

**ROLE OF FATTY ACID BINDING PROTEIN IN
LIVER REGENERATION AND CELLULAR PROTECTION**

A Thesis

Presented to

The University of Manitoba

In Partial Fulfillment of the Requirements

For the Degree of Doctor of Philosophy

By

Gu-Qi Wang

(c) 2004

Faculty of Pharmacy

The University of Manitoba

Winnipeg, Manitoba

THE UNIVERSITY OF MANITOBA
FACULTY OF GRADUATE STUDIES

COPYRIGHT PERMISSION PAGE

Role of Fatty Acid Binding Protein in Liver Regeneration and Cellular Protection

BY

Gu-Qi Wang

**A Thesis/Practicum submitted to the Faculty of Graduate Studies of The University
of Manitoba in partial fulfillment of the requirements of the degree**

of

DOCTOR OF PHILOSOPHY

GU-QI WANG ©2005

Permission has been granted to the Library of The University of Manitoba to lend or sell copies of this thesis/practicum, to the National Library of Canada to microfilm this thesis and to lend or sell copies of the film, and to University Microfilm Inc. to publish an abstract of this thesis/practicum.

The author reserves other publication rights, and neither this thesis/practicum nor extensive extracts from it may be printed or otherwise reproduced without the author's written permission.

This work is dedicated to

my parents, Shao-Tong Wang and Fu-xiang Duan

my wife, Qing-ming and

my daughters, Jing and Hannah

TABLE OF CONTENTS

Abstract.....	VII
Acknowledgements.....	VIII
List of Figures.....	IX
List of Tables.....	XII
Abbreviations.....	XIII
 I. Introduction	 1
A. Fatty Acid Binding Proteins (FABPs)	1
B. FABPs Gene Organization.....	3
C. FABPs Structure and Subfamily.....	6
D. Functions of FABPs.....	10
E. Membrane-Associated Fatty Acid Binding Protein.....	13
F. Liver Fatty Acid Binding Protein.....	14
1. L-FABP (FABP1).....	14
2. L-FABP Gene and Expression.....	18
3. Role of L-FABP in Hepatic Fatty Acid Uptake and Transportation.....	24
4. Role of L-FABP in Hepatocytes Proliferation.....	27
5. Antioxidation Function of L-FABP.....	30
6. L-FABP Expression and Antioxidation in Bile-Duct Ligated Rats.....	36
II. Hypothesis and Objectives.....	39
III. Materials and Methods.....	41

A. Materials.....	41
B. Methods.....	41
1. Animal Care.....	41
2. Isolation and purification of L-FABP and cytosolic proteins.....	42
3. In-gel Tryptic Digestion for Protein Mass Spectrometric Analysis.....	44
4. Protein Blotting and Protein Extraction.....	45
5. In-solution Proteolytic Digestion.....	46
6. MALDI QqTOF Mass Spectrometry.....	47
7. Protein MS Data Processing.....	47
8. 70% Hepatectomy.....	49
9. Bile-duct ligation (BDL) animal model.....	50
10. Histopathologic examination.....	51
11. L-FABP antisera production.....	51
12. Western blot analysis.....	52
12.1. Protein sample preparation from tissue.....	52
12.2. Protein sample preparation from cell culture.....	52
12.3. Western blot	52
13. Northern blot analysis.....	53
13.1. RNA isolation	53
13.2. Random Primer DNA Labelling	54
13.3. Northern Blot.....	55
14. Determination of liver regenerating activity	56
14.1. PCNA Western blot assay.....	56

14.2. [³ H]-thymidine incorporation.....	56
14.3. DNA assay.....	57
15. Hepatic fatty acid uptake studies.....	57
15.1. Purification of [³ H]-palmitic acid	57
15.2. Hepatocyte isolation.....	58
15.3. Uptake Procedure	60
16. Cell culture conditions.....	60
17. Transformation of competent E. coli cells with Plasmid.....	61
18. Mini-preparation of Plasmid.....	61
19. Large-scale Preparation of Plasmid.....	62
20. Restriction Enzyme Digestion.....	64
21. Agarose Gel Electrophoresis.....	64
22. Subcloning of DNA fragment.....	65
22.1. DNA extraction from agarose gels.....	65
22.2. DNA ligation and transformation.....	65
23. Construction of mammalian expression plasmid of human L-FABP.....	66
24. Selection of Stable Transfected Chang liver cells.....	67
25. Reverse transcriptase polymerase-chain reaction (RT-PCR) analysis of FABP mRNA expression.....	67

26. L-FABP mRNA expression assay with quantitative real-time RT-PCR.....	68
26.1. L-FABP mRNA standard curve preparation	68
26.2. Quantitative real-time RT-PCR.....	70
27. Inducing Oxidative Stress and DCF fluorescence assay.....	70
27.1. Oxidative stress induced by H ₂ O ₂	71
27.2. Oxidative stress induced by Hypoxia- Reoxygenation	71
27.3. DCF fluorescence measurement	73
27.4. DCF fluorescence imaging.....	73
28. Lipid peroxidation (TBARS) assay.....	74
29. Biochemical Assay.....	75
29.1. Serum collection.....	75
29.2. Alanine aminotransferase (ALT) assay.....	77
29.3. Ammonia assay.....	78
29.4. Lactate dehydrogenase (LDH) assay.....	79
29.5. Total bilirubin determination.....	80
29.6. Lowry protein assay.....	82
29.7. Bradford protein assay.....	84
30. Statistical analysis.....	86
IV. Results and discussions.....	87
Section A. Identification and sequencing of rat liver FABP and other cytosolic proteins by mass spectrometry following electrophoretic separation and extraction....	87
Section B. Expression and effects of liver FABP on hepatic fatty acid uptake and liver regeneration following partial hepatectomy.....	107

Section C. Cellular Antioxidative Function of L-FABP in L-FABP Stable Transfected	
Chang Liver Cells.....	119
Section D. Expression and antioxidant function of L-FABP in normal and bile-duct	
ligated rats.....	140
V. Overview of FABP.....	156
VI. References.....	159

ABSTRACT

Liver fatty acid binding protein (L-FABP) is intricately involved in the intracellular disposition of long-chain fatty acids. L-FABP also is known to be a carrier of certain hydrophobic reactants from cytosol to nucleus, suggesting that L-FABP is an important mediator between ligand and ligand activated nuclear receptors, affecting gene expression. L-FABP contains one cysteine and seven methionine residues that are known to be effective antioxidant agents. Accordingly, the present studies were designed to determine: 1) the role of L-FABP in liver regeneration following partial hepatectomy (PHx); 2) the role of L-FABP as an effective endogenous cytoprotectant against oxidative stress; 3) the expression and antioxidative function of L-FABP in an animal model of cholestatic liver disease induced by bile duct ligation (BDL).

Results of this thesis showed: 1) L-FABP mRNA and protein level increased in a time-dependent manner following PHx. The increased L-FABP level was associated with an increased hepatic [^3H]-palmitate clearance. Down-regulation of L-FABP by dexamethasone reduced hepatocellular mitotic activity. The data suggest that L-FABP plays an important role in liver regeneration acting as a carrier of mediators required for cell proliferation; 2) compared with vector-transfected Chang cells, L-FABP transfected cells showed lower levels of ROS in oxidative stress induced by H_2O_2 and hypoxia/reoxygenation. The LDH released from cells was also lower in the L-FABP expressed cells during oxidative stress. These results suggest that L-FABP plays a significant role as an endogenous cellular protectant against oxidative stress; 3) cholestatic liver disease (BDL model) results in hepatic oxidative stress. L-FABP mRNA and protein level were decreased after BDL. The decreased L-FABP correlated with an increased lipid peroxidation and hepatic dysfunction. Clofibrate treatment restored L-FABP protein level back to 79% of sham and improved hepatic function. Clofibrate treatment also reduced hepatic lipid peroxidation products. This finding indicated that reduction of L-FABP in the BDL model was related to increase ROS. L-FABP expression may be important in preventing the progression of cholestatic liver disease.

The present study made novel and important findings concerning the roles of L-FABP as an intracellular mediator of cell proliferation and an important cellular antioxidant during hepatocellular oxidative stress.

ACKNOWLEDGEMENTS

A big thanks to my supervisor, Dr. Frank J. Burczynski, for his tremendous support and guidance throughout all aspects of this project. I really appreciate his patience in our discussions and his encouragement of independent thinking. I am very grateful to Drs. Yuewen Gong and Dongfeng Sun for their excellent technical help in molecular biology, their kindness and patience whenever I needed help.

Dr. Yiming She has given me much support and research cooperation on the Mass Spectrometrics of Liver Fatty Acid Binding Protein and other proteins. Thank you for the venture in Proteomics.

Over the last four years, Patricia, Ganesh, Denise, Pat, and Ping Jiang have been especially supportive as friends and fellow students. Their friendship and support have made the time enjoyable and full as it should be.

I would like to express my gratitude to Dr. Gerald Minuk for his generous support during my experiments in his laboratory. It was an honor and joy to work with his liver research team. I would also like to thank Drs. Brian Hasinoff and Yuewen Gong for their ideas and constructive discussions. I am very grateful to Drs. Frank Burzynski, Gerald Minuk, Brian Hasinoff, and Yuewen Gong for their letters of reference in support of my applications for scholarships and awards. I would like to extend my thanks to all professors and fellow graduate students in our faculty for their friendship, encouragement, and interesting discussions.

I gratefully acknowledge CIHR and Rx&D for my studentship support.

I owe a great debt of gratitude to my wife Qing-ming, and my daughters, Jing and Hannah, for their love, understanding and continual support throughout my years as a graduate student.

LIST OF FIGURES

Figure 1. Comparison of gene structures of FABPs	5
Figure 2. Crystal structure and cavity location of L-FABP	7
Figure 3. FABPs subfamily	8
Figure 4. Physiological function of FABP	11
Figure 5. Amino acid sequence of rat L-FABP	15
Figure 6. <i>Cis</i> - acting elements and transacting factors of rat L-FABP	20
Figure 7. L-FABP and nuclear receptor activation	22
Figure 8. Schematic presentation of cellular fatty acid uptake	25
Figure 9. Oxidative stress and putative antioxidation function of L-FABP	31
Figure 10. S-thiolation/dethiolation of cysteine residue in antioxidation	33
Figure 11. Cyclic oxidation and reduction of methionine residues scavenge oxidants catalytically.....	34
Figure 12. Chromatography and electrophoresis of rat liver proteins.....	43
Figure 13. Diagram of MALDI QqTOF tandem mass spectrometer.....	48
Figure 14. Experimental arrangement for <i>in situ</i> perfusion of rat liver.....	59
Figure 15. Hypoxia/reoxygenation apparatus.....	72
Figure 16. HPLC chromatograms of TBARS-(TBA) ₂ complex.....	76
Figure 17. Reaction of bilirubin with diazotized sulfanilic acids.....	81
Figure 18. Reaction schematic for the Lowry Protein Assay.....	83
Figure 19. Reaction schematic for the Bradford protein assay	85

Figure 20. Summary of procedures in cytosolic proteins identification and amino acid sequence analysis	89
Figure 21. SDS-PAGE gel of rat liver cytosolic protein fraction	90
Figure 22. MALDI mass spectra of in-gel digests of L-FABP	92
Figure 23. CID mass spectrum of the ion at m/z 1539.71	94
Figure 24. MALDI mass spectra of the FABP digests.....	97
Figure 25. CID mass spectrum of the ion at m/z 1587.71	98
Figure 26. MALDI mass spectrum of the endoprotease Glu-C digested Cu-Zn superoxide dismutase.....	101
Figure 27. CID mass spectrum of the ion at m/z 2632.14 from a tryptic FABP.....	102
Figure 28. MALDI mass spectrum of a tryptic protein.....	103
Figure 29. Northern blot analysis of rat L-FABP mRNA expression following PHx.....	109
Figure 30. Western blot analysis of rat L-FABP levels following PHx	110
Figure 31. Western blot analysis of L-FABP levels in dexamethasone treated rat livers following PHx.....	112
Figure 32. [³ H]-Thymidine incorporation into hepatic DNA in dexamethasone treated rat livers.....	113
Figure 33. PCNA protein levels in regenerating rat livers.....	114
Figure 34. [³ H]-Palmitate clearance by rat hepatocytes.....	115
Figure 35. Expression of L-FABP cDNA in hepatoma cell lines.....	122
Figure 36. Selection of the pcDNA-FABP transfected Chang liver cells.....	123
Figure 37. L- FABP mRNA expression levels in the selected clones.....	124

Figure 38. Western Blot analysis of L-FABP expression in the experimental pcDNA-FABP transfected Chang cells.....	125
Figure 39. The morphological images of pcDNA-FABP and pcDNA3.1 (vector) transfected Chang liver cells.....	126
Figure 40. Effect of L-FABP on the fluorescence intensity of DCF.....	128
Figure 41. Effect of DMSO on DCF fluorescence intensity.....	129
Figure 42. DCF fluorescence of pcDNA-FABP transfected Chang cells in oxidative stress induced by hydrogen peroxide.....	130
Figure 43. Colour DCF images of pcDNA-FABP transfected Chang cells in oxidative stress induced by hydrogen peroxide.....	131
Figure 44. DCF fluorescence in pcDNA-FABP transfected Chang cells subjected to hypoxia-reoxygenation.....	133
Figure 45. LDH release from pcDNA-FABP transfected Chang cells subjected to hypoxia/reoxygenation.....	134
Figure 46. Liver sections from Sham and BDL rats.....	142
Figure 47. RT-PCR analysis of rat L-FABP mRNA expression following BDL.....	143
Figure 48. Western blot analysis of rat L-FABP levels following BDL.....	144
Figure 49. Increased TBARS production in liver tissues in BDL rats.....	147
Figure 50. Clofibrate reverses reduction of L-FABP mRNA and L-FABP level in BDL rats.....	148
Figure 51. High mortality rate of BDL animals fed with high fat diet	154
Figure 52. L-FABP mRNA and protein levels of BDL rats fed high fat diet.....	155

LIST OF TABLES

Table 1. Members of FABPs family.....	2
Table 2. Chromosomal location of FABPs gene and protein length.....	4
Table 3. Ligand and correlative functions of L-FABP	17
Table 4. PCR conditions and primer structures.....	69
Table 5. Comparison of mass differences between adjacent b fragments at m/z 1539.71 with calculated mass	95
Table 6. Complete sequence of some rat liver proteins by MALDI QqTOF mass spectrometry.....	96
Table 7. Protein sequence analyses by MALDI QqTOF mass spectrometry following peptide extraction of the tryptic digests.....	104
Table 8. Serum Levels of Bilirubin, Ammonia, TBARS, and liver TBARS level.....	146

ABBREVIATIONS

ACBP	Acyl-CoA-binding protein
BDL	bile duct ligation
A	deoxyadenosine
ALT	alanine aminotransferase
bp	basepair(s)
BSA	bovine serum albumin
C	deoxycytidine
C-14	radioisotope carbon-14
cDNA	complementary DNA
CID	collision-induced dissociation
CRABP	cellular retinoic acid binding protein
CRBP	cellular retinol binding protein
dATP	deoxyadenosine triphosphate
DCF	dichlorofluorescein
dCTP	deoxycytidine triphosphate
DE	delayed extraction
dGTP	deoxyguanosine triphosphate
DHA	docosahexaenoic acid
DHB	2,5-dihydroxybenzoic acid
DMEM	Dulbecco's modified Eagle's medium
DMSO	dimethyl sulfoxide

DNA	deoxyribonucleic acid
dNTP	deoxyribonucleotide triphosphate
dNTP	deoxyribonucleotide triphosphate
dpm	disintegrations per minute
dTTP	deoxythymidine triphosphate
ECL	enhanced chemiluminescence
EDTA	ethylenediaminetetraacetic acid
EtBr	ethidium bromide
FA	fatty acid
FAARs	fatty acid activated receptors
FABP	fatty acid binding protein
FABPpm	plasma membrane fatty acid binding protein
FAT	fatty acid translocase
FATP	fatty acid transport protein
FBS	fetal bovine serum
FTICR	Fourier transform ion cyclotron resonance
<i>g</i>	gravity
g	gram
G	deoxyguanosine
G418	geneticin
GAPDH	glyceraldehyde 3-phosphate dehydrogenase
GDB	human genome database

GSH	reduced glutathione
GST	glutathione S-transferase
GTPx	glutathione peroxidase
HETEs	hydroxyeicosatetraenoic acids
HNF	Hepatocyte nuclear factor
HPETEs	hydroperoxyeicosatetraenoic acids
kDa	kilodalton
LCFA	long chain fatty acid
LDH	lactate dehydrogenase
L-FABP	liver fatty acid binding protein
LXR	liver X receptor
M	molarity
MALDI QqTOF	matrix-assisted desorption ionization quadrupole time-of-flight
MDA	malonaldehyde
MGD	mouse genome database
min	minute(s)
MMLV	monoley murine leukemia virus
mRNA	messenger RNA
MS	mass spectrometry
MS/MS	tandem mass spectrometric measurement
N	normality
NADH	nicotinamide adenine dinucleotide, reduced form

NADP	nicotinamide adenine dinucleotide phosphate
NADPH	nicotinamide adenine dinucleotide phosphate, reduced form
OD	optical density
OGP	n-octyl α -D-glucopyranoside
PAGE	polyacrylamide gel electrophoresis
PBS	phosphate buffered saline
PCNA	proliferating cell nuclear antigen
PCR	polymerase chain reaction
PHx	partial hepatectomy
PMSF	phenylmethanesulfonyl fluoride
PPARs	peroxisome proliferator activated receptors
PPREs	peroxisome proliferator responsive elements
PVDF	polyvinylidene difluoride
RARs	retinoic acid receptors
RGD	rat genome database
RIPA	radioimmunoprecipitation
RNA	ribonucleic acid
Rnase	ribonuclease
ROS	reactive oxygen species
rpm	revolutions per minute
RT	reverse transcription
RXR _s	retinoic acid X receptors

SDS	sodium dodecyl sulfate
sec	second(s)
SEM	standard error of measurement
SOD	superoxide dismutase
T	deoxythymidine
TBA	thiobarbituric acid
TBARS	thiobarbituric acid-reactive substances
TBS	tris-buffered saline
TPCK	N ^a -tosylsulfonylphenylalanylchloromethyl ketone
Tris	tris(hydroxymethyl)amino methane
U	unit(s)
v/v	volume per volume
w/v	weight per volume

I. Introduction to Fatty Acid Binding Protein

A. Fatty acid binding proteins (FABPs)

Fatty acid binding protein (FABP) is a class of cytoplasmic binding proteins that are abundantly present in the cytoplasm of tissue and involved in cellular long chain fatty acid (LCFA) uptake, translocation, and metabolism. FABP was first discovered in 1969 when Levi and his co-workers studied the binding of bilirubin and bromosulphophthalein to rat liver cytosol (Levi, Gatmaitan et al. 1969). They found two fractions involved in the binding of these ligands; the fraction with molecular mass of 30 - 50 kDa known as Y protein and the fraction with molecular mass of 10 - 20 kDa termed Z protein. Z protein was the original name of fatty acid binding protein. In the early 1970s, Ockner (Ockner, Manning et al. 1972), Mishkin (Mishkin, Stein et al. 1972), and Ketterer (Ketterer, Tipping et al. 1976) performed a series of experiments, where cytosolic proteins were incubated with C-14 labeled oleic acid followed by a gel chromatography. The radioactive label was recovered in two fractions, one with a molecular mass of about 68 kDa that contained albumin, the second with a molecular mass of approximately 15 kDa that was termed fatty acid binding protein (FABP). With the progress of gene and protein structure analysis, scientists realized FABPs belong to a large group of water soluble lipid binding proteins having low molecular mass (14-16 kDa, 127-137 residues) and similar gene and protein structure that perform similar functions. To date, thirteen FABPs have been identified with at least nine distinct types of FABP (Table 1).

Table 1. Members of FABP family

FABP type	Abbreviation	Tissue occurrences	Ligands
Liver FABP	L-FABP	liver, intestine, kidney, lung, pancreas	FA, acyl-CoAs, heme, bilirubin, eicosanoids
Intestinal FABP	I-FABP	intestine, stomach	FA
Heart FABP	H-FABP	heart, kidney, skeletal muscle, aorta, adrenals, brain, testes, ovary, lung, stomach, placenta	FA
Adipocyte FABP	A-FABP	adipose tissue	FA, retinoic acid
Epidermal FABP	E-FABP	skin, brain, lens, capillary endothelium, retina	FA, eicosanoids
Ileal FABP	IL-FABP	intestine, ovary, adrenals, stomach	FA, bile acids
Brain FABP	B-FABP	brain	FA
Myelin FABP	M-FABP	peripheral nervous system	FA, retinoids
Testicular FABP	T-FABP	Testis	FA
Cellular RABP I	CRABP I	testis, brain, kidney, skin	retinoic acid
Cellular RABP II	CRABP II	skin, adrenals	retinoic acid
Cellular RBP I	CRBP I	liver, lung, intestine, kidney, testis	retinol
Cellular RBP II	CRBP II	small intestine	retinol

An FABP type does not mean its presence in all cell types of that tissue, and also not specific for a given tissue. A specific FABP may be limited to specific cells or may be present at certain developmental stages.

B. FABPs gene organization

Although the locations of FABP genes are at different sites on the chromosomes (Table 2), they show a large structural homology. Each gene contains four exons separated by three introns (Figure 1). Although the length of introns varies, the length of exons has been maintained such that exon/intron positions are similar in all genes. This common gene structure suggests that FABPs developed from a single precursor gene by gene duplication and branching. The divergence of distinct FABPs from a common ancestral gene is estimated to have occurred approximately 650 million years ago, before the invertebrate-vertebrate divergence (Chan, Wei et al. 1985). The genes of cellular retinol binding protein (CRBP) and cellular retinoic acid binding protein (CRABP) also contain four exons and three introns, although the average length of introns far exceeds that of the FABP genes (Li and Norris 1996). Therefore, CRBP and CRABP are classified into FABPs multigene family. Most of the FABP genes exist in a single copy on the chromosome. However, murine heart FABP is an exception, which is represented three times (Heuckeroth, Birkenmeier et al. 1987). FABPs are named after the tissues in which they were first identified or the primary ligand type. Some of them are expressed in one tissue, while others are expressed in multiple tissues (Bernlohr, Simpson et al. 1997). For example, adipocyte FABP, intestinal FABP, epidermal FABP, myelin FABP, brain FABP, and testis FABP are expressed in each single tissue. Liver FABP, ileal FABP are expressed in a limited number of tissues. Heart FABP shows the broadest tissue distribution occurring in heart, skeletal muscle, mammary, lung, brain, kidney, testis, ovary, stomach, and adrenal tissues.

Table 2. Chromosomal location of FABP genes and protein length

FABP type	Gene symbol	Chromosome (region)			Protein length
		Human	Mouse	Rat	
L-FABP	FABP1	2p11	6	4q33	127
I-FABP	FABP2	4q28–q31	3	2q41	131
H-FABP	FABP3	1p32–p33	4	5q36	132
A-FABP	FABP4	8q21	3	2q23	131
E-FABP	FABP5	8q21.13	3(3A1-3)	-	134
IL-FABP	FABP6	5q23–q35	11	10q21	127
B-FABP	FABP7	6q22–q23	10	20q11	131
M-FABP	FABP8	8q21.3–q22.1	3	-	131

The information are retrieved from the human genome database (GDB), mouse genome database (MGD), and rat genome database (RGD), respectively. Gene nomenclature according to human genome database conventions. The length of the mature protein is given in amino acids.

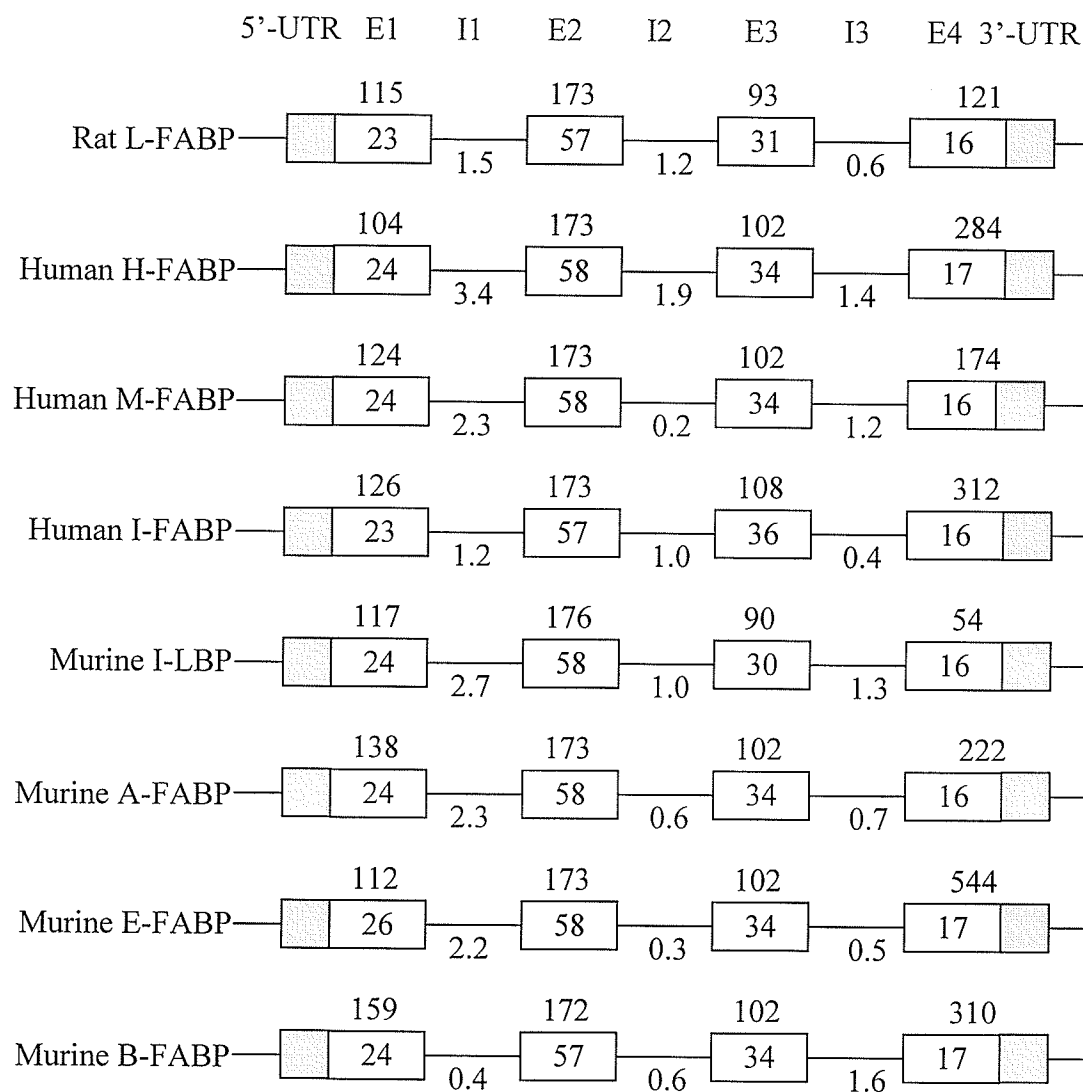


Figure 1. Comparison of the gene structures of FABP. E, exon; I, intron; the shaded box represents the 5' and 3' untranslated regions (UTR) of exon 1 and exon 4, respectively. Numbers in boxes indicate the number of amino acids encoded within each exon. Intron lengths are in kilobase pairs and exon lengths in base pairs. This figure is adapted from Zimmerman, 2002.

C. FABPs structure and subfamily

Each type of FABP exhibits a characteristic pattern of tissue distribution. Heart FABPs from human, rat, and bovine have approximately 90 % amino acid sequence homology (Offner, Troxler et al. 1986; Billich, Wissel et al. 1988; Offner, Brecher et al. 1988). An 82 % sequence homology was found between human and rat liver FABPs (Lowe, Boguski et al. 1985). However, rat liver FABP only has 26 % and 38 % sequence homology with intestinal and heart FABP in the rat respectively (Alpers, Strauss et al. 1984; Sacchettini, Said et al. 1986). Although the amino sequence homology of each protein varies, all FABPs have ten antiparallel β -strands and two α -helices in their tertiary structures (Figure 2). Within the confines of β -strands is the binding pocket of the protein (Banaszak, Winter et al. 1994). Two α -helices form a cap for the binding pocket. These short α -helices are arranged as a helix-turn-helix segment in the sequence. It is believed that this helical domain functionally determines the different transfer mechanism of fatty acids from the protein-binding pocket (Hodsdon and Cistola 1997; Corsico, Cistola et al. 1998; Corsico, Liou et al. 2004). For example, fatty acids transfer from I-FABP is a collisional transfer mechanism, while for L-FABP, transfer is thought to occur by diffusion through the aqueous phase.

The N-terminal amino acid in FABP is acetylated, indicating its cytoplasmic protein destination, not secreted (Gordon, Alpers et al. 1983; Alpers, Strauss et al. 1984). Based on statistical analyses of cDNA, protein sequence data, and binding properties, FABPs can be divided into four subfamilies (Hohoff and Spener 1998)(figure 3): (1) subfamily-1 contains all the retinoid binding protein, CRBP (I and II), CRABP (I and II).

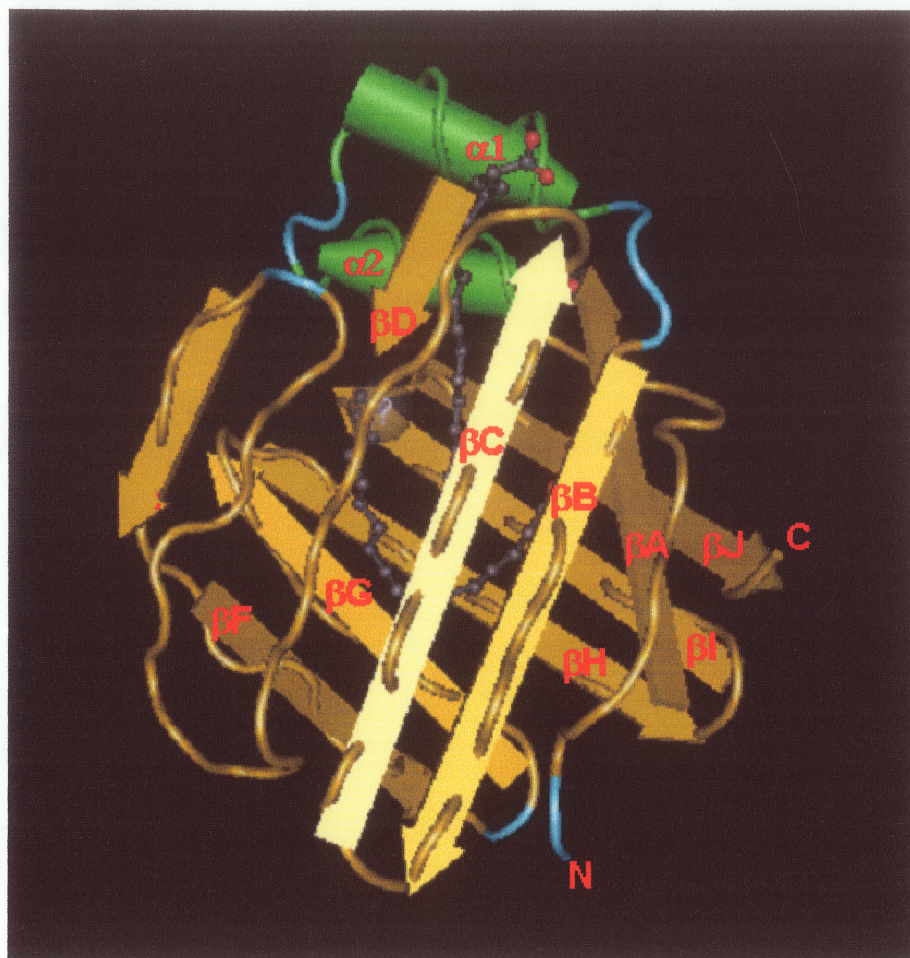
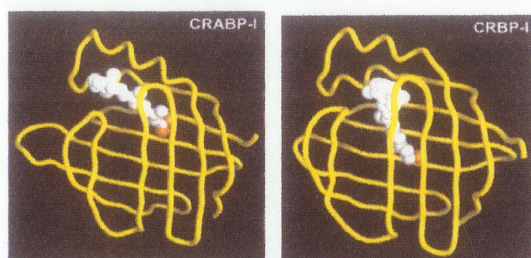
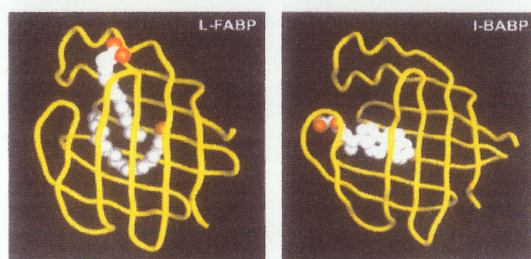


Figure 2. The crystal structure and cavity location of L-FABP. Ten antiparallel β -strands (A to J) form a β -barrel. Two oleate ligands (dark gray) are bound in the cavity of L-FABP. One oleate is completely buried within the confines of the cavity. The carboxyl group of the other is exposed to solvent such that the hydrocarbon chains of the two fatty acids can interact with each other. The two α -helices form the portal cavity. N-terminal is acetylated. Based on rules of hydrogen bonding, the β F strand could be divided into two connecting β -strands. However, they are homologous with the β F in other FABPs. This figure was referred and modified from NCBI-MMDB(6159) at <http://www.ncbi.nlm.nih.gov/Structure/MMDB/mmdb.shtml>.

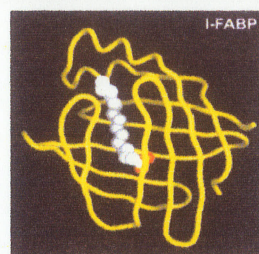
Subfamily-1



Subfamily-2



Subfamily-3



Subfamily-4



Figure 3. Graphic representation of FABP-ligand complexes that are exemplary of four FABPs subfamilies. The bound ligand is represented as a space-filling model in red (carboxylate group) and white. The protein backbone is shown as a yellow tube. Subfamily-1 shows CRABP-I and CRBP-I complexes with retinoic acid and retinol respectively. In subfamily-2, L-FABP binds two molecules of oleic acid, whereas I-BABP binds glycocholate. I-FABP of subfamily-3 is shown in complex with one molecule of palmitic acid in a linear conformation. The subfamily-4 proteins, E-FABP (with palmitic acid), H-FABP (with oleic acid), and B-FABP (with DHA), generally bind one molecule of fatty acid in a U-shaped conformation. Figures were produced with GRASP (Christian Lucke, Frankfurt, Germany).

CRBPs and CRABPs are specialized in binding vitamin A and its derivatives. The ligands generally consist of three parts: a β -ionone ring, a polyisoprene chain and a polar headgroup (carboxylate in retinoic acid, aldehyde in retinal and alcohol in retinol). In the binding confirmation, the β -ionone ring is usually located near the ligand entrance under the helix-turn-helix domain. The polyisoprene chain extends through the protein cavity. The polar headgroup rests in the deep of the binding pocket. (2) Subfamily-2 consists of liver FABP and intestinal bile acid binding protein (I-BABP). These proteins interact with a wide variety of bulky ligands in addition to long chain fatty acids (LCFAs). Less residues in β -strand G and H of this family create an additional opening in the protein surface for a favorable second ligand entry portal. Their ability to bind more bulky groups may be due to the considerably higher backbone flexibility (Lucke, Zhang et al. 1996). In all FABP families, L-FABP is the only one able to bind two LCFAs simultaneously. Presumably, the high-affinity fatty acid ligand sits at the bottom of the protein cavity in a bent conformation. The second, low-affinity fatty acid ligand stretches from the center of the first ligand to the portal with its solvent-accessible carboxyl group at the protein surface. (3) Intestinal FABP is the sole member of subfamily-3, which preferentially binds a single fatty acid in a linear conformation. The ligand adopts a reversed orientation compared to the low affinity binding ligand in L-FABP. (4) Subfamily-4 contains the most diverse assortment of FABPs, including E-FABP, H-FABP, B-FABP, T-FABP, M-FABP, A-FABP. All members of this family preferentially bind a single long chain-fatty acid in a highly bent or U-shaped conformation, thus creating intra-molecular non-polar contacts for favorable LCFA energetically.

D. Functions of FABPs

In the last 30 years, remarkable advances have been made in understanding the structural biology of FABPs. There are not many other protein families for which their tertiary structures and in vitro binding properties are as well studied. Nevertheless, the biological functions of FABPs are still being investigated. A large amount of evidence suggests FABPs are involved in at least seven biological pathways (Glatz and van der Vusse 1996)(Figure 4). These pathways include: 1) FABP shuttles fatty acids from the inner plasma membrane into the cytosol, transporting ligands to the mitochondrial matrix, where fatty acids are oxidized for energy production; 2) FABP compartmentalizes fatty acids in microsomes for the synthesis of acyl-CoA, triacylglycerols, and phospholipids; 3) FABP translocates fatty acids and their metabolites to the nuclear membrane where fatty acids are bound by a nuclear receptor. This complex dimerizes with other liganded nuclear receptor and targets the response element to regulate gene expression. Good candidate nuclear receptors are some members of the steroid/thyroid hormone nuclear receptor superfamily, such as peroxisome proliferator activated receptors (PPARs) and fatty acid activated receptors (FAARs). In the mechanism of retinoic acid-induced gene regulation, retinoic acid receptors (RARs) and retinoid X receptors (RXRs) form heterodimeric complexes that work as ligand-controlled transcription factors; 4) FABP can transport fatty acids to a hormone receptor to compete with the steroid hormone for the binding site, therefore, modulating the signals originating from other pathway in a reversible manner; 5) with hormone stimulated intracellular fatty acid production, fatty acids serve as secondary messengers being carried to the nuclei by FABP to regulate gene

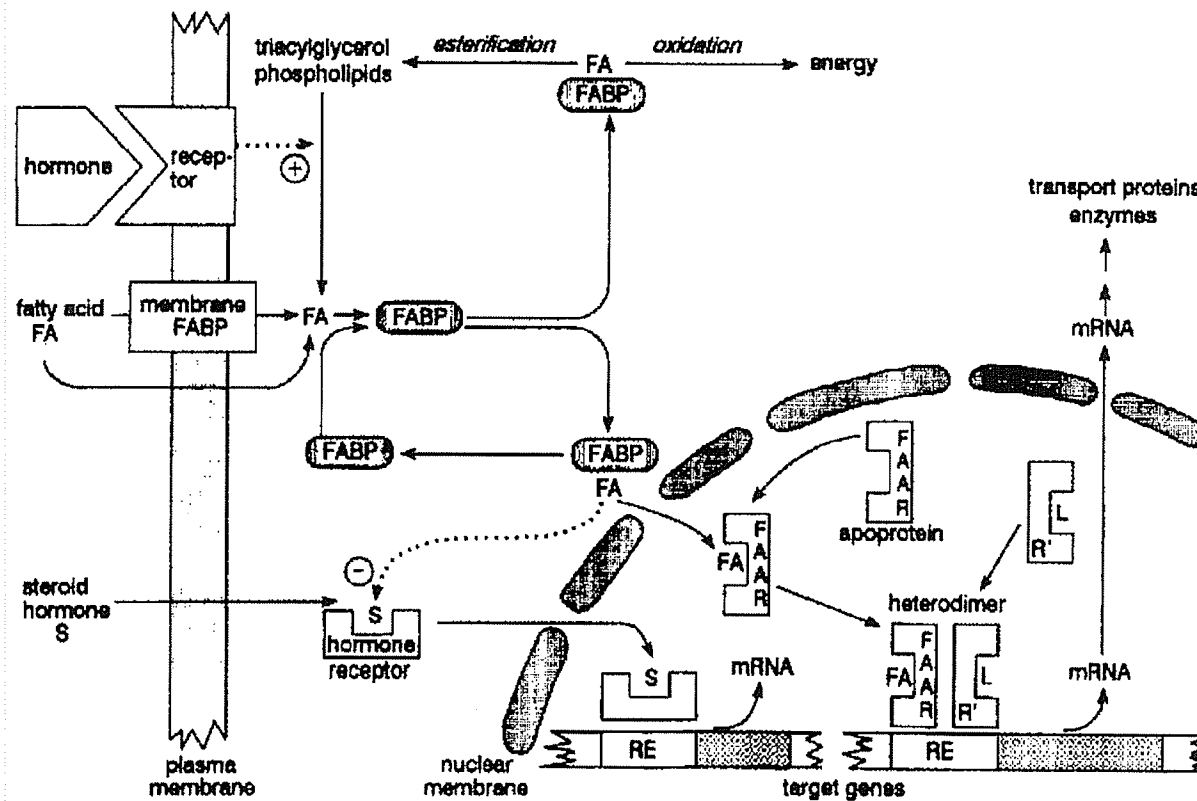


Figure 4. The physiological functions of FABP in LCFA transport, metabolism, and signal transduction. Exogenous or endogenous FA as second messengers are bound by FABPc and diffuse to nucleus to transfer the ligand to the nuclear receptor FAAR. The complex then dimerizes with another liganded nuclear receptor and targets a specific response element to stimulate transcription. L, ligand; R', nuclear receptor; RE, response element; S, steroid hormone; +, stimulation; -, inhibition. The figure is adapted from Glatz, 1996.

Expression; 6) FABP can serve as an intracellular buffer of fatty acids and their CoA and carnitine esters to maintain a low concentration of the unbound form of these substances within the cell; 7) FABP may act as a trapper or scavenger to inhibit or clear cytotoxin and reactive oxygen species (ROS) to protect cells.

FABPs are very stable proteins, with a high resistance to enzymatic digestion (Peeters, in't Groen et al. 1989) and radiation (Sacchetti, Meininger et al. 1987). The binding of FABPs with LCFAs appears to increase this resistance (Takahashi, Odani et al. 1982). At 50 °C and pH of 4.0, activity of FABP was not affected significantly during bovine FABP isolation (Haunerland, Jagschies et al. 1984; Jagschies, Reers et al. 1985). The degradation rate of FABP under physiological conditions was determined with a half-life of 3.1 days in liver (Bass, Manning et al. 1985). Release of FABP from damaged cells occurs rapidly and simultaneously since FABPs are smaller and highly soluble intracellular proteins. It has been reported that some specific FABPs can be detected in elevated levels in the plasma or urine of patients with heart, liver and other diseases. Thus, FABP analysis is being applied as a valuable diagnostic tool for the early detection in acute myocardial infarction and stroke (Tsuji, Tanaka et al. 1993; Van Nieuwenhoven, Kleine et al. 1995; Yoshimoto, Tanaka et al. 1995; Zimmermann-Ivol, Burkhard et al. 2004), in cancer (bladder, prostate cancer) (Rasmussen, Orntoft et al. 1996; Das, Hammamieh et al. 2001), in liver diseases (hepatitis, cirrhosis) (Kamisaka, Maezawa et al. 1981; Pelsers, Morovat et al. 2002), in intestinal ischaemia (Kanda, Nakatomi et al. 1992; Kanda, Fujii et al. 1996), and chronic renal disease (Kamijo, Kimura et al. 2004).

E. Membrane-associated fatty acid-binding protein

It is necessary to mention the other category of fatty acid binding proteins (classified as membrane-associated fatty acid binding proteins) in the discussion of FABPs. Three membrane-associated fatty acid binding proteins have been identified to date, which are distinctly different from cytosolic FABPs. These proteins are the 43-kDa plasma membrane FABP (FABPpm), the 88-kDa fatty acid translocase (FAT/CD36), and a family of five fatty acid transport proteins (FATP1-5) with molecular weight of 60-kDa (Abumrad, Coburn et al. 1999; Luiken, Schaap et al. 1999; Glatz and Storch 2001). Membrane-associated fatty acid binding proteins are expressed in multiple tissues. In some species and strains, FAT/CD36 is not expressed in liver and brain (Van Nieuwenhoven, Willemsen et al. 1999). These membrane-associated fatty acid binding proteins facilitate the cellular LCFA uptake in protein-mediated transmembrane transportation (Berk, Bradbury et al. 1996; Luiken, Arumugam et al. 2001). FABPpm is a peripheral membrane protein (Stump, Zhou et al. 1993). LCFAs are likely trapped by FABPpm and then cross the membrane by passive diffusion. FAT/CD36 is an integral membrane glycoprotein that has two transmembrane-spanning regions (Abumrad, Coburn et al. 1999). It is suggested that FAT/CD36 facilitates LCFA uptake through the cellular membrane mainly through trapping LCFAs to the plasma membrane, and then increasing the LCAF concentration near the sarcolemma for transmembrane flux (Glatz and Storch 2001). FATP was found to have one transmembrane and multiple membrane-associated domains (Lewis, Listenberger et al. 2001). FATP also has acyl-CoA

synthetase activity, particularly for very long chain fatty acids, so that the enhanced uptake of LCFAs may be due to their metabolic trapping (Coe, Smith et al. 1999; Herrmann, Buchkremer et al. 2001).

Cytoplasmic FABPs, as well as membrane-associated FABPs play central roles in the cellular uptake and transport of LCFA and/or their derivatives. Their physiological significance most likely involves increasing LCFA transport capacity and controlling cellular LCFA homeostasis, thus performing a dual role that transport ligands to certain sites and sequester from others. Transcription factors PPARs, RXRs, RARs, LXR, and HNF4 bind LCFA and/or their derivatives and play a central role in regulating the storage and metabolism of dietary fats. Essential metabolic pathways of lipids appear to be under control of one or more genes regulated by these transcription factors. They are involved in the pathogenesis of inflammatory disorders, obesity, cancers, and atherosclerosis. Since these transcription factors need fatty acids or their derivatives as ligands, FABPs certainly play an important role in ligand transport, and therefore affect health and disease outcomes.

F. Liver fatty acid binding protein

1. L-FABP (FABP1)

Liver fatty acid binding protein (L-FABP, also called as Z protein, h-FABP) is a 14-kDa protein mainly presented in the cytoplasm of hepatocytes including the nucleus

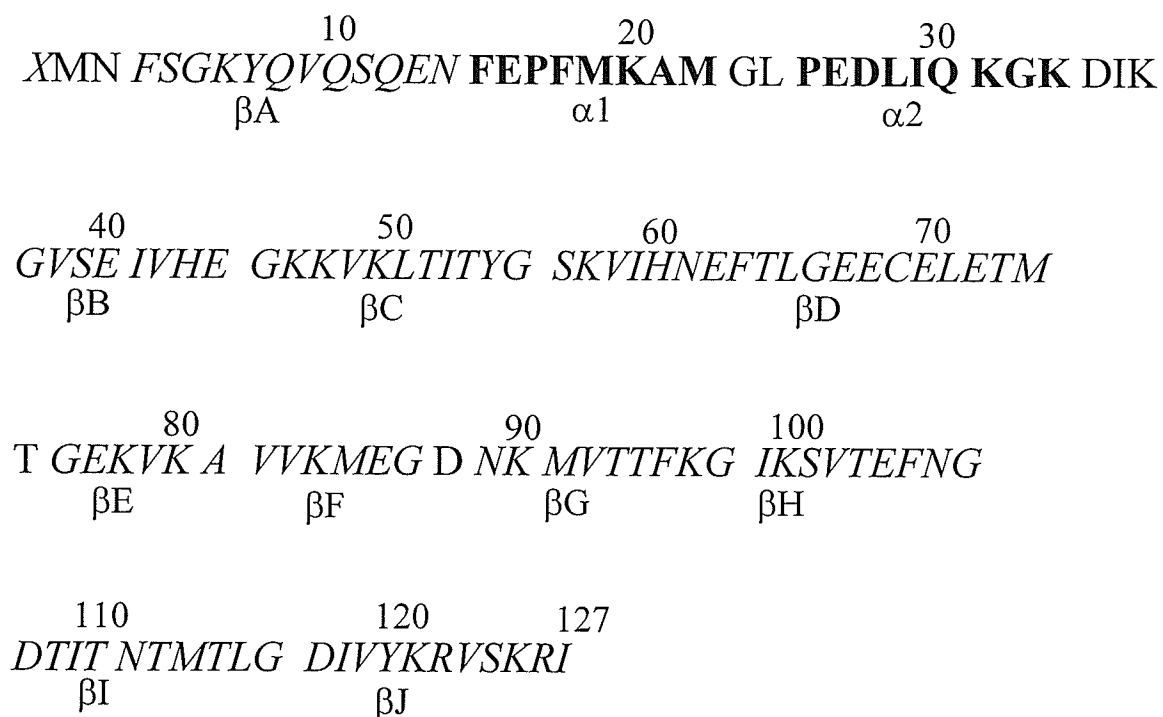
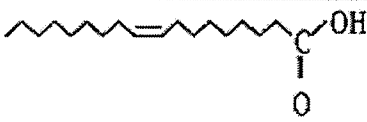

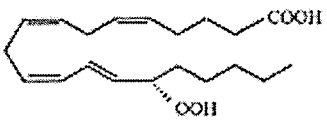
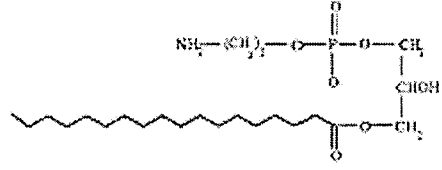
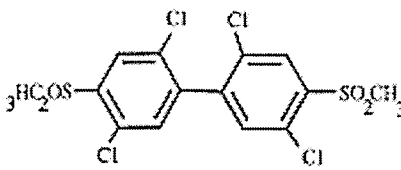
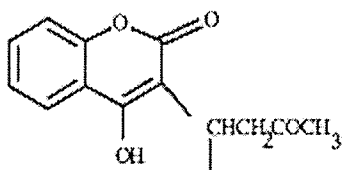
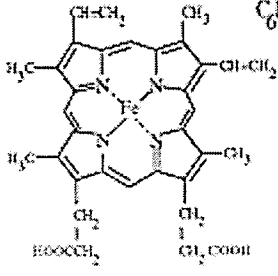


Figure 5. Amino acid sequence of rat liver FABP. The secondary structure (in Bold and Italic) determined from its crystal confirmation. One cysteine residue is located at position 69. Seven methionine residues located at positions 1, 19, 22, 74, 85, 91, and 113. *x* indicates that the N-terminal methionine residue is acetylated. This figure is modified from the Protein Data Bank (ID code 1LFO).

(Bordewick, Heese et al. 1989; Fahimi, Voelkl et al. 1990). In addition to liver, L-FABP may also be found, to a lower level, in intestine, kidney, and lung. L-FABP appears to have several different forms that result from post-translational modification, bound ligand or alternative folding pathways, but their amino acid fragments and fatty acid binding are identical (Murphy, Edmondson et al. 1999). L-FABP has 127 amino acids (Figure 5). One molecule of L-FABP contains one cysteine residue at position 69 and seven methionine residues. The cysteine residue may be involved in the binding of other hydrophobic ligands or serve as an antioxidant participating in S-thiolation/dethiolation (Thomas, Poland et al. 1995; Sato, Baba et al. 1996). Methionine residues have nucleophilic sulfur atoms and are regarded as cellular scavengers of activated xenobiotics such as carcinogens (Bassuk, Tsichlis et al. 1987). Cellular oxidative stress may also be suppressed by oxidation of methionines in liver FABP to sulfoxides, that are then reduced back by the protein methionine sulfoxide reductase (Levine, Berlett et al. 1999; Moskovitz, Berlett et al. 1999).

Unlike other members in the FABP family, L-FABP is capable of binding two molecules of fatty acid. One is in the centre of binding pocket, the other in the opposite orientation, keeps the carboxyl group on the surface of protein, near the helix-turn-helix that caps the “portal” of binding cavity (Figure 2). The primary and secondary fatty acid binding sites appear to be interdependent, because both aliphatic chains form favorable hydrophobic interaction. This binding property may directly affect interactions with ligands, enzymes, or membrane systems (Thompson, Reese-Wagoner et al. 1999) and cause an isoelectric point (pI) range of 5.2 – 6.9. L-FABP accounts for approximately 5% of the cytoplasmic proteins. This translates to an estimated cellular concentration of

Table 3. Ligand and correlative functions of L-FABP

Class	Structure	Potential Function(s)
Fatty acids (oleate)		energy storage/mobilization modulate enzyme function
Acyl-CoAs (palmitoyl CoA)		beta-oxidation
Eicosanoids (5-HPETE)		modulate enzyme function (inflammatory response) anti-oxidation
Lysophospholipids (lysophosphatidyl- ethanolamine)		Signaling
Carcinogens (methylsulfone PCB)		Detoxification
Anti-Coagulants (warfarin)		Uptake/mobilization of Warfarin
Heme		Heme catabolism

This table is modified from Coe, 1998

approximately 0.4 mM (Burnett, Lysenko et al. 1979). In addition to binding LCFA, L-FABP binds fatty acyl-CoAs, peroxisome proliferators, prostaglandins, bile acids, bilirubin, hydroxyl and hydroperoxyl metabolites of fatty acids, lysophosphatidic acids, selenium, heme, and other hydrophobic ligands. The extensive ligand binding preference appears to imply that L-FABP has distinct functional roles (Coe and Bernlohr 1998) (Table 3). Collectively, L-FABP can work as a trafficking and delivery controller of various ligands to cellular destinations such as enzymes, membranes, and the nucleus, therefore, affect enzyme function by its effects on fatty acid flux and disposition, modulate enzyme activity by changing membrane structure and fluidity, and regulate gene expression through activating nuclear receptors.

2. L-FABP gene and expression

L-FABP is the first of the family of cytoplasmic lipid binding proteins to be recognized, cloned and purified from recombinant sources. The L-FABP gene contains 3791 nucleotides, and consists of four exons and three introns (Sweetser, Lowe et al. 1986). A peroxisome proliferator response element (PPRE) is present at L-FABP promoter, which is located at nucleotides -76 to -66 (Simon, Roth et al. 1993). This element can be recognized by peroxisomal-proliferator-activated receptors (PPARs) and their similarities, such as all-*trans* retinoic acid receptor (RAR), retinoid X receptor (RXR), thyroid hormone and vitamin D3 and several orphan receptors. The specific activators of PPAR are long chain fatty acids and their metabolites, hypolipidemic drugs, and various peroxisome proliferators. PPAR is a multigene family with α , γ , and

δ isoforms. It is thought that PPAR α is involved in lipid catabolism, PPAR γ is related in lipid anabolism, PPAR δ is less well characterized in its function (Schoonjans, Staels et al. 1996). In addition to PPARs, L-FABP promoter also contains three CCAAT/enhancer binding protein alpha (C/EBP α) binding sites located at - 402 to - 385, - 356 to - 345, and - 306 to - 275 bp, and two additional hepatic nuclear factors (HNF1) binding sites (Figure 6). Transcription of L-FABP gene is regulated through these binding sites in the promoter. Unlike other FABPs, liver FABP is able to bind peroxisome proliferators, which may play a role in regulating the availability of ligands for PPARs. L-FABP and its mRNA show a declining gradient of expression from periportal to pericentral hepatocytes (Veerkamp and Maatman 1995).

The most recent research on L-FABP has focused on its cross-talk with ligand activated nuclear receptors. L-FABP is able to transport different compounds to nuclear receptors and functions as modulator of ligand activated nuclear receptor activity. PPARs and L-FABP are found in the nucleus and likely interact directly for an involvement in signal transduction (Lawrence-JW, Kroll-DJ et al. 2000; Huang, Starodub et al. 2004). Thus, L-FABP acts as a signaling pathway to nucleus for these PPAR α and PPAR γ agonists (Wolfrum, Borrmann et al. 2001). The intracellular concentration of L-FABP directly correlates with the activities of PPAR α and PPAR γ , suggesting that L-FABP is a positive regulator of PPAR expression. In the treatment of hypercholesterolemia, statins inhibit cholesterol synthesis and also decrease plasma triglyceride and non-esterified fatty acid level. L-FABP is up-regulated and involved in the statins treatment. A molecular mechanism for this induction is suggested by the fact that statins transactivate the PPAR α promoter (Landrier, Thomas et al. 2004). This

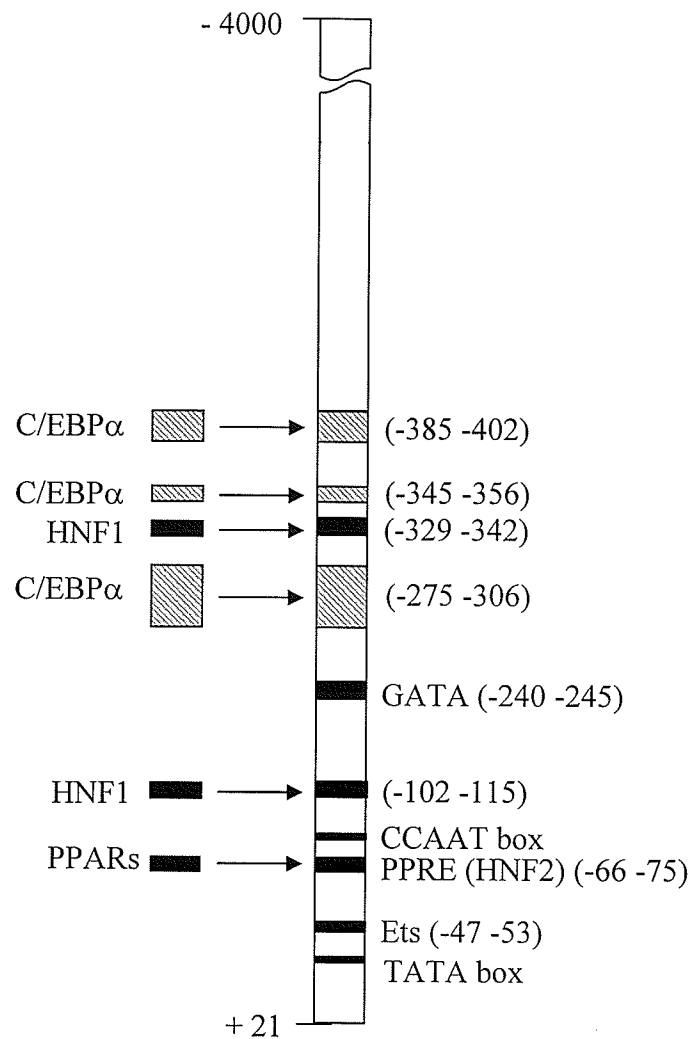


Figure 6. *Cis* – acting elements and transacting factors in the 5' flanking region of rat liver FABP. Transcription of L-FABP gene is regulated through three C/EBPα binding sites located at –402 to –385, –356 to –345, and –306 to –275 bp. Peroxisome proliferator response element (PPRE) is present at –76 to –66, which differs by one nucleotide from the hepatic nuclear factor 2 (HNF2) binding site in the other promoter. Two additional HNF1 are present. This figure is adapted from (Veerkamp and Maatman, 1995).

finding provides a molecular basis for the hypolipidemic effect of these drugs. The signal transduction pathways of L-FABP interaction with nuclear receptors could be summarized in a sequential five-step process (Figure 7): (1) L-FABP binds ligand; (2) the bound L-FABP interacts with nuclear receptor; (3) Ligand-loaded receptor binds to responsive element; (4) transactivation of nuclear receptor; (5) induction of target genes. The design of drugs affecting gene regulation usually focuses on ligand-activated receptor. However, it is worthy to call attention on to the cellular delivery system that function to transport drugs to their target sites. Therefore, L-FABP and other FABPs could serve as novel therapeutical targets that modulate nuclear receptor activity.

The L-FABP content appears to be very responsive to changes in physiological and pharmacological conditions. For example, L-FABP is known to be higher in females. The gender influence on L-FABP corresponds to the effects of steroid hormones. Testosterone decreases but estrogens increases L-FABP level (Ockner, Lysenko et al. 1980). L-FABP in rat increases from fetal day 16 up to adulthood. L-FABP mRNA level is low in prenatal rat liver, rises markedly around birth and again between 35 and 70 days (Gordon, Elshourbagy et al. 1985; Berry, Yoon et al. 1993). This is thought to be regulated by growth hormone (Berry, Yoon et al. 1993). Starvation and high fat content diets have clearly an effect on L-FABP level (Stein, Mishkin et al. 1976; Brandes and Arad 1983; Paulussen, Jansen et al. 1986). A high-carbohydrate diet also increases L-FABP content (Haq and Shrago 1985). Chronic alcohol consumption induced an increase of L-FABP dramatically in rats (Pignon, Bailey et al. 1987; Shevchuk, Baraona et al. 1991). Choline-deficient diet increased rat L-FABP three fold (Dutta-Roy, Trinh et al. 1988). Peroxisomal proliferators also have a marked effect on increasing liver FABP

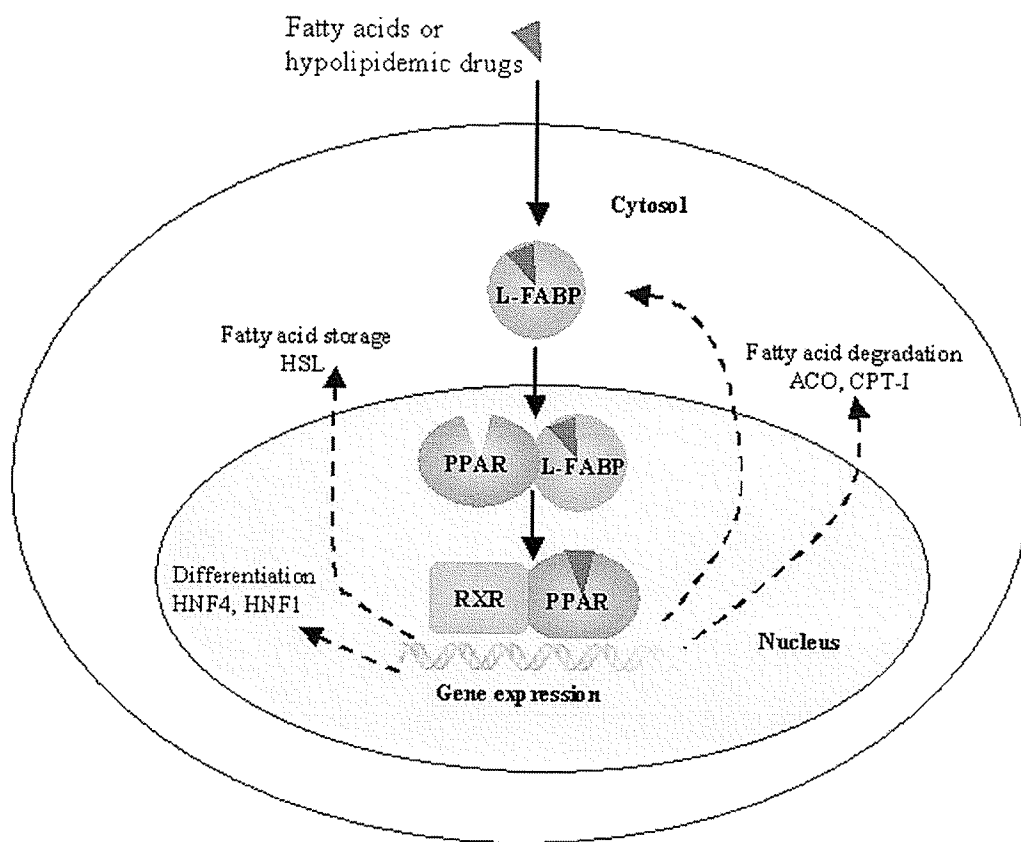


Figure 7. L-FABP and nuclear receptor activation. Ligand is transported through cytoplasm to nucleus by L-FABP. Upon entering the nucleus, the L-FABP:ligand complex binds to the receptor. The ligand activated receptor in turn regulates the expression of L-FABP as well as other genes involved in fatty acids degradation or storage and embryonic development. PPAR and RXR, nuclear receptors; ACO, acyl-CoA oxidase; CPT-I, carnitine palmitoyl transferase; HNF, hepatocyte nuclear factor; HSL, hormone-sensitive lipase.

(Kawashima, Nakagawa et al. 1983). Clofibric acid increased L-FABP content in various hormonal states of rats, indicating a common mechanism that peroxisomal proliferators enhance the transcription rate of L-FABP gene and causes a rise in L-FABP mRNA level (Nakagawa, Kawashima et al. 1994). The upregulation of L-FABP and its mRNA by peroxisomal proliferators is correlated with protein content and peroxisomal fatty acid oxidation significantly (Kawashima, Nakagawa et al. 1983). Dexamethasone is reported to down-regulate liver FABP by changes in cellular lipid metabolism (Foucaud, Niot et al. 1998). Long chain fatty acids are strong inducers of L-FABP gene expression (Meunier-Durmort, Poirier et al. 1996). The higher level of L-FABP in female rats, as well as the increased L-FABP content in male animals treated by clofibrate, is not related to differences in the turnover rate of L-FABP but appears to be correlated with an increase content of tissue L-FABP mRNA (Bass, Manning et al. 1985). Endotoxin, bacterial lipopolysaccharide downregulated L-FABP and H-FABP in rats but only L-FABP was downregulated by cytokines (Memon, Bass et al. 1999). Mostly, L-FABP content in tissue is considered to be regulated at transcriptional level, but the post-transcriptional regulation of L-FABP was found in livers of pregnant and lactating rats (Besnard, Foucaud et al. 1995).

Genetic disorder has not been reported to affect L-FABP level in human or animals. Under some pathological or experimental conditions, L-FABP in tissues was reportedly changed. Diabetes was found to markedly decrease the content of L-FABP in liver (Brandes and Arad 1983). Liver FABP was reported lower in colon cancer (Davidson, Ifkovits et al. 1993), hepatomas (Mishkin, Morris et al. 1977; Roomi, Vincent et al. 1988), but higher in human hepatoblastomas (Suzuki, Watanabe et al. 1990). In

Reye's syndrome, L-FABP in human liver was increased (Vergani, Fanin et al. 1990). Hypothyroidism decreased the level of L-FABP and hyperthyroidism caused an increase (Nakagawa, Kawashima et al. 1994). Various liver diseases (hepatitis, cirrhosis) largely decrease L-FABP content in liver, whereas their concentration in serum are higher than in normal liver (Kamisaka, Maezawa et al. 1981). The cause and consequences of changing L-FABP in tissue under pathological conditions have not been well understood.

3. Role of L-FABP in hepatic fatty acid uptake and transportation

The primary function of liver FABP is the involvement in cellular long chain fatty acid uptake and translocation. However, this does not mean L-FABP is only a vehicle for transportation. The extension of this function may include: 1) trapping, selecting, or sensing specific types of fatty acid or of lipophilic substances; 2) generating or distributing local high concentrations of unbound fatty acids; 3) directly regulating fatty acid metabolism and related reactions.

The precise molecular mechanism of fatty acid transportation across cellular membranes (uptake process) is still under investigation. Various alternative mechanisms have been proposed (Burczynski and Luxon 1995; Berk 1996; Van Nieuwenhoven, Van der Vusse et al. 1996; Zakim 1996). Long chain fatty acid movement across the cell membrane could take place (Figure 8): 1) by plasma membrane-bound FABP transporter, which "flips" the fatty acid from the extra cellular to the intracellular leaflet; 2) by simple diffusion of fatty acid through the membrane bilayer; 3) by a combination of both.

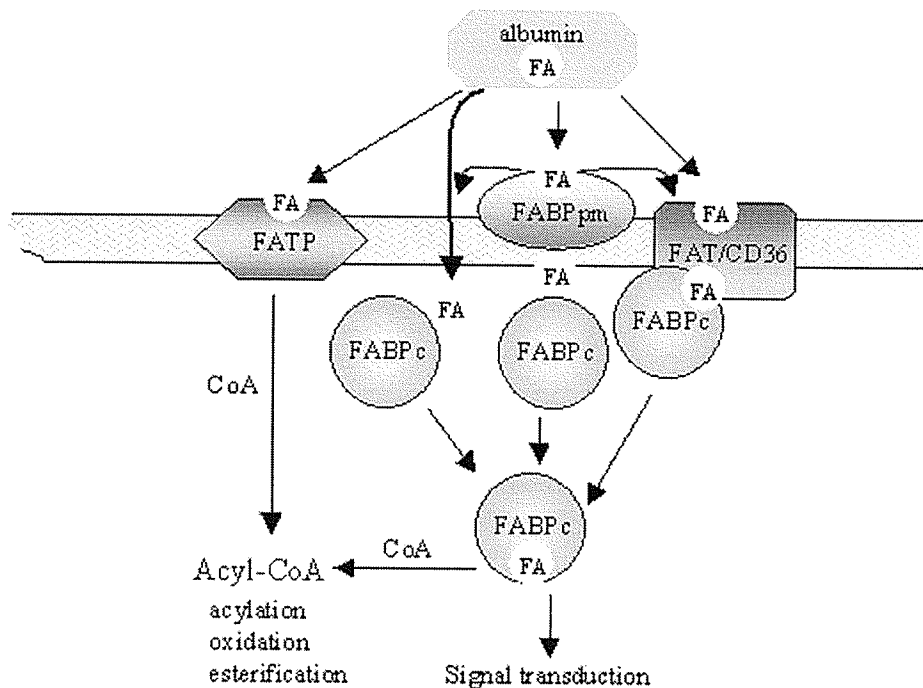


Figure 8. Schematic representation of cellular fatty acid uptake. Following the dissociation from plasma albumin, LCFA transmembrane flux takes place either by passive diffusion through the lipid bilayer and facilitated by membrane-associated proteins. FABPpm and FAT/CD36 act as fatty acid transporters. FABPc-FAT/CD36 complexes have been identified. FATP most likely is involved in fatty acyl-CoA synthesis. Intracellular LCFAs are bound by FABPc (cytosolic FABP).

Once the long chain fatty acids are located to the inner side of the cell membrane, they are translocated to the site of metabolism (or site of action) by cytosolic FABP in the protein-bound form or diffuse through the cytoplasm in unbound form. A direct interaction between cytosolic FABP and LCFAs on the inner membrane leaflet and/or membrane-associated FABP is likely to account for maintaining or facilitating the fatty acid transmembrane flux. Complexes of H-FABP-FAT and L-FABP-FAT have been identified (Spitsberg, Matitashvili et al. 1995; Wolfrum, Borrmann et al. 2001). Thus, L-FABP facilitates fatty acid transmembrane flux through a diffusion mechanism (Corsico, Liou et al. 2004). Binding to cytosolic FABP serves to increase the aqueous solubility of fatty acids in the cytoplasm. In this manner the overall transport of fatty acids through the cytoplasm is increased several-fold (Luxon 1996). Our previous work using hypophysectomized rats showed a 49% reduction in L-FABP level that was associated with a 40% decrease in hepatocyte long chain fatty acid uptake. Conversely, stimulating FABP synthesis by clofibrate treatment enhanced the level by 73%, which also resulted in an increased uptake of long chain fatty acid (Burczynski, Zhang et al. 1997; Burczynski, Fandrey et al. 1999). L-FABP was increased by almost 2-fold at 24 hours after partial hepatectomy in rats, which resulted in a 29% increase in palmitic acid clearance by hepatocytes (Wang, Chen et al. 2004). Our studies indicated that L-FABP level determines the extent of long chain fatty acid uptake from the extracellular fluid.

Molecular biological techniques provide a more precise assessment for the role of FABPs in fatty acid uptake, by specifically altering the cellular level of L-FABP. Transfection of L-FABP into fibroblasts stimulated fatty acid uptake rate and extent,

and increased the esterification of fatty acid into lipid pools (Prows, Murphy et al. 1995; Murphy, Prows et al. 1996). In the human hepatoma cell line HepG2, peroxisome proliferators increased L-FABP content and then stimulated fatty acid uptake. However, stable transfecting HepG2 cells with L-FABP antisense reduced the L-FABP level by 84% and decreased the rate of oleate uptake by 66% (Wolfrum, Buhlmann et al. 1999). Consistent with the role of L-FABP in fatty acid uptake, hepatocytes isolated from L-FABP gene knockout mice displayed significantly less oleate uptake compared with wild type mice in fed and fasted conditions (Newberry, Xie et al. 2003).

4. Role of L-FABP in hepatocytes proliferation

In many aspects L-FABP appears to represent the intracellular equivalent to serum albumin, participating in the intracellular storage and transport of fatty acids, their acyl-CoA esters, and influencing the metabolic utilization and compartmentalization of long-chain fatty acids (Bass 1988). L-FABP also may be a possible carrier of certain hydrophobic reactants in their passage from cytosol to chromatin (Wolfrum, Borchers et al. 2000) and thus have a direct or indirect effect on cell growth.

Several studies provide evidence for the notion that L-FABP is associated with hepatocyte mitotic activity and growth. First, L-FABP binds and transports many ligands that are of potential importance in the regulation of hepatocyte growth. These include the essential fatty acids such as linoleic acid and arachidonic acids (Bass 1988; Veerkamp, Peeters et al. 1991), the growth modulatory hydroxy and hydroperoxy

metabolites of arachidonic acid (i.e., HETEs and HPETEs) (Raza, Pongubala et al. 1989), prostaglandin E₁ (Dutta-Roy, Gopalswamy et al. 1987), the growth inhibitory prostaglandins (Khan and Sorof 1990), mitogenic lysophosphatidic acids (Vancura and Haldar 1992), antiproliferative and anticancer selenium (Bansal, Cook et al. 1989).

Second, increased levels of L-FABP have been reported in hepatocytes undergoing mitotic activity. Hepatocytes within the hyperplastic and malignant foci of livers in rats fed with the hepatic carcinogen N-2-fluorenylacetamide or aminoazo dyes have been reported to contain higher L-FABP levels (Sorof and Custer 1987). L-FABP also is the target protein of rat liver carcinogens, binding the genotoxic metabolites of aminoazo dyes (Ketterer, Tipping et al. 1976), N-2-fluorenylacetamide (Bassuk, Tschlis et al. 1987) (Vinores, Churey et al. 1984), as well as the nongenotoxic hepatocarcinogenic peroxisome proliferators such as the amphipathic carboxylates and tetrazole-substituted acetophenones. The latter two carcinogens require the presence of L-FABP, resulting in cell multiplication in hepatoma cells (Keler and Sorof 1993; Khan and Sorof 1994).

Third, a synergistic effect occurs between the action of L-FABP and unsaturated fatty acids (e.g. linoleic acid) in the promotion of DNA synthesis and cell growth (Keler and Sorof 1993). Normally, L-FABP serves as a specific cytoplasmic receptor of unsaturated fatty acids, particularly linoleic acid, thereby promoting the multiplication of hepatocytes. This process can be modified by peroxisome proliferators, which are supposed to displace the endogenous mitogenic ligands from L-FABP. These endogenous ligands, in turn, may activate the nuclear peroxisome proliferators-activated receptor (PPAR), or the nuclear fatty acid-activated receptor (FAAR), therefore inducing

mitogenesis. A higher level of L-FABP in hepatocytes can be elicited reversibly by unsaturated fatty acids and peroxisome proliferators. The increased L-FABP level may induce the responsiveness of hepatocytes for the same compounds.

Fourth, the level of immunostained L-FABP is markedly increased during all stages of mitosis (Sorof and Custer 1987) (Custer and Sorof 1985). In addition, L-FABP improves the efficiency of the utilization of unsaturated fatty acids in the formation, maintenance of integrity, and fluidity of cell membranes as needed for the growth, preservation of morphology, and survival of the hepatocytes (Woodford, Jefferson et al. 1993). Transfection of L-FABP cDNA into embryonic stem cells shows L-FABP altering embryonic stem cells morphology and regulating cell differentiation by acting in nucleus as well as cytoplasm (Schroeder, Atshaves et al. 2001).

Collectively these reports support the notion that L-FABP binds and transports ligands that promote hepatocyte division and also may transport certain activated chemical carcinogens. However, these reports were based on experiments conducted on animal models or hepatoma cell lines using chemical carcinogens. Whether a physical conducted model (non pharmacological) such as hepatectomy affects L-FABP mRNA expression and L-FABP levels, the time course of the increase, relationship between regeneration activity and L-FABP level, and if the hepatic fatty long chain fatty acid uptake rate is enhanced in regenerating livers following partial hepatectomy are not known. In this thesis work, I examined the mRNA expression and protein abundance of L-FABP as well as hepatocyte [^3H]-palmitic acid clearance during liver regeneration after 70% partial hepatectomy.

5. Antioxidation function of L-FABP

Many pathophysiological states are associated with notable changes in cellular lipid metabolic homeostasis, which usually result in changes in cellular FABP level. L-FABP may play a regulatory or protective role by controlling availability of free fatty acids and their metabolites (Raza, Pongubala et al. 1989; Atshaves, Storey et al. 2002), modulating the interaction of fatty acids with nuclear receptors (Huang, Starodub et al. 2004), and trapping or scavenging reactive oxygen species (ROS) (Samanta, Das et al. 1989; Catala, Cerruti et al. 1995; Ek, Cistola et al. 1997; Ek-Von Mentzer, Zhang et al. 2001).

Oxidative Stress (Figure 9) is a general term used to describe the steady state level of oxidative damage in a cell, tissue, or organ, caused by reactive oxygen species (ROS). It occurs in the following conditions: 1) an increase in oxidant generation; 2) a decrease in antioxidant protection; or 3) a failure to repair oxidative damage. ROS includes free radicals, superoxide and its anion, molecules containing oxygen atoms that can either produce free radicals or are chemically activated by them. The excess ROS can damage cellular lipid, protein or DNA, and interfere in normal cell signaling pathways. Because of these, oxidative stress has been implicated in disease states as well as in the aging process. Many liver diseases are associated with cellular oxidative stress, such as cirrhosis, hepatitis, and hepatoma (Yamamoto, Yamashita et al. 1998). Cellular oxidative stress may result from ROS being liberated during metabolic processes (e.g., metabolism of long chain fatty acid may lead to the generation of highly reactive oxygen and

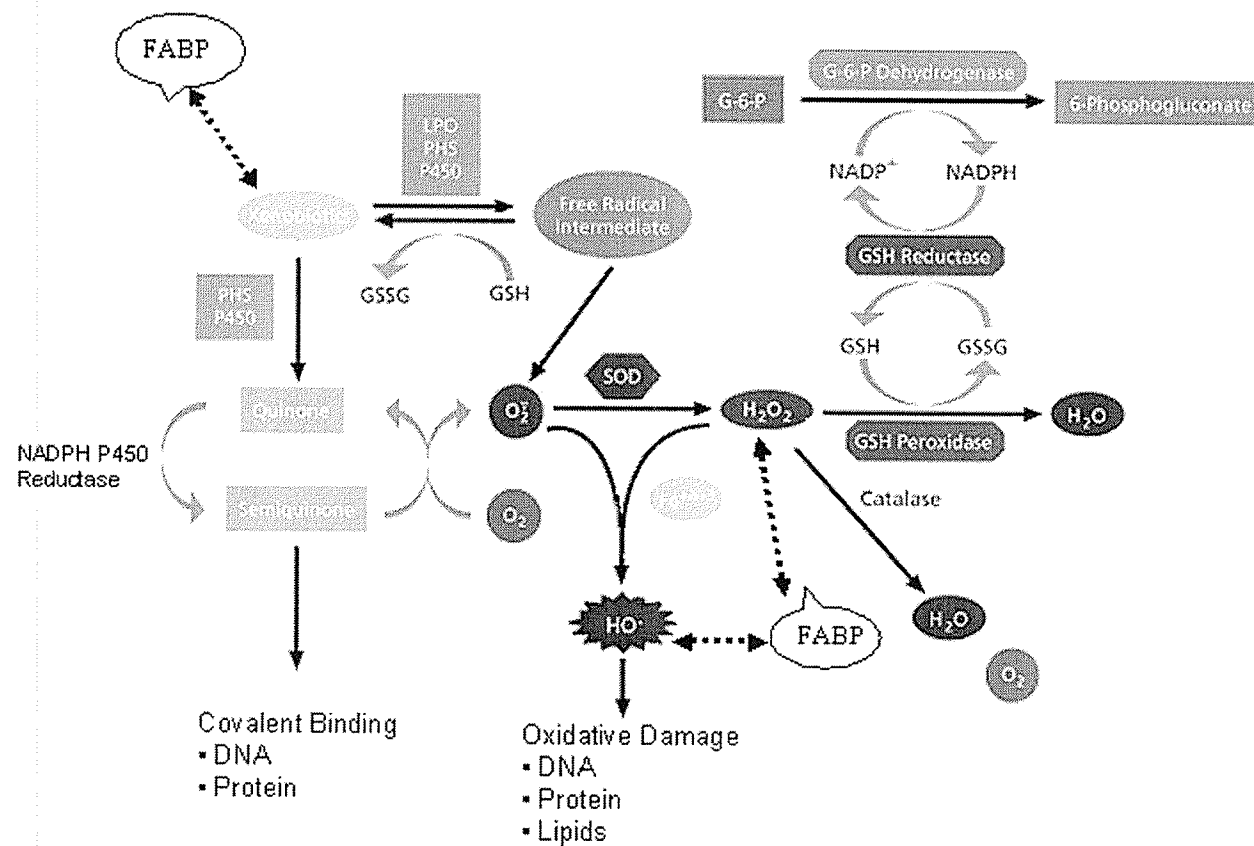


Figure 9. Oxidative stress and putative antioxidant function of L-FABP. ROS are cleared from the cell by the action of superoxide dismutase (SOD), catalase, or glutathione (GSH) peroxidase in normal condition. Prolonged exposure to ROS leads reducing enzymes depletion or inhibition. Dotted arrows represent the potential involvement of FABP in antioxidant. This figure is modified from Sigma-Aldrich pathway slide.

hydroxyl radicals) (Day and James 1998) or those derived from interrupted oxygen metabolism (hypoxia/reperfusion). As a primary defence mechanism antioxidant enzymes in cell, e.g. superoxide dismutase (SOD), catalase, and glutathione peroxidase (GPx), are present to scavenge these reactive species (Figure 9). Prolonged exposure to oxidative stress, however, may deplete the cellular antioxidant capacity (Csonka, Pataki et al. 2000). It is very likely that L-FABP plays a critical role in the defence process since it has been identified to: 1) contain a cysteine group at position 69. Proteins containing a cysteine amino acid are known to be effective antioxidant agents participating in S-thiolation/dethiolation reactions (Thomas, Poland et al. 1995) (Figure 10); 2) contain 7 methionine groups. Methionine residues have nucleophilic sulfur atoms and are regarded as cellular scavengers of activated xenobiotics such as carcinogens (Odani, Namba et al. 2000). Oxidative damage to cellular components may be suppressed by oxidation of methionines in liver FABP to sulfoxides, which can be reduced back by the protein methionine sulfoxide reductase (Levine, Berlett et al. 1999; Moskovitz, Berlett et al. 1999). Methionine sulfoxide reductase is highly expressed in liver (Moskovitz, Jenkins et al. 1996), and is considered as a regulator of cellular antioxidative defence (Moskovitz, Bar-Noy et al. 2001; Stadtman 2004). Cyclic oxidation and reduction of protein methionine residues causes a net effect of catalytic scavenging ROS, thus delineating an important mechanism of antioxidant defense in cellular regulation (Stadtman, Moskovitz et al. 2002) (Figure 11); 3) bind many lipid peroxidation products; and 4) L-FABP is highly expressed in hepatocyte (approximately 5% of cytoplasmic protein). The accessible volume enclosed by the molecular surface of L-FABP is $28,600 \text{ \AA}^3$ (Thompson, Reese-Wagoner et al. 1999). The concentration of total methionine

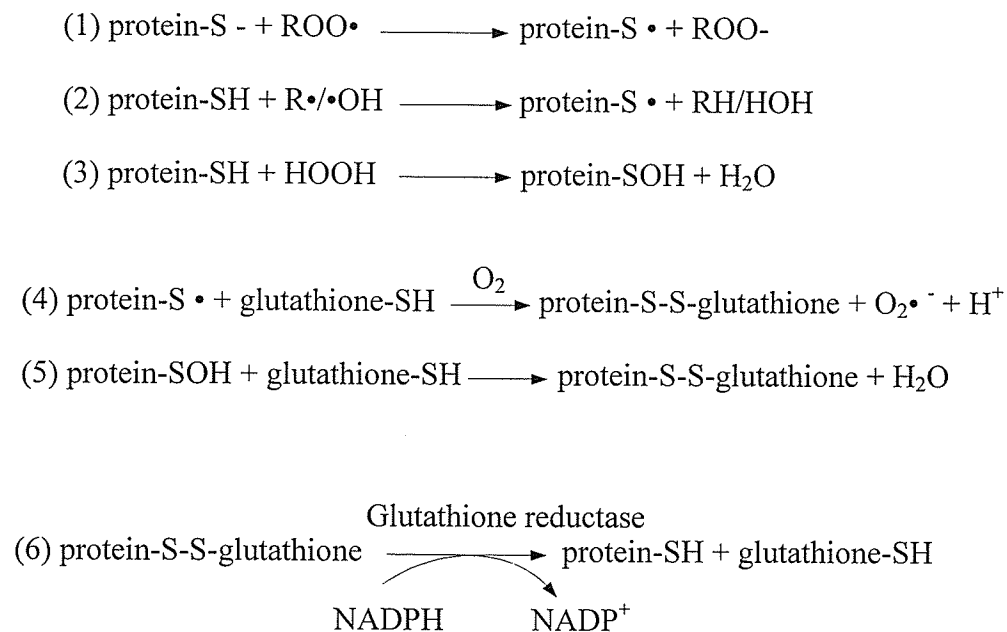
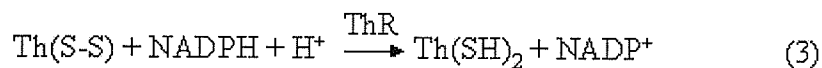
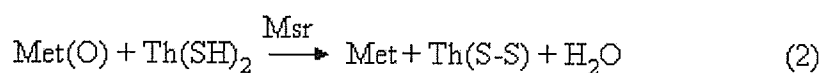
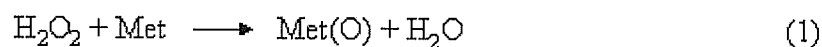
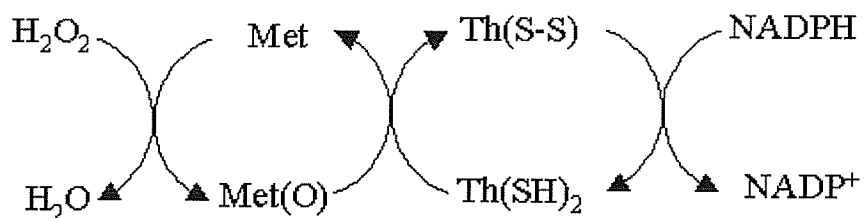


Figure 10. Protein cysteine residues participate as antioxidants by S-thiolation/dethiolation. In reaction (1), (2), and (3), oxidative species lead to rapid modification of protein sulfhydryls, producing sulfenic acids and thiyl radicals. These partially oxidized proteins are trapped in a reversible manner by formation of S-glutathiolated protein forms in reaction (4) and (5). S-glutathiolated proteins are continuously reduced by the reducing power of the glutathione cycle through glutathione reductase and small proteins like glutaredoxin and thioredoxin. If not trapped by glutathione, further oxidation can lead to irreversibly oxidized forms such as protein sulfinic and sulfonic acids.



Sum 1, 2, 3:

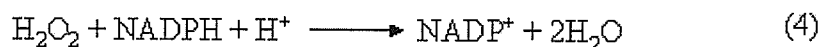


Figure 11. Cyclic oxidation and reduction of methionine residues scavenge oxidants catalytically. Methionine (Met) is readily oxidized to methionine sulfoxide [Met(O)] by many different forms of reactive oxygen species (ROS), such as hydrogen peroxide (H_2O_2), ozone, hypochlorous acid, alkyl peroxides, and peroxynitrite. In reaction 1, H_2O_2 is used to represent ROS. The oxidation of Met residues is readily reversed by catalysing thioredoxin [Th(SH)_2]-dependent reduction of Met(O) to form Met and oxidized thioredoxin [Th(S-S)] under the action of methionine sulfoxide reductase (Msr) (reaction 2). The produced Th(S-S) is readily reduced back to Th(SH)_2 by thioredoxin reductase (ThR), which uses NADPH as an electron donor (reaction 3). The overall reactions are summarized in reaction 4, which shows the cyclic oxidation and reduction of methionine residues scavenges ROS and oxidizes NADPH.

residues in L-FABP can be as high as ~ 400 mM. For these reasons L-FABP might serve as an endogenous cellular protectant, participating as a scavenger of highly reactive oxidants resulting from metabolic reactions and/or binding of products that induce cellular oxidative damage on the surface of membranes or in the cytosol (Sato, Baba et al. 1996; Palacios, Piergiacomini et al. 1999).

To date, no studies have critically examined the role of liver FABP as an endogenous antioxidant in hepatocytes. Levels of L-FABP have been reported to be in the order: pregnant females > clofibrate-treated male > female > male (Hung, Burczynski et al. 2003), possibly consistent with the greater need for cytoprotection in pregnancy. We do know that L-FABP binds metabolic oxidative products such as oxidized fatty acids (Raza, Pongubala et al. 1989; Ek-Von Mentzer, Zhang et al. 2001), and that higher lipid peroxide levels are present in some pathologic conditions. An earlier report showed that 10 μ M H-FABP was able to bind both $O_2^{\cdot -}$ and OH^{\cdot} radicals in cardiac myocytes (Samanta, Das et al. 1989; Jones, Prasad et al. 1990). 4-Hydroxynonenal, a cytotoxic aldehyde that is response to oxidative stress and aging, was inactivated by E-FABP through covalent modification of protein Cys-120 (Bennaars-Eiden, Higgins et al. 2002). Moreover, we know that some forms of liver disease, such as NASH (Non-alcoholic steatohepatitis), are associated with higher levels of fatty acids (de Almeida, Cortez-Pinto et al. 2002). The increased levels are thought to trigger lipid peroxidation products, which as a source of free radicals leads to hepatic necroinflammation or fibrosis (Day and James 1998). Thus, understanding factors that suppress levels of reactive oxygen species, such as those occurring in the liver (Fong, Nehra et al. 2000) during chemotherapy (Farrell 1995; Lieber and Abittan 1999) or chemical injury

(Albano, Gorla-Gatti et al. 1993), and those involving intracellular bacterial infections, e.g. Chlamydia (McClarty 1994), would lead to new therapeutic treatment strategies for those diseases.

To test the hypothesis that L-FABP is an endogenous cellular protectant against oxidative stress (Figure 9), I found that Chang liver cells normally do not carry the L-FABP gene and selected it as experimental model, and successfully transfected liver FABP cDNA into this cell. Using this model, I determined the cellular ROS levels of L-FABP transfected cells with different L-FABP expression levels in the oxidative stress induced by hydrogen peroxide and hypoxia/reoxygenation. The cell damage state was monitored by LDH release measurement. The positive results are reported and discussed in the following chapter.

6. L-FABP expression and antioxidation in bile-duct ligated rats

FABPs are cytoplasmic lipid binding proteins possessing the task of protecting cellular lipid homeostasis. Recent studies have indicated that several diseases have been associated with a malfunction or deficiency of cellular lipid binding proteins, such as hyperlipidemia, diabetes, and atherosclerosis. Liver disease is one of the most common diseases in the world with cholestatic liver disease being of a major concern in the North American population. A depletion of L-FABP in an animal model of steatosis has been reported (Hung, Siebert et al. 2005). However, the mechanism of cholestatic liver disease is not well understood. Several hypotheses have been proposed with one of which includes oxidative stress (Ljubuncic, Tanne et al. 2000; Aboutwerat, Pemberton et al.

2003). According to the oxidative stress hypothesis, endogenous antioxidant systems could prevent liver damage during cholestatic liver disease progression.

The experimental model used widely to study cholestatic liver disease includes the bile duct ligation model (BDL). BDL is a typical model of biliary disease in animals, which features proliferation of bile duct epithelial cells, hepatocellular necrosis and apoptosis, stellate cell activation, and eventually formation of liver fibrosis and cirrhosis (Scobie and Summerskill 1965; Kountouras, Billing et al. 1984). It has been reported that BDL is associated with decreased antioxidant activities of hepatic catalase, superoxidase (SOD) and glutathione peroxidase (GTPx) (Orellana, Rodrigo et al. 2000). Moreover, liver mitochondria antioxidative capacity and glutathione (GSH) are known to be decreased in bile-duct-ligated rats (Krahenbuhl, Talos et al. 1995). Furthermore, the detergent action and cytotoxicity of bile salts is likely to be responsible for the plasma membrane damage which leads to cellular oxidative stress. The exogenous antioxidants, vitamin E (lipophilic) and Trolox (hydrophilic), improved lipid peroxidation and oxidation of glutathione in BDL rats, but had no effect on liver injury (Baron and Muriel 1999). Therefore, it would be interesting and important to examine other endogenous anti-oxidant systems in the liver. Since L-FABP forms a large portion of the intracellular protein pool, its reducing methionines and cysteine residues, and its great binding capacity make L-FABP a potential intracellular antioxidant in liver cholestasis. Moreover, previous reports showed that short-term cholestasis (BDL) in rats impaired mitochondrial ketogenesis, and thus disturbing hepatic fatty acid metabolism (Lang, Berardi et al. 2002). It has been known that L-FABP is an important determinant of hepatic lipid composition and turnover, and contributes to cytosolic fatty acid binding

capacity, hepatic fatty acid oxidation and ketogenesis (Martin, Danneberg et al. 2003; Erol, Kumar et al. 2004). An increase in L-FABP abundance by clofibrate is related to increased fatty acid uptake (Burczynski, Fandrey et al. 1999) and fatty acid β -oxidation (Kaikaus, Chan et al. 1993). Reduction of L-FABP is likely to facilitate production and accumulation of free radicals in the mitochondria and increase the load of free radicals in the liver (Sokol, Devereaux et al. 1991). As an important protein involved in LCFA uptake and metabolism, L-FABP expression in cholestatic liver has not been documented. Therefore, in this thesis I investigated and documented the expression and antioxidative function of L-FABP in an animal model of cholestatic liver disease induced by bile duct ligation (BDL).

II. Hypotheses and Objectives

L-FABP is known to bind and transport many ligands that are deemed important in the regulation of hepatocyte growth. In this thesis, I tested the hypothesis that L-FABP is increased following partial hepatectomy, the increase enhances hepatocyte fatty acid uptake and liver regeneration; and modulating L-FABP affects liver regeneration.

The liver contains various antioxidants available to the cell. One of them that has escaped study is L-FABP. Our laboratory has uncovered an antioxidation property of L-FABP through our intracellular protein identification work using SDS electrophoresis and mass spectrometric analysis. Thus, I tested the hypothesis that L-FABP plays an endogenous antioxidant role against cellular oxidative stress; up-regulating L-FABP expression would protect hepatocyte from oxidative injury.

The objective of this study was in determining if L-FABP enhances liver regeneration and fatty acid uptake after 70% partial hepatectomy, and if L-FABP plays a role as an endogenous cytoprotectant against cellular oxidative stress. Specifically, experiments were designed to (1) determine the time course of L-FABP mRNA and L-FABP protein levels during liver regeneration following partial hepatectomy; (2) determine if the increased L-FABP expression enhances hepatocyte fatty acid uptake during liver regeneration; (3) determine if down-regulating L-FABP expression pharmacologically suppresses liver regeneration; (4) select an ideal cell line to examine if L-FABP is an effective cellular antioxidant; (5) transfect L-FABP cDNA into Chang liver cells which have undetectable L-FABP level; (6) examine the antioxidative function of L-FABP in cellular oxidative stress model induced by hydrogen peroxide and

hypoxia/reoxygenation; (7) examine the cytoprotective (antioxidation) role of L-FABP using an intact animal model of cholestatic oxidative stress - bile duct ligation (BDL).

III. Materials and methods

A. Materials

Unless specified otherwise, all chemicals were purchased from Sigma-Aldrich. All chemicals and reagents were analytical grade or high quality commercially available.

Rat L-FABP cDNA was generously provided by Dr. J.I. Gordon (Washington University, St. Louis, MO). Dulbecco's modified Eagle's medium (DMEM), pyruvate, penicillin, streptomycin, Geneticin (G-418), Fungizone, and Lipofectamine were purchased from GIBCO/BRL (Life Technology, Burlington, ON). Fetal bovine serum was purchased from Sigma (Sigma, Co., St. Louis, MO). Human hepatoma cell lines: Chang liver cell, HepG2, and PLC/PRF/5 were purchased from ATCC; Huh7 was obtained from Dr. G.Y. Minuk (University of Manitoba, Canada). The pcDNA3.1/v5-his vector was purchased from Invitrogen (Ontario, Canada). Marathon-ready human liver cDNA and Marathon PCR amplification kits were purchased from Clontech Laboratories (Palo Alto, CA). L-FABP polyclonal antibody was generated in our laboratory as described below methods.

B. Methods

1. Animal Care

Procedures were performed in accordance with guidelines specified by the University of Manitoba Animal Care Committee. Sprague-Dawley rats (body weight (BW) 200-300 g), purchased from University of Manitoba breeding stock, were housed in

a temperature-light controlled room (22 °C with lights set on a 12-hour on and 12-hour off cycle starting at 06:00 hour), and were allowed Agway Prolab Animal Diet (Agway County Foods; Syracuse, NY) and water *ad libitum*.

2. Isolation and purification of L-FABP and cytosolic proteins

L-FABP was isolated and purified according to a modification of the Murphy et al. method (Murphy, Edmondson et al. 1999) at 4 °C. Male Sprague-Dawley rat livers were minced in cold homogenisation buffer (50 mM Tris, 0.5 mM phenylmethylsulfonyl fluoride, 1 mM EDTA, 1 µg/ml leupeptin, and 1.5 µg/ml pepstatin, pH 8.0). The minced tissue was homogenized using a Tissue Tearor homogenizer in the volume of 2.5 g tissue/ml homogenisation buffer. Homogenates were centrifuged, initially for 10 min at 600 g, followed by 100 min at 25,000 g and 4 °C. The top clear supernatant, representing the cytosolic fraction, was retained and precipitated by slowly adding ammonium sulphate up to 70 % of saturation (44.2 g/100 ml supernatant) with stirring. After 60 min, the precipitated proteins were sedimented by centrifugation at 25,000 g for 100 min and the supernatant dialyzed against 10 mM Tris-HCl (pH 8.0) overnight at 1:100 volume ratio. The dialysate was concentrated by ultrafiltration using Millipore BIOMAX-5K NMWL membrane. The concentrated protein was subjected to anion exchange on AKTApurifier 10/100 (Amersham Biosciences) with a DEAE-Sepharose column (HiPrep 16/10 DEAE FF*, Amersham Biosciences). 12 mM Tris (pH 8.0) and 1 M NaCl (in 12mM Tris, pH 8.0) were used as the gradient elution buffer (at the program of 1 M NaCl content: 1) 0 % wash out 0.25 column volumes; 2) 0-20 % for 2 column volumes; 3) 20-

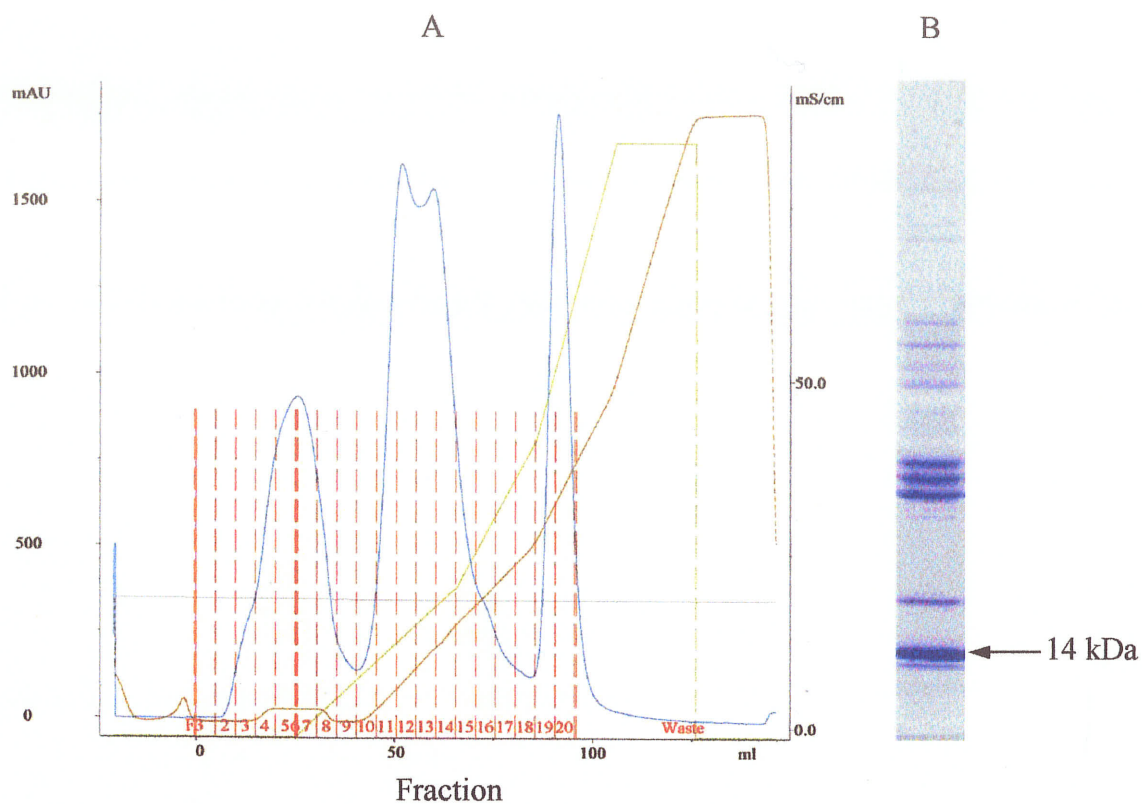


Figure 12. A, DEAE-Sepharose column chromatogram of rat liver cytosolic protein fraction by AKTApurifier. The green curve represents the concentration change of eluents. The brown curve indicates the conductance of eluents. Protein eluted from the column was monitored by the absorption at UV 280 nm (in blue). The first fraction containing L-FABP was collected for further separation using SDS-polyacrylamide gel electrophoresis. B, Proteins on the gel were visualized by Coomassie blue staining. The 14 kDa band represented L-FABP.

50 % for 1 column volume; 4) 50-100 % for 1 column volume (Figure 12A). The first fraction was collected and concentrated by ultrafiltration. This protein fraction was then separated using a Bio-Rad Protean II sodium dodecyl sulfate-polyacrylamide gel electrophoresis (SDS-PAGE) system with a 12 % polyacrylamide gel according to the manufacturer's directions. The proteins (Figure 12B) on the gel were visualized by Coomassie blue staining and used for MS analysis. The 14 kDa band represented L-FABP. To make a large amount of L-FABP, the concentrated first fraction from AKTApurifier was passed over a G-50 superfine Sephadex column (2.6 X 100 cm) equilibrated and eluted with 10 mM Tris-HCl, pH 8.0. The L-FABP fraction at 14 kDa (checked by SDS Page) was collected and multiple runs were conducted to achieve good purity.

3. In-gel Tryptic Digestion for Protein Mass Spectrometric Analysis

A modification of the procedure described by Shevchenko *et al.* (Shevchenko, Wilm et al. 1996) was used for the in-gel tryptic digestion of proteins. The SDS-PAGE-separated proteins were visualized by staining with Coomassie blue. The protein-containing band was excised and destained with 100 mM ammonium bicarbonate/acetonitrile solution. Gel pieces were dried in a SpeedVac centrifuge (Savant, Fisher Scientific, Nepean, ON). Reduction and alkylation of the proteins were performed using 10 mM dithiothreitol (DTT) and 55 mM iodoacetamide respectively (50 μ l per piece of gel). In-gel digestion used 0.02 to 0.03 μ g/ μ l of trypsin in 25 mM ammonium bicarbonate solution (~25 μ l per piece of gel). After overnight digestion at 37 °C, the proteolytic peptide products were extracted 3 times by sonicating with 0.1 %

trifluoroacetic acid (TFA) and acetonitrile (50 μ l per piece of gel). The extracts were combined and dried using a SpeedVac.

4. Protein Blotting and Protein Extraction

Immediately following gel electrophoresis (described above), the gel-separated proteins were electroblotted onto a nitrocellulose membrane, using a transfer buffer of 25 mM Tris, 192 mM glycine and 10 % methanol at a constant current of 200 mA overnight at 4 °C. The resulting protein bands were visualized by staining with amido black for 3 min, and then destained in 10 % (v/v) acetic acid solution containing 5 % (v/v) 2-propanol. The membrane was washed with several changes of deionized water, placed onto a filter paper and allowed to dry. Protein bands were cut as close as possible to the stained areas in order to minimize the background level, and stored at – 20 °C until required.

The protein-nitrocellulose band was washed twice with 100 mM ammonium bicarbonate/methanol (v/v, 1:1) to remove the amido black stain, and then dried at room temperature. The protein band was transferred to a 0.8 ml tube containing 80 μ l ethyl acetate and ~1 mg silica gel as adsorbing agent. The suspension was vortexed for 2 min to facilitate extraction. The suspension was subsequently centrifuged (Hettich Zentrifugen, Tuttlingen, Germany) at 15,000 g for 15 min, followed by removal of the liquid phase. A 10 μ l volume of 0.1 % OGP in 20 mM ammonium bicarbonate solution was added to the residue, and the suspension was vortexed to facilitate desorption of the protein from the absorbent. The resulting protein solution was diluted with 120 μ l deionized water, an additional volume of ethyl acetate (40 μ l) was added in, and the

mixture was vortexed. After centrifugation (10,000 *g* for 10 min) the mixture was observed to separate into two phases. The upper supernatant including the interface (ethyl acetate containing nitrocellulose) was carefully discarded and the lower layer (the aqueous phase containing the soluble protein) was extracted with 40 μ l ethyl acetate to remove any residual nitrocellulose. The final protein solution was collected after two further extractions with ethyl acetate, solvents were evaporated, and the residual protein was dried using a SpeedVac.

5. In-solution Proteolytic Digestion

Two different procedures were applied to digest proteins. The first method, preferable for small water-soluble proteins, required protein purification followed by digestion. The second procedure involved digestion first, followed by purification of the resulting peptides. The digestion yielded proteolytic peptides with high solubility and mobility, such that this procedure was suitable for large proteins, particularly hydrophobic proteins since their large hydrophobic interaction with the nitrocellulose was weakened.

Method 1: The extracted proteins from above procedures were digested overnight at 37 °C in 10 μ l 25 mM ammonium bicarbonate containing 0.02 μ g enzyme for trypsin, Lys-C or Glu-C digestions; for endoproteinase Asp-N digestion, 10 mM Tris-HCl buffer solution (pH 7.6) was used in place of the ammonium bicarbonate. Enzymatic reaction was terminated by freezing the solution at – 20 °C.

Method 2: The destained protein band was pre-dissolved in 80 μ l ethyl acetate (do not add silica gel in this method), and proteins were precipitated by centrifugation at

15,000 g for 15 min. Subsequently, the majority of the nitrocellulose (dissolved in the liquid phase) was removed and the protein components at the bottom were immediately placed in 10 μ l 25 mM ammonium bicarbonate solution containing 0.02 μ g trypsin and digested overnight at 37 °C. To remove the nitrocellulose completely, the resulting peptide fragments were diluted with 120 μ l deionized water and extracted twice with 40 μ l ethyl acetate by centrifugation at 10,000 g for 10 min. As in the protein extraction procedure described above, the upper organic layer (containing nitrocellulose) was carefully discarded and the lower aqueous phase containing the peptides was harvested and dried using the SpeedVac.

6. MALDI QqTOF Mass Spectrometry

In each case, peptide mapping and MS/MS sequencing were performed on the Manitoba/Sciex prototype MALDI QqTOF tandem mass spectrometer (Loboda, Krutchinsky et al. 2000) (Figure 13). A UV nitrogen laser (337 nm) irradiated the target, which was movable in both transverse dimensions under computer control. The dried sample was dissolved in 5 μ l deionized water, and 0.5 μ l of the solution was mixed in a 1:1 (v/v) ratio with 160 mg/ml DHB solution in acetone/water (v/v, 1:1) matrix. The acceleration voltage was set to 10 kV, and the m/z scale was calibrated externally with a known peptide mixture (dalargin, substance P, and melittin). Argon was used as the collision gas in the collision-induced dissociation (CID) experiments. Collision energies were adjusted between 30 and 170 eV to give optimum fragmentation of the parent ions.

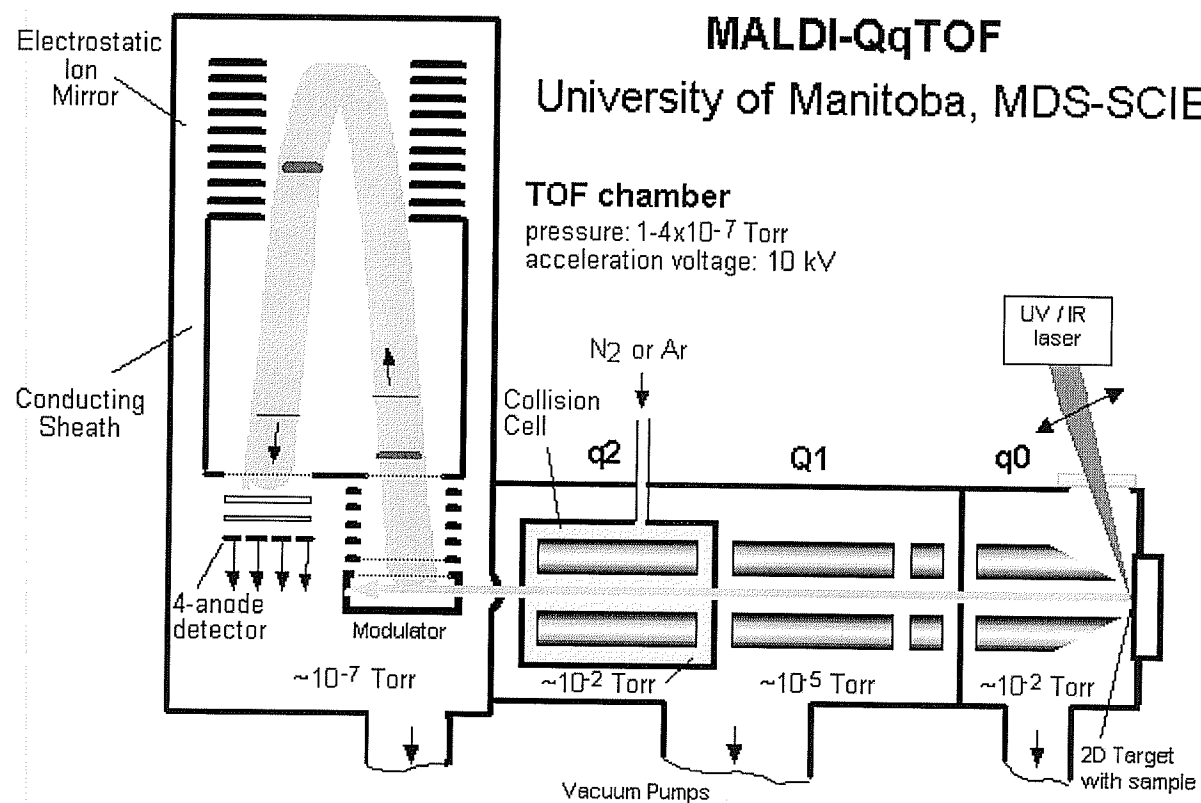


Figure 13. Diagram of the Manitoba/Sciex prototype MALDI QqTOF tandem mass spectrometer.

7. Protein MS Data Processing

Both peptide mass fingerprinting (MS Fit) and MS/MS fragment sequencing (MS-Tag) from the in-gel tryptic digests were routinely used for the internet protein database search at the UCSF web site (<http://prospector.ucsf.edu/>). The selected search parameters included the NCBI nr database with tryptic digestion and monoisotopic mass tolerance of ± 20 ppm, allowing possible post-translational modifications of S-carboxyamidated cysteines and oxidated methionines.

After protein sequence identification using the database search, masses of proteolytic peptides and their MS/MS fragmentations (b- and y- series ions) were predicted using the ProMaC 1.5.3.1 software (PE SCIEX). A comparison between the calculated masses and measured values was then carried out on those peptides observed in the MALDI MS measurements. To evaluate any abnormal peaks, the peptide sequences were carefully analyzed on their CID spectra and further validated by different enzymatic digests.

8. 70% Hepatectomy

Male Sprague-Dawley rats (250-300 g) were subjected to 70 % PHx following ether anesthesia according to the procedure of Higgins and Anderson (Higgins and Anderson 1931). Rats were divided into two groups: partial hepatectomy (PHx) group and sham operation group. Following an incision on the middle line of the abdomen, the middle and left hepatic veins were ligated, and the median and left lateral lobes were then resected (70 % PHx). Sham operation was undertaken only by laparotomy plus slight

mobilization on liver without resection. After surgery, each rat was given water *ad libitum* for 8 h, and then allowed free access to standard rat chow. Animals were sacrificed at various time points following PHx after being anesthetized with ether. The remnant liver tissue was removed, rinsed in ice-cold saline solution, flash-frozen in liquid nitrogen and, stored at -80°C until required. Dexamethasone treated animals received 2 mg dexamethasone/kg body weight/day subcutaneously for 5 days prior to PHx, while control animals received saline.

9. Bile-duct ligation (BDL) animal model

Adult male Sprague-Dawley rats were divided in three groups. The first group was sham operation where the animals underwent laparotomy without bile duct ligation. Rats in second group underwent common bile duct ligation. Briefly, animals were anesthetized using ether. Following anesthetic induction the common bile duct was exposed by median laparotomy and occluded by double ligature with a non-resorbable suture (7-0 silk). The first tie was made below the junction of the hepatic ducts and the second was made above the entrance of the pancreatic ducts. The common bile duct was then resected between the two ligatures, and the abdominal incision was closed. The third group consisted of bile duct ligation rats that received Clofibrate (50 mg/100 g body weight) for 6 days. Clofibrate was suspended in 60 % glycerol and administered by gastric gavage two weeks following bile duct ligation. Surgery control rats were administered only 60 % glycerol in the same way. Animals were sacrificed at different time as indicated in the results. Livers were removed and frozen in liquid nitrogen

immediately. Blood samples were taken from the hearts just before sacrifice. Livers and the serum samples were stored at -70 °C until required.

10. Histopathologic examination

Sections of liver tissue from sham and BDL animals were fixed in 10 % buffered formalin after sacrifice. The fixed tissues were embedded in paraffin, and then sectioned for Hematoxylin and Eosin (H&E) stain. The slides were reviewed for degree of bile duct proliferation and liver inflammation.

11. L-FABP antisera production

Generally, the immune response induced by gel slices is typically higher. L-FABP was purified by gel electrophoresis. The gel was stained lightly with Coomassie Blue. L-FABP band was excised and destained with an acetic acid wash, then washed with distilled water to remove residual stain. Lysozyme was used as the standard to estimate the amount of L-FABP protein. The gel slides were smashed in saline with a glass homogeniser manually.

Rat L-FABP anti serum was raised in New Zealand white rabbits by the intradermal injection of 250 µg of L-FABP followed by two subcutaneous injections of L-FABP (200 µg each) into the loose skin behind the neck and shoulders at biweekly intervals. A maintenance injection was followed at six weeks apart. Test bleeds of 10 to 25 ml and production bleeds of 50 ml were taken by puncture of the central ear artery with a sterile 19 or 20 gauge needle. The frequency of collection was once every two weeks. Blood was collected into a suitable tube and allowed to clot and retract at room

temperature for up to 24 hours before the serum was collected following centrifugation. The quality and titer were determined using pure L-FABP and Western Blot.

12. Western blot analysis

12.1. Protein sample preparation from tissue

Liver protein was prepared by homogenizing liver tissue (0.1 g/ml) in PBS (containing 1 % of Protease Inhibitor Cocktail, Sigma, pH 7.4) on ice using a Tissue Tearor homogenizer. After homogenisation, samples were centrifuged at 8000 g (4 °C) for 20 min. The supernatant was further centrifuged at 21,000 g for 60 min at 4 °C. The new supernatant was collected and stored at – 20 °C. The total protein amount of each sample was measured by Bradford protein assay as described in this chapter using bovine serum albumin as the standard.

12.2. Protein sample preparation from cell culture

Protein extracts were prepared from cell cultures by RIPA Buffer (50 mM Tris-HCl pH 7.4, 150 mM NaCl, 1 mM PMSF, 1 mM EDTA, 5 µg/ml Aprotinin, 5 µg/mL Leupeptin, 1 % Triton x-100, 1 % Sodium deoxycholate, 0.1 % SDS) lysis. Briefly, cell pellets (~10⁸ cells) were washed once with ice-cold PBS and incubated with 1 ml RIPA buffer on ice for 20 min, vortex 2 to 3 times. The lysate was centrifuged for 5 min at 4 °C at 20,000 g in a microfuge tube. Supernatant was transferred into a clean tube. Protein concentration was measured using the Lowry protein assay as described in this chapter. Samples were stored at – 80 °C until use.

12.3. Western blot

Proteins (20 µg) were mixed with 4X gel loading buffer (4X = 250 mmol/L Tris-HCl, pH 6.8, 8 % SDS, 20 % glycerol, 0.2 % bromophenol blue and 5 % β-mercaptoethanol), separated on 12 % sodium dodecyl sulfate-polyacrylamide (SDS-polyacrylamide) gel under reducing conditions, and transferred onto Nitroplus-2000 membrane (Micron Separations Inc. Westborough, MA). Nonspecific antibody binding was blocked by pre-incubation of the membranes in 5 % dry skim milk in 1X Tris-buffered-saline-Tween (TBS-T, 2.42 g Tris base, 29.25 g NaCl, 0.5 ml Tween 20 per liter) for 1 hour at room temperature. Membranes were then incubated with primary antibody in 1X TBS-T containing 2 % skim milk at 4 °C overnight. The titration of primary antibody was 1:2500 for rat L-FABP antiserum, 1:500 for monoclonal mouse anti-PCNA (proliferating cell nuclear antigen, an index of regenerating activity) (PC-10, Dako Corporation, California), and 1:2000 for monoclonal mouse anti-GAPDH (IMG-5019A-2, Imgenex Corp., California) respectively. Membranes were subsequently incubated with horseradish peroxidase-conjugated secondary antibody (goat anti-rabbit antibody for L-FABP, rabbit anti-mouse antibody for PCNA and GAPDH (1:5000 dilution)). The antigen-antibody complexes were detected by enhanced chemiluminescence (ECL system, Amersham). The optical density (OD) values of each target protein band were determined by using NIH Imaging software. Protein loading variation was corrected by normalization of GAPDH.

13. Northern blot analysis

13.1. RNA isolation

Total RNA was extracted from liver tissue by the phenol-chloroform-LiCl method (Itoh, Nose et al. 1979). Briefly, livers were homogenized for 1 min (full speed) on ice using a Tissue Tearor homogenizer in LiCl/Urea solution (3M/6M, 2.5 g tissue/ml). Homogenate was kept at -20°C for at least 1 hour, and then centrifuged at 3000 rpm for 10 min. The supernatant was transferred into a polyallomere tube (for SW41 Ti rotor) and further centrifuged for 20 min at 25,000 rpm at 4°C . The supernatant was removed carefully by aspiration, and the tube was dried upside down. The pellet was dissolved in 1.0 ml fresh ES solution (0.1 % SDS and 0.2 mM EDTA), and was transferred into a 5 ml tube, which contained 1.0 ml phenol and 1.0 ml chloroform. The tube was shaken for 40 shakes by hand, then centrifuged for 10 min at 3000 rpm at 4°C . The lower layer was removed, and 1 ml of chloroform was added in the same tube and vortexed for 1 minute, after centrifuging the tube for 10 min at 3000 rpm, the upper layer (aqueous phase) was transferred to a 5 ml tube which contain 125 μl 3 M NaAc (pH 5.2) and 2 ml 100 % ethanol, and kept at -70°C for at least 30 min (or overnight). This solution was centrifuged for 20 min at 13,000 rpm at 4°C . The supernatant was removed completely. The pellet was dissolved in ddH₂O. RNA concentration was determined using Bio-Rad SmartSpec 3000 Spectrophotometer.

13.2. Random Primer DNA Labelling

The detection of target RNA sequences in northern blot hybridization required a radiolabeled DNA strand (probe). One of common DNA labelling methods was to use a

random-primer labelling kit (GibcoBRL Random Primer DNA labeling system). This method required only 25 ng of DNA and 50 μCi of 3,000 Ci/mmol $[\alpha\text{-}^{32}\text{P}]\text{-dCTP}$ per reaction. This form of labelling is based on polymerization from a single strand template primed with a random six-base oligodeoxyribonucleotide. Priming and synthesis of DNA by DNA polymerase I (Klenow fragment) occurs along the entire length of the DNA fragment of interest. Twenty-five ng DNA template in 20 μl was added into a screw cap vial, denatured by heating in a boiling water bath for 10 min, and then immediately placed on ice. The denatured DNA was mixed with the reaction mixture (2 μl each of dATP, dGTP, dTTP, and 15 μl of reaction buffer, 5 μl of $[\alpha\text{-}^{32}\text{P}]\text{-dCTP}$, 1 μl of Klenow polymerase) gently but thoroughly. The reaction was carried out by incubating for 15 min at 37°C, and then stopped by adding 2 μl 0.2 M EDTA and heating to 65 °C for 10 min. The unincorporated label was removed by chromatography on a 3.5 ml column of Sephadex G-50 or G-75 (Pharmacia, DNA grade, medium) equilibrated with TE (10 mM Tris, 1mM EDTA, pH 7.5) or water.

13.3. Northern Blot

Total RNA (20 μg) was separated by gel electrophoresis using a 1% agarose gel containing formaldehyde and transferred to Hybond-Nylon membrane (Amersham, RPN 303N) using 10 x SSC (where 1 x SSC was 150 mM NaCl, 15 mM sodium citrate, pH 7.0). The RNA was crosslinked to the membrane using a GS Gene Linker UV Chamber (BIO-RAD). Membranes were then prehybridized for 10 min with hybridization buffer followed by hybridization with ^{32}P labeled rat L-FABP cDNA at 42°C overnight. Rat L-FABP cDNA was generously provided by Dr. J.I. Gordon (Washington University, St.

Louis, MO). Following hybridization, membranes were washed twice in 2 x SSC containing 0.1 % SDS at room temperature for 15 min of each and once in 0.1 x SSC containing 0.1 % SDS at 65 °C for 15 min. Membranes were then exposed to x-ray film. After stripping the ^{32}P -labeled L-FABP probe, the same membrane was hybridized with ^{32}P -labeled 28S RNA probe, which served as the loading control. X-ray films were scanned using an Umax scanner and density of the bands was quantitated using the NIH Image computer program. Relative expression of L-FABP mRNA was calculated by dividing the densities of L-FABP mRNA by the loading control (28S RNA).

14. Determination of liver regenerating activity

Hepatic regenerating activity was measured by [^3H]-thymidine incorporation into DNA and Western blot analysis of PCNA as outlined by Assy (Assy, Gong et al. 1998).

14.1. PCNA Western blot assay

PCNA determination was described in Western blot assay.

14.2. [^3H]-Thymidine incorporation

In the [^3H]-thymidine incorporation analysis, rats received 10 μCi [^3H]-thymidine / 200 g body weight (specific activity, 42 Ci/mmol; Amersham) by intraperitoneal injection one hour prior to anesthesia. Following anesthesia, livers were excised, weighed, and homogenized in 2.5 mM EDTA solution (10 % of mass/volume), pH 7.4. [^3H]-Thymidine radioactivity was determined in homogenate pellets following precipitation with 50 % trichloroacetic acid (100 $\mu\text{l/ml}$ homogenate) by liquid scintillation counting (Beckman LS6500TA). The remaining liver homogenates were

used for DNA determination with the diphenylamine reaction as described by Hashimoto (Hashimoto and Sanjo 1997). The results of [^3H]-thymidine incorporation into DNA were expressed as dpm/ μg DNA.

14.3. DNA assay

Liver homogenate (1 ml) was mixed with 2.5 ml ice-cold 10 % trichloroacetic acid (TCA) in a glass tube. The mixture was centrifuged at 3000 rpm for 10 min in a Beckman Allegra® X-12 Benchtop Centrifuge. The pellet was washed with 2.5 ml 10 % TCA, and then suspended in 4 ml 95 % ethanol. The ethanol suspension was centrifuged at 3000 rpm for 10 min, and the supernatant was removed. The precipitate was suspended in 5 ml of 3 % perchloric acid in a boiling water bath for 20 min for DNA extraction. The sample was cooled down on ice and the supernatant was collected after centrifugation. The extraction step was repeated once and the supernatants were combined for DNA assay. Calf thymus DNA was used as standard. DNA assay reagent was made by mixing 100 ml of 1 % diphenylamine (in 98 ml of glacial acetic acid plus 2 ml of sulphuric acid) and 500 μl of acetaldehyde solution (406 μl of 1.6 % acetaldehyde in 19.594 ml distilled water). 1 ml of DNA extract or standard was mixed with 2.5 ml of DNA assay reagent, and incubated at 50 °C for 3 hours. Absorbance at 600 nm was read in a Pharmacia Biotech UV spectrophotometer. DNA concentration of the sample was calculated according to DNA standard.

15. Hepatic fatty acid uptake studies

15.1. Purification of [^3H]-palmitic acid

Commercial [^3H]-palmitic acid (PerkinElmer Life and Analytical Sciences) was further purified by the ethanol extraction procedure as previously described by our lab (Elmadhoun, Wang et al. 1998). A 1 ml sample of the manufacturer-supplied [^3H]-palmitic acid in ethanol was added to 0.98 ml research quality distilled water (18 M Ω /cm) containing 0.1 ml of 1 N NaOH and \sim 0.1 mg thymol blue. To this solution heptane (1.2 ml) was added, and the mixture was vortexed for 60 sec and allowed to separate. The heptane phase was discarded, and fresh heptane added, and the procedure repeated. After two such extractions, the aqueous phase was acidified using two drops of 6 N HCl, heptane was added, and the mixture was vortexed for 60 sec. The purified palmitate contained in the heptane phase was harvested, fresh heptane was added to the acidified aqueous phase, and the procedure was repeated. The second heptane phase was combined with the first. The harvested heptane was evaporated by blowing N_2 on heptane phase. At the end, 1 ml of 100 % ethanol was added. The purified [^3H]-palmitic acid was stored in ethanol at -20°C until used.

15.2. Hepatocyte isolation

Rat hepatocytes were isolated from male Sprague-Dawley rats of sham and 24 hours post 70 % PHx groups by the *in situ* collagenase perfusion technique (Figure 14) previously described by our lab (Burczynski, Fandrey et al. 1999). Briefly, a mid-line incision was made up to sternum. Portal vein was cannulated and inferior vena cava tied

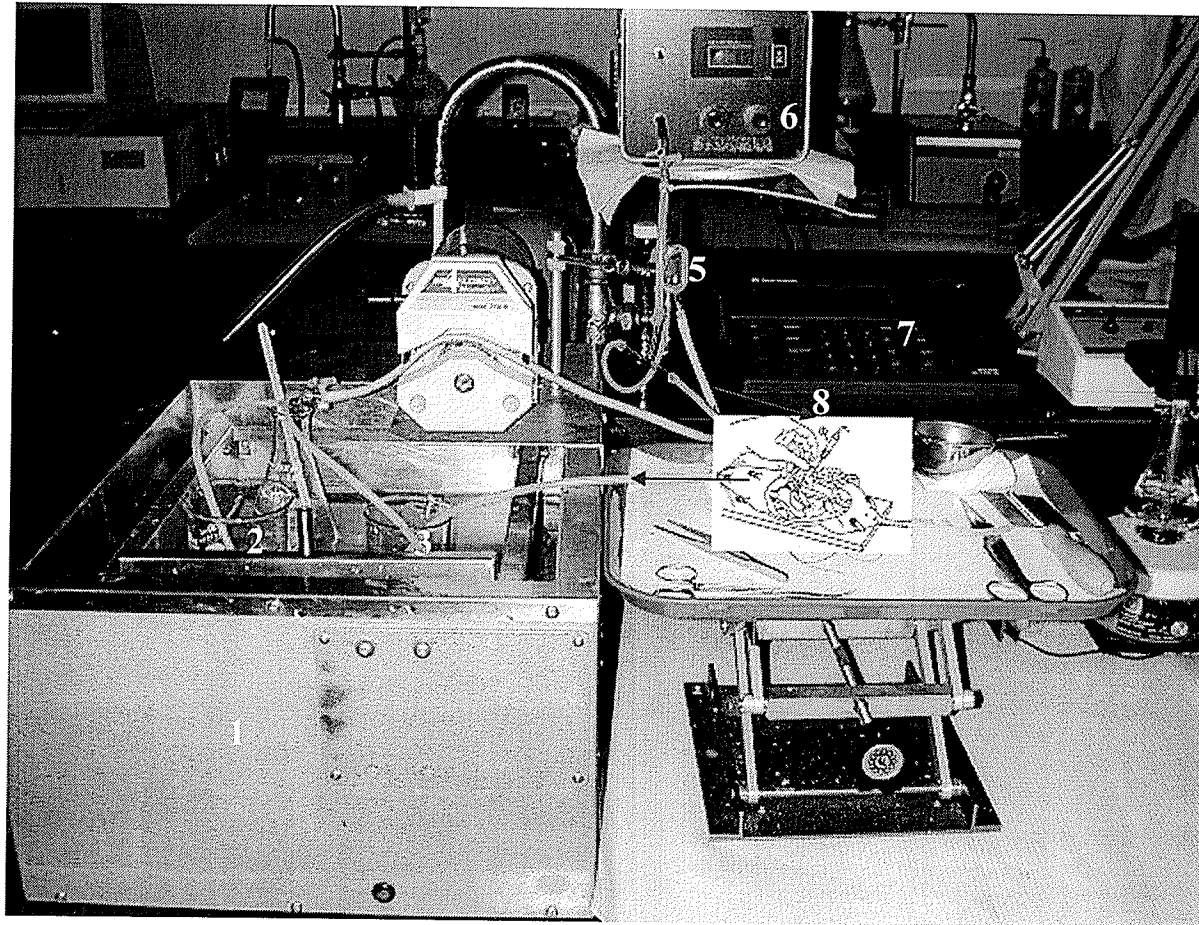


Figure 14. Experimental arrangement for in situ perfusion of rat liver. 1, water bath (37 °C); 2, Swim's *S*-77 medium containing EDTA; 3, Swim's *S*-77 medium containing collagenase; 4, pump; 5, bubble trap; 6, line pressure monitor; 7, pH meter; 8, catheter for the insertion of portal cannula. Arrows indicate the circulation of collagenase solution.

with a ligature. A cannula was inserted into thoracic vena cava and tightened with the ligature around it. Liver was perfused in situ at 20 ml/min initially with oxygenated Swim's S-77 medium containing 5 mM EDTA for 5 min and then with Swim's S-77 medium containing 40 mg/100 ml collagenase and 5 mM CaCl_2 for 1 minute. Finally, liver was recirculated with the collagenase solution for about 15 min. The pH of the collagenase solution was monitored and maintained at 7.5 by bubbling with 100 % O_2 or 95 % O_2 /5 % CO_2 . Perfused livers were excised, combed free of connective tissue, and filtered through 80-mesh followed by 150-mesh stainless-steel filters (Sigma Chemical Company). The resulting cell suspension was washed four times with D-MEM/F-12 supplemented with NaHCO_3 (1.2 g/L), penicillin G (100 U/mL), and streptomycin (100 $\mu\text{g/mL}$) by resuspension and centrifugation. Freshly isolated hepatocytes were stored at room temperature and were used for studies within 2 hours of isolation. Viability of hepatocytes was greater than 90 % before and after uptake experiments as determined by trypan blue exclusion.

15.3. Uptake Procedure

Hepatocytes (final cell density in uptake medium was 2×10^5 cells/ml) were added to solutions of PBS (composition in mM: 137 NaCl, 2.68 KCl, 1.65 KH_2PO_4 , and 8.92 Na_2HPO_4 , pH 7.4) containing 500 μM fatty acid-free albumin and purified [^3H]-palmitic acid (~ 2 nM). At specified time intervals 1.0-ml aliquots of the continuously stirred cell suspension (hand agitation) were immediately filtered through GF/C glass microfibre filters (Whatman) by vacuum and washed with 7 ml ice-cold PBS to stop uptake and remove adherent extracellular fluid. Cell-associated radioactivity was

assessed by liquid scintillation counting (Beckman LS6500TA). The final cell density resulted in total ligand depletion of less than 3 % in the uptake medium.

16. Cell culture conditions

Cells were grown in DMEM supplemented with 100 U of penicillin/ml, 100 µg of streptomycin/ml, 10 % fetal bovine serum, 1 % fungizone, and 0.011 % sodium pyruvate in a humidified, 37 °C incubator in an atmosphere of 95 % air and 5 % CO₂. Neomycin-resistant transfected Chang cells were maintained in the presence of G418 (Geneticin) at concentration of 200 mg/L.

17. Transformation of competent E. coli cells with Plasmid

Transformation was carried out by adding a maximum of 4 µl plasmid DNA solution to 100 µl of competent cells on ice for 5 to 30 min. This mixture was subjected to heat shock by immersion in a 42 °C water bath for 30 to 60 sec without shaking. Then 0.2 ml of LB (Luria-Bertani) medium (1 % tryptone, 0.5 % yeast extract, 1 % NaCl, pH 7.0) was added to the mixture and the transformation was spread on LB-agar (15 g agar/l LB) plates containing the appropriate antibiotics (50-100 µg/ml of ampicillin or 50 µg/ml kanamycin) for selection of transformed colonies. The plate was incubated at 37 °C overnight for bacteria growth.

18. Mini-preparation of Plasmid

The selected transformed colony was picked up into a 12 ml culture tube containing 1.5 or 3.0 ml of LB with appropriate antibiotics. The bacteria were incubated in a shaking

incubator overnight at 37 °C with the tube covered. The bacteria were pelleted at 600 g at 4 °C for 1 min. The pellets were resuspended in 100 µl lysis buffer (25 mM Tris-HCl pH 8.0, 10 mM EDTA-2Na, 50 mM D-glucose) and stored at 22 °C for 5 min. A 200 µl fresh prepared alkaline solution (1% SDS, 0.2 N NaOH) was added. The tubes were mixed by inverting tube rapidly three times and stored on ice for 5 min. 150 µl 3 M sodium acetate (pH 5.6) was added and the tubes were vortexed gently by inversion for 10 sec and stored on ice for 5 min. The tubes were centrifuged at 10,000 g at 4 °C for 5 min. The approximately 450 µl supernatant was transferred to an Eppendorf tube and extracted with equal amount of phenol/chloroform. The 300 µl supernatant was transferred to another Eppendorf tube and 2 volume of ethanol was added and stored at room temperature for 5 min. The DNA precipitation was pelleted at 10,000 g at room temperature for 5 min and the pellet was washed with 1 ml 70 % ethanol and centrifuged as above. The pellet was dried under vacuum and resuspended in 30 µl TE (10 mM Tris, 1 mM EDTA, pH 8.0) with 2 µg/ml RNase.

19. Large-scale Preparation of Plasmid

The bacteria were cultured in 250 ml LB overnight with shaking (for best result, the culture does not go over 12 hours). The bacteria culture was pelleted by centrifugation at 1,000 g (4 °C) for 15 min. The supernatant was removed completely. Cell pellets were resuspended in a total volume of 10 ml of ice-cold lysis buffer (25 mM Tris-HCl pH 8.0, 10 mM EDTA, 50 mM D-glucose, and 5 mg/ml lysozyme) in the 250 ml centrifuge bottles and transferred into 50 ml screw-cap Oakridge tubes on ice. The cells were incubated on ice for 15 min with occasionally gentle rolling of the tubes. Subsequently 10 ml of 0.2 N

NaOH, 0.2 % SDS solution was added to the partially lysed bacterial slurry and incubated for 15 min on ice as above, followed by the addition of 10 ml 3 M NaAc (pH 5.6). This latter addition facilitated precipitation of bacterial genomic DNA and was left on ice for 30 min. This viscous slurry was centrifuged at 40,000 *g* (4 °C) for 30 min to pellet the bacterial debris. The approximately 30 ml supernatant was transferred to a 50 ml centrifuge tube. The 0.6 volume of isopropanol was added to precipitate the remaining DNA and left at room temperature for about 1 hour or until a white precipitate was evident. This was then pelleted by centrifugation at 1,500 *g* for 10 min at room temperature. The white pellets were then desiccated and dissolved in 6 ml of sterile TE pH 8.0 (10 mM Tris-HCl pH 8.0, 1 mM EDTA). After the white pellets were dissolved in TE at 65°C completely, 6.6 g of CsCl was added into the solution and then 500 µl of 10 mg/ml ethidium bromide (EtBr) was added and gently mixed and centrifuged at 1,500 *g* for 20 min at room temperature. The supernatant was transferred to Beckman quick-seal Ti75 polyallomer centrifuge tubes via a glass Pasteur pipet. The Ti75 centrifuge tubes were filled with mineral oil, balanced and heat-sealed. Centrifugation was performed at 55,000 rpm in a Beckman Ti75 rotor at 22 °C for 16 hours.

Visualization of the lower plasmid band in the CsCl gradient was performed by fluorescence under long wavelength ultraviolet light. The centrifuge tube was penetrated with an 18-gauge needle and recovery of the plasmid band was facilitated by insertion of a 3 ml syringe fitted with an 18-gauge needle just below the plasmid band. Slowly, the plasmid band (1-1.5 ml) was drawn into the syringe and then expelled through its open end into a sterile 15 ml centrifuge tube. Approximate 10 ml isopentyl alcohol was added and the mixture was gently mixed and the upper pink organic phase discarded. This isopentyl

alcohol extraction was repeated several times until no pink colour was evident in the upper phase. Sterile water was added to make volume up to 4ml followed by 160 μ l 5 M NaCl and 2.5 volumes of cold ethanol (-20°C), agitated and placed at -20°C for at least 2 hours to precipitate DNA. The plasmid DNA was then centrifuged at 10,000 g (4°C) for 20 min, the pellet washed with 70 % EtOH, desiccated and dissolved in an appropriate volume of water and stored at 4°C . The quantity of plasmid DNA isolated was determined spectrophotometrically at 260 nm.

20. Restriction Enzyme Digestion

Purified plasmid DNA was digested with various restriction endonuclease. The incubation buffer and conditions were provided by the manufacturer. The total reaction volume consisted of plasmid DNA (0.1 to 5 mg DNA), restriction buffer, restriction endonuclease (3 to 20 units), sterile distilled water and amounted to 20 ml (larger volumes may be necessary for preparative digests or for chromosomal DNA digests). The digestion could be checked by running a small aliquot on a gel. If the DNA is to be used for another manipulation, inactivate the enzyme by heating at 70°C for 15 min, and purified by phenol/chloroform extract and ethanol precipitate, or purified on Qiagen DNA purification column.

21. Agarose Gel Electrophoresis

The fragmentation pattern of the plasmid DNA digested with restriction enzymes was analyzed by electrophoresis through horizontal agarose slab. The choice of regular agarose or low melting point agarose gel was determined by the molecular weight range of

the DNA fragments of interest. Visualization of the restriction fragmentation pattern was facilitated by the addition of EtBr to the melted agarose gel at 0.5 $\mu\text{g}/\text{ml}$ of gel solution. The banding pattern was photographed while the gel was transilluminated with long wavelength ultraviolet light. Fragment sizes were determined by plotting the distance travelled (mm) from the gel wells against the size (basepairs) of the DNA markers in the semi-log paper.

22. Subcloning of DNA fragment

22.1. DNA extraction from agarose gels

The DNA subfragment of interest was purified from agarose gels before subcloning. Approximately 50 μg of plasmid DNA was digested with the appropriate restriction enzymes at a ratio of 2 units/ μg DNA overnight in a volume of 100 μl . Long and thin wells were made in the agarose gel to facilitate loading of the large digest volume and reduce the possibility of smearing of the DNA due to overloading. The DNA on the agarose gel was cut off carefully using a scalpel blade on a UV light-box (a transilluminator) (it is good to trim off as much empty agarose as possible). The excised band was kept in a 1.5ml microfuge tube, and dissolved in 3 volumes of chaotropic agent (Qiagen) at 50 $^{\circ}\text{C}$ for 10 min. The solution was applied to a spin-column (Qiagen) and spin for 1 minute (DNA remains in the column). The column was washed by passing 70% ethanol through (DNA remains in the column, salt and impurities are washed out). Finally, the DNA was eluted in a small volume (30 μl) of water or buffer. DNA concentration was assayed by Bio-Rad Spectrophotometer.

22.2. DNA ligation and transformation

The amount of purified DNA fragment used for ligation was calculated using this formula:

$$\text{insert (ng)} = \frac{\text{length of insert (in bp)}}{\text{length of plasmid (in bp)}} \times 3 \text{ to } 6 \text{ for cDNA or } 12 \text{ for linker} \times \text{plasmid (ng)}$$

Routinely the ligation reactions consisted of 200 ng of plasmid vector digested to produce compatible ends with the fragment to be subcloned, the purified DNA fragment calculated from above formula, 1x One-Phor-All Buffer Plus (Amersham Biosciences), 0.001 M ATP, 1-6 units of T4 DNA ligase in a total volume of 20 µl. The reaction was allowed to proceed overnight at room temperature or at 16 °C. The reaction was terminated by incubation at 65 °C for 10 min. Then 4-5 µl of the ligation mixture was used to transform 100 µl of bacterial cells as described above. Five to ten white colonies (putative subclones) were picked with sterile loop to inoculate individual 1.5 ml aliquot of LB plus 200 µg/ml ampicillin or 50 mg/ml kanamycin. The subclones were grown overnight in a shaking incubator at 37 °C and plasmid DNA was isolated following the mini-prep plasmid DNA method as described above. The plasmid for insert was analysed by restriction analysis (refer to the vector map). The digested DNA was analyzed by agarose gel electrophoresis as described above.

23. Construction of mammalian expression plasmid of human L-FABP

Human L-FABP cDNA was generated by PCR using CLONTECH's Marathon-Ready cDNA kit. The primers were 5'-CTA TTG CCA CCA TGA GTT-3' (sense), encompassing nucleotides 5-23, and 5'-AAT AAT ATG AAA TGC AGA CTT G-3'

(antisense), encompassing nucleotides 401-423. The PCR product (418 bp) containing the full length L-FABP cDNA was subcloned into PCR-Blunt II-TOPO plasmid vector. The plasmid was then cut with Hind III and Xba I to generate a digested product of 530-base pair cDNA containing full length L-FABP coding region, which was then subcloned into pcDNA3.1/V5-His B mammalian expression vector (Invitrogen). The produced plasmid was referred as pcDNA-FABP.

24. Selection of Stable Transfected Chang liver cells

Chang liver cells were transfected with pcDNA-FABP plasmid and stable transfectant was selected by G418. In brief, 1×10^6 Chang liver cells in 3.5-cm culture dishes were transfected with 1 μ g of linearized pcDNA-FABP or pcDNA3.1/V5-His using Lipofectamine according to the manufacturer's instructions. Transfected cells were selected in the presence of G418 (800 μ g/ml) for 4 weeks. G418-resistant clones were then isolated with cloning cylinders and maintained in culture medium containing G418 (200 μ g/ml). Clones were analyzed individually by RT-PCR for the expression of L-FABP.

25. Reverse transcriptase polymerase-chain reaction (RT-PCR) analysis of FABP mRNA expression

Gene-specific PCR primers for human and rat L-FABP were designed with Oligo 5.1 program from the cDNA sequences obtained from GenBank. Primers were synthesized by Life Technologies (Burlington, ON, Canada). Total RNA was isolated from liver cells or liver tissues by TRIzol LS reagent (Life Technologies, Inc.). The first

strand cDNA was synthesized with CLONTECH First-cDNA RT-PCR kit. Briefly, 1 µg of total RNA was dissolved in diethylpyrocarbonated-treated doubled-distilled water (ddH₂O) to achieve a final volume of 12.5 µl. Subsequently, 1 µl oligo dT primer, 4 µl 5X reaction buffer, 1 µl 10 mmol/L dNTP mix, 0.5 µl recombinant RNase inhibitor, and 1 µl MMLV reverse transcriptase were added and incubated for 1 hour at 42 °C. At the end of the reverse-transcription procedure, the reaction mixture was heated to 94 °C for 5 min and brought up to a final volume of 100 µl with ddH₂O. Reaction products (5 µL) were used for PCR. The oligonucleotide primers of L-FABP and PCR conditions are listed in Table 4. The specific rat GAPDH control amplimers (Clontech, Cat. No. 5507-3) was used as loading control and the expected size of GAPDH was 986 base pairs. PCR amplification was carried out using Eppendoff MasterCycler (Eppendoff, Westbury, NY). PCR products were analyzed by electrophoresis in a 1.5 % agarose gel.

26. L-FABP mRNA expression assay with quantitative real-time RT-PCR

26.1. L-FABP mRNA standard curve preparation

A 215-bp fragment of L-FABP mRNA was generated by PCR using CLONTECH's Marathon-Ready cDNA kit. The primers and PCR condition were described in Table 4. The PCR product was subcloned into pCR 4-TOPO plasmid vector using TOPO TA cloning kit (Invitrogen). L-FABP positive clone was selected and amplified. The L-FABP plasmid DNA was isolated and linearized by restriction enzyme (Not I) digestion. L-FABP mRNA fragment was synthesized by *in vitro* RNA transcription with Ribprobe *in vitro* Transcription Kit (Promega). RNA concentration was

Table 4. PCR conditions and primer structures

mRNA	Human L-FABP	Human L-FABP (full length)	Rat L-FABP
cDNA reference	GenBank M10050	GenBank M10050	GenBank M35991
Upper Primer	5'-TGT CGG AAA TCG TGC AG-3'	5'-CTA TTG CCA CCA TGA GTT-3'	5'-GGA AAC CTC ATT GCC ACC A-3'
Position	155 - 172	5-23	22 - 41
Lower Primer	5'-GAT TAT GTC GCC GTT GAG TT-3'	5'-AAT AAT ATG AAA TGC AGA CTT G-3'	5'-GCC TTG TCT AAA TTC TCT TGC TGA-3'
Position	350 - 370	401-423	407 - 431
Product Length	215 base pairs	418 base pairs	409 base pairs
PCR conditions	<ul style="list-style-type: none"> • First cycle Denaturation: 94°C, 2 min • 29 cycles Denaturation: 94°C, 45 sec Annealing: 56°C, 30 sec Elongation: 72°C, 45 sec • Final extension: 72 °C, 7 min 	<ul style="list-style-type: none"> • First cycle Denaturation: 94°C, 2 min • 30 cycles Denaturation: 94°C, 45 sec Annealing: 54°C, 30 sec Elongation: 72°C, 60 sec • Final extension: 72 °C, 7 min 	<ul style="list-style-type: none"> • First cycle Denaturation: 94°C, 3 min • 30 cycles Denaturation: 94°C, 45 sec Annealing: 58°C, 30 sec Elongation: 72°C, 90 sec • Final extension: 72 °C, 10 min

assayed using Bio-Rad SmartSpec 3000 Spectrophotometer. L-FABP mRNA standard curve was constructed using logarithmic dilutions.

26.2. Quantitative real-time RT-PCR

Quantitative real-time PCR was performed in a LightCycler instrument (Roche Diagnostics) using the RNA Master SYBR Green I kit (Roche Diagnostics). Results were analyzed using the LDCA software supplied with the instrument. L-FABP mRNA fragment (215-bp) was amplified using primers as mentioned in Table 4. Each 20 μ L real time PCR reactants contained 100 ng of sample RNA or standard RNA, 3.5 mM $MnCl_2$, 0.5 μ M of each primer, and 7 μ L of the master mix supplied with the kit. The following real-time PCR protocol was employed: reverse transcription at 61 °C for 20 min; PCR reaction started at 95 °C for 30 sec; 45 cycles in four steps: 95 °C for 1 sec, 56 °C for 5 sec, 72 °C for 13 sec and 72 °C for 25 sec.

27. Inducing Oxidative Stress and DCF fluorescence assay

Reactive oxygen species produced in oxidative stress were assessed by the fluorescence intensity of DCF using a fluoro-microplate reader as modified by Wang and Joseph (Wang and Joseph 1999). Briefly, 10 mM (4.87 mg/ml) stock solution of 2,7-dichloro-fluorescein diacetate (H_2DCFDA) was prepared daily in ethanol, kept at – 20 °C, and diluted to 100 μ M with DMEM medium prior to each study. This cell-permeable compound is converted into a nonfluorescent product (H_2DCF), after intracellular deacetylation by intracellular esterases, and is rapidly oxidized to a highly fluorescent

compound dichlorofluorescein (DCF). The DCF and H₂DCF are retained more effectively in the cytosol than H₂DCFDA.

27.1. Oxidative stress induced by H₂O₂

Chang transfected cells with different L-FABP expression levels were cultured in a 96 well culture plate (Costar #3603) at a cell density of 25,000 cells per well. After 8 hours incubation in DMEM-10% FBS, cultures were washed twice with PBS and then incubated with 100 μ M H₂DCFDA in 95 % air/5 % CO₂ for 30 min at 37 °C. Extracellular H₂DCFDA was removed by washing the culture twice with warm PBS. Cellular oxidative stress was induced by incubating cells with 400 μ M H₂O₂ in PBS containing Ca⁺⁺ and Mg⁺⁺ for 20 min at 37 °C in the dark. Cellular fluorescence intensity of each well was measured and immediately recorded as described below.

27.2. Oxidative stress induced by Hypoxia- Reoxygenation

The hypoxia-reoxygenation experiments were done according to the protocol described by Hasinoff (Hasinoff 2002). The hypoxia apparatus (Figure 15) was a cylindrical plastic container that was slightly larger than a 35 mm culture dish. The container had a small hole at the center of the top and the bottom of the dish chamber through which gas was passed. The flow of gas was directed onto the top surface of liquid in the culture dish. The gas was humidified by bubbling it through water in a gas-washing tower in order to prevent evaporative loss of water from the culture dish. The whole apparatus was housed in a 37 °C incubator (Figure 15). pcDNA-FABP transfected Chang liver cells with different L-FABP expression levels were parallel seeded in 35 mm

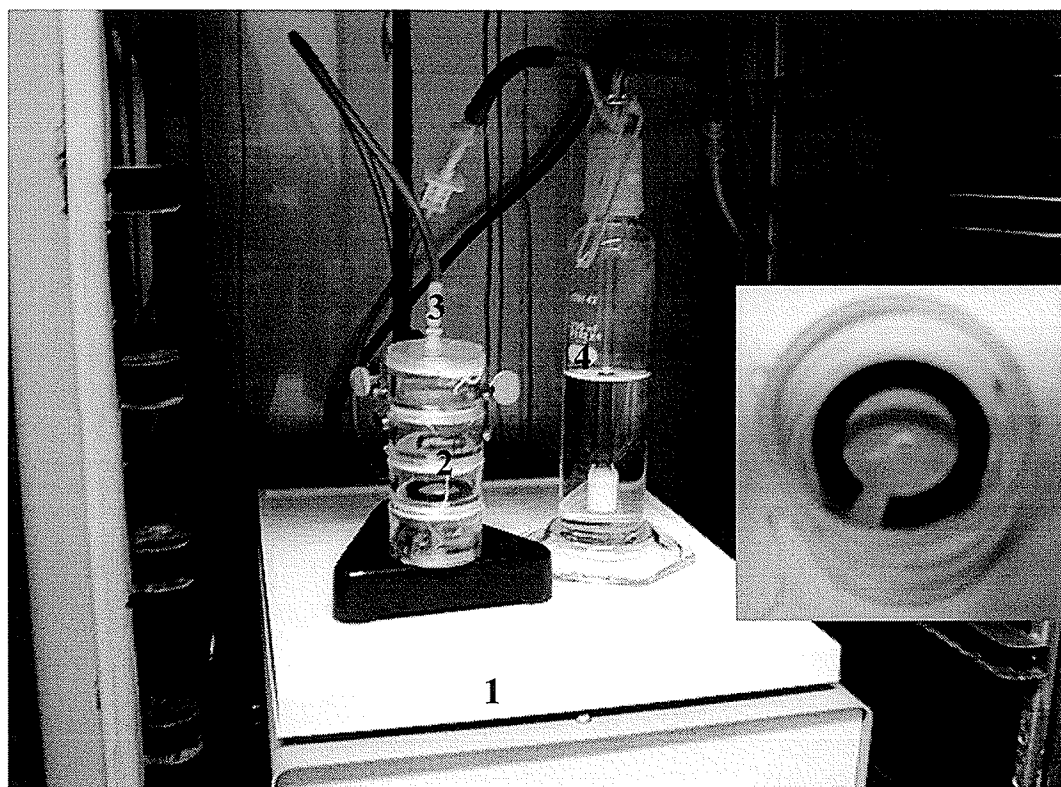


Figure 15. Hypoxia/reoxygenation apparatus. 1, shaker; 2, cylindrical plastic containers; 3, gas line; 4, gas-washing tower. The small picture shows the inside of the chamber. The hole and space ring are for gas passage.

culture dish at the cell density of one million cells per dish. After 8 hours incubation in DMEM-10 % FBS, the culture medium was replaced three times with 1 ml DMEM-0 % FBS to minimize any background LDH levels. Culture dishes were placed in the hypoxia apparatus and made hypoxic by passing 95 % N₂/5 % CO₂ over the surface of the liquid for 3 hours at a flow rate of 80 ml/min. Cells were subsequently reoxygenated with medical-grade 95 % O₂/5 % CO₂ for 3 hours at the same flow rate. To maximize gas exchange during hypoxia, the hypoxia apparatus was gently shaken at 40 rpm/min. In control studies, samples were kept in the incubator with 95 % air and 5 % CO₂ for 6 hours. At the end of hypoxia-reoxygenation, a 100- μ l sample of the supernatant was collected and centrifuged for 5 min at 500 g to remove any floating cells. Samples were kept at - 80 °C until LDH assay requirement. After the supernatant was sampled, plates were loaded with 1 ml 100 μ M H₂DCFDA for 30min in the incubator. Plates were then washed twice with PBS and the cultures were lysed with 0.5 ml DMSO for 15 min at room temperature in dark. A 200 μ l of lysate was collected for immediate DCF fluorescence assay.

27.3. DCF fluorescence measurement

H₂DCFDA-loaded cells were placed in a FLUOstar Galaxy plate reader (BMG Labtechnologies, Germany). The excitation filter was set at 485 nm and the emission was 520 nm. The temperature was maintained at 25 °C. Fluorescence in each well was captured, digitized, and stored on a computer using FLUOstar Galaxy V4.11. DMSO was tested to ensure that DMSO had no quenching effect on DCF fluorescence.

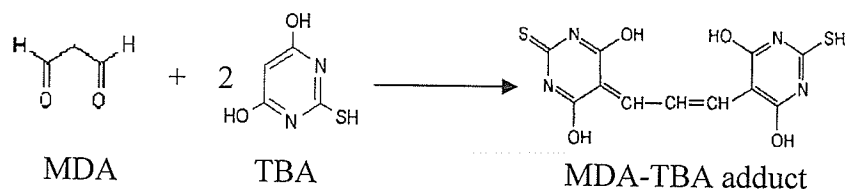
Fluorescence signals were stable for more than one hour in DMSO (Data are presented in the results section).

27.4. DCF fluorescence imaging

The DCF fluorescence images were obtained by the method described previously by our lab (Wang, Burczynski et al. 2002). Briefly, after removing the extracellular probes from the cell culture, images were acquired individually at 488 nm excitation/515 nm emission for each staining using a Nikon Diaphot inverted microscope with an Axon Integrated Imaging System (Axon Instruments Inc. CA). All images were collected at room temperature, and were pseudocolored using the same software.

28. Lipid peroxidation (TBARS) assay

Thiobarbituric acid reactive substances (TBARS) is one of the methods for screening and monitoring lipid peroxidation, a major indicator of oxidative stress (Armstrong and Browne 1994). Biological samples contain a mixture of TBARS, including lipid hydroperoxides and aldehydes, which increase as a result of oxidative stress. The assay is based on that malonaldehyde (MDA) forms a 1:2 adduct with thiobarbituric acid (TBA) and produces the following:



with a maximum absorption at 532 nm.

In this study, immediately following sacrifice, rat livers were frozen in liquid nitrogen. Livers were homogenized in PBS using a Tissue Tearor homogenizer on ice. Supernatants obtained by centrifugation at 21000 g at 4 °C were measured for total protein amount using Lowry protein assay and then subjected to lipid peroxidation assay (Chirico, Smith et al. 1993). Liver protein fraction (2 mg) was added to 1.5 ml micro centrifuge tube containing 25 µl ethanolic antioxidant butylated hydroxytoluene (BHT 2 g/liter). To the tube was added 750 µl 0.44 M H₃PO₄ and the volume of the mixture adjusted to 1000 µl with doubled-distilled water. The mixture was set aside for 10 min at room temperature, and then 250 µl TBA (6 g/l ethanol solution) added. The mixture was vortexed and heated to 100 °C for 30 min. The mixture was subsequently cooled on ice for 5 min, and then centrifuged at 1000 g for 10 min. To eliminate the hemolyzed and icteric interference or other possible chromogens from TBA-MDA adducts at wavelength 532 nm, the cooled sample was subjected to a high-performance liquid chromatography (HPLC). The TBA reaction mixture (20 µl) was injected onto an reversed-phase C-18 column (Xterra MS, 4.6 x 250 mm) with Waters 2690 alliance HPLC system (Waters Corporation, USA) and eluted with 50 % 50 mM KH₂PO₄-KOH at pH 7.0 and 50 % methanol at a flow rate of 0.75 ml/min. Absorbance was read at 532 nm with the retention time (R_T) at 5.9 min (Figure 16). An MDA standard (1,1,3,3-tetramethoxypropane; Sigma) was used to construct the standard curve. The degree of lipid peroxidation was expressed as concentration of thiobarbituric acid-reactive substances (TBARS) in terms of MDA equivalents per gram of liver protein.

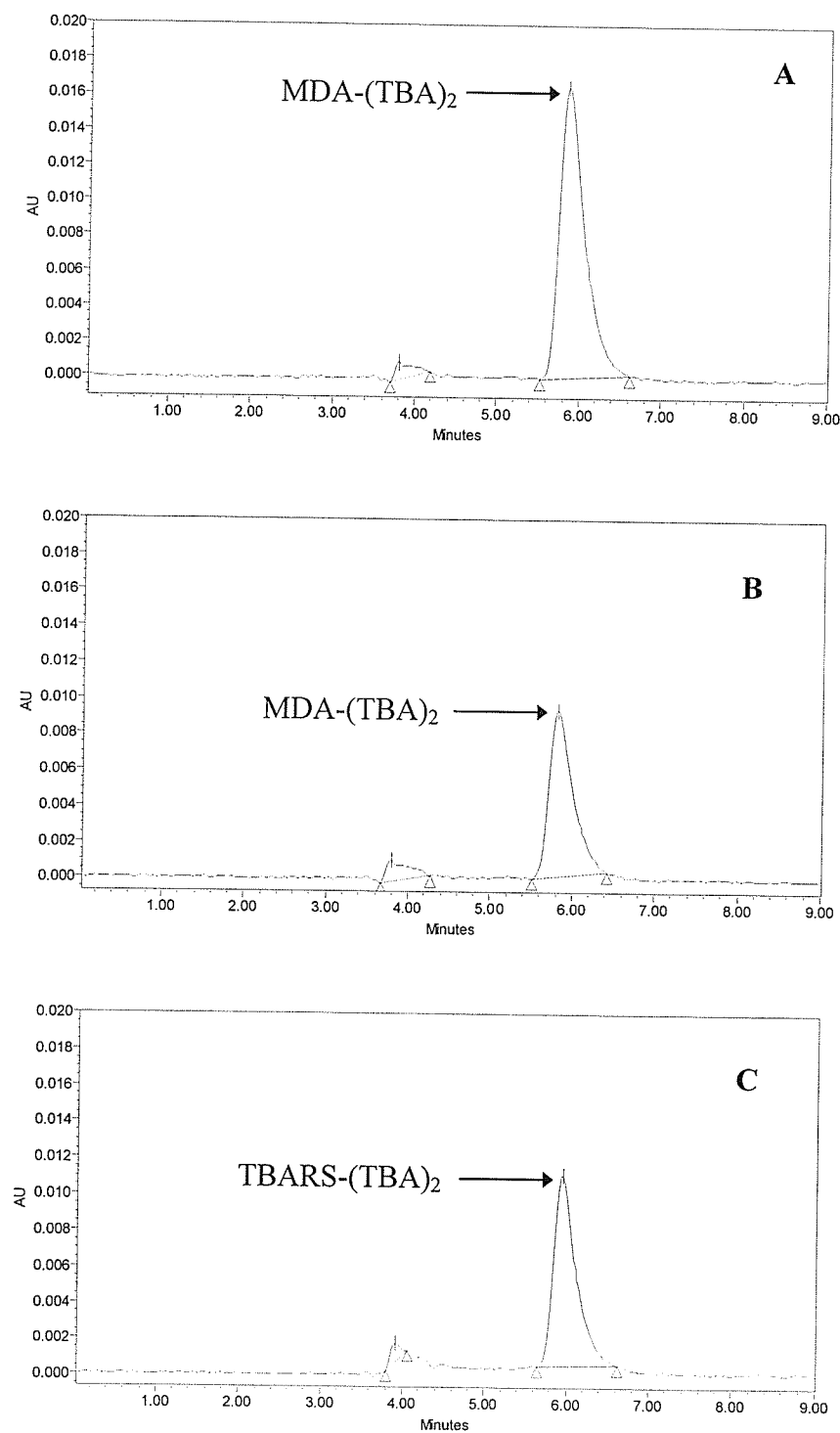


Figure 16. HPLC chromatograms of MDA-(TBA)₂ and TBARS-(TBA)₂ complex prepared from standard MDA and liver samples of BDL rats. A, Standard (0.4 $\mu\text{g/ml}$), R_T 5.86 min; B, Standard (0.2 $\mu\text{g/ml}$), R_T 5.82 min; C, Sample, R_T 5.95 min.

29. Biochemical Assay

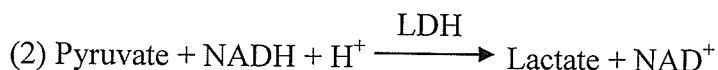
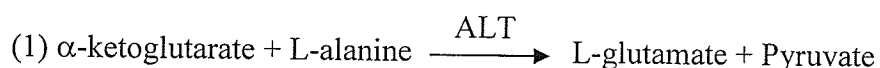
29.1. Serum collection

Blood was collected from the experimental animals, and transferred into a blood collection tube (contains serum separating gel barrier, no preservatives). Blood was allowed to clot for 30 min in an upright position followed by centrifugation at 2200-2500 rpm for 15 min. The stopper was kept during centrifugation. The clear serum was transferred to a labeled plastic vial and stored at -80°C until assayed within 3 months.

29.2. Alanine aminotransferase (ALT) assay

Elevated serum alanine aminotransferase (ALT) levels is commonly taken as an indicator of liver disease. In cases of hepatic necrosis, elevations of ALT levels occur prior to the onset of clinical symptoms such as jaundice.

ALT levels were determined by spectrophotometer analysis (Bergmeyer and Horder 1980). This assay is based on the following enzyme catalyzed reaction:



The ALT catalyzes the conversion of L-alanine and α -ketoglutarate to pyruvate and L-glutamate. In reaction (2), LDH catalyzes the oxidation of NADH to NAD. The rate of decrease in absorbance of the reaction mixture at 340nm is directly proportional to the ALT activity.

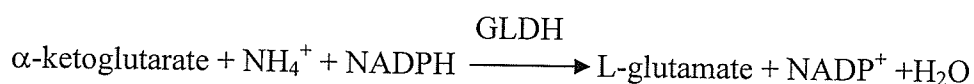
All solutions used for this assay were made fresh on the day of the assay. The working reagent was made by mixing 4 parts of the enzyme reagent (500 mM L-alanine and >1200 U/L LDH in 50 mM Tris buffer, pH 7.5 at 25 °C) with 1 part of the substrate reagent (15 mM 2-oxoglutarate and 0.18 mM NADH). The working reagent was equilibrated to 25 °C in a water bath prior to use. Serum (50 µl) was added to a quartz cuvette at 25 °C that contained 1000 µl of the working reagent in a Cary Win UV spectrometer. Solution was mixed and incubated for 1 min. Absorbance was recorded until the absorbance change was constant. ALT activity was expressed as units per liter (U/L) and calculated by the following equation using 6.22 as the absorbance coefficient of NADH at 340 nm:

$$\text{ALT U/L} = \frac{\Delta A/\text{min} \times \text{assay volume (ml)} \times 1000}{6.22 \times \text{light path (cm)} \times \text{sample volume (ml)}}$$

$\Delta A/\text{min}$ = change in absorbance per minute

29.3. Ammonia assay

In normal physiology, circulating ammonia is relatively low, despite the fact that ammonia is continuously produced from food and amino acid metabolism. Blood ammonia elevation is commonly associated with hepatic dysfunction. Ammonia determination is very useful in the diagnosis and prognosis of liver disease. The enzymatic method for serum ammonia assay is based on the following reaction:



Ammonia reacts with α -ketoglutarate and reduced nicotinamide adenine dinucleotide phosphate (NADPH) to form L-glutamate and NADP. This reaction is catalyzed by glutamate dehydrogenase (GLDH). The decrease in absorbance at 340nm due to the oxidation of NADPH is proportional to the ammonia concentration (Ratcliff 1982).

Ammonia Reagent (2.2 mM ADP, 3.5 mM α -ketoglutarate and 0.2 mM NADPH), Ammonia Standard (an aqueous solution of ammonium sulfate containing ammonia 294 $\mu\text{mol/L}$) and Ammonia GLDH Reagent (1200U/mL GLDH) were purchased from Diagnostic Chemicals Limited (Charlottetown, P.E.I., Canada, Catalog No. 200-02).

All solutions were reconstituted with deionized water on the day of the assay. 3.0 ml of reagent and 200 μl of deionized water (blank), ammonia standard, or sample were added into an ammonia free test tube. The mixture was incubated for 1 minute at room temperature. Initial absorbances of the blank (A_b), standard (A_s) and samples (A_p) at 340 nm vs. deionized water were recorded. Then, 200 μl of GLDH reagent was added to each test tube. The mixture was incubated for an additional 6 min. The final absorbance of the solutions at 340 nm vs. deionized water was recorded.

Ammonia was calculated by the equation below and expressed as $\mu\text{mol/L}$.

$$\text{Ammonia } (\mu\text{mol/L}) = \frac{(\Delta A_p - \Delta A_b)}{(\Delta A_s - \Delta A_b)} \times 294 \text{ (concentration of the standard, } \mu\text{mol/L)}$$

ΔA_b = initial blank absorbance – final blank absorbance

ΔA_p = initial plasma absorbance – final sample absorbance

ΔA_s =initial standard absorbance – final standard absorbance

29.4. *Lactate dehydrogenase (LDH) assay*

LDH is a cytosolic enzyme present within all mammalian cells. The normal plasma membrane is impermeable to LDH. When cell membranes become damaged, membrane permeability changes and results in subsequent leakage of LDH into the extracellular fluid. Release of LDH into culture supernatant correlates with cell membrane integrity and cell viability. LDH activity was measured spectrophotometrically based on the following reaction (Bergmeyer 1974):



All solutions used for this assay were made fresh on the day of the assay. The substrate for lactate dehydrogenase reaction was made by mixing 10 % (v/v) of 2.5 mM NADH and 10 % (v/v) of 25 mM pyruvate in a Tris-KCl buffer (50/150 mM, pH 7.40) and equilibrated to 25 °C in a water bath prior to use. Quadruplicate 20 µl aliquots of the culture supernatants collected from hypoxia-reoxygenation sample (containing LDH) were added to a quartz cuvette at 25 °C that contained 800 µl of the substrate solution in a Cary Win UV spectrometer. The change in absorbance at 340 nm is directly proportional to LDH activity in the supernatant samples.

29.5. Total bilirubin determination

Serum bilirubin determination is commonly used as a test for hepatic function. Hepatocellular dysfunction or biliary tract obstruction results in an elevation of bilirubin concentration. The colorimetric determination of total bilirubin in serum is based on reaction of total bilirubin with diazotized sulfanillic acid in the presence of DMSO to give azobilirubin (Figure 17).

Total bilirubin reagent (0.1 % Sulfanillic acid and 50 % DMSO in 0.2 M HCl), sodium nitrite solution (0.07 M), and bilirubin standard (5.1 mg/dL) were purchased from Sigma. Total bilirubin assay solution was prepared by mixing 30 ml total bilirubin reagent with sodium nitrite solution. For each sample and standard, two test tubes were labelled as Test and Blank. Total bilirubin reagent (2.5 ml) was added to Blank and 2.5 ml total bilirubin assay solution was added to Test. To specimen Test and specimen Blank, 0.1 ml specimen was added respectively. Into standard Test and standard Blank, 0.1 ml standard was added respectively. Tubes were mixed thoroughly and then incubated at 30 °C for 5 min in water bath. After transferred to cuvetts, the absorbance at 560 nm vs water was recorded. Total bilirubin was calculated by:

$$\text{Total bilirubin (mg/dL)} = \frac{\Delta A_{\text{specimen}}}{\Delta A_{\text{standard}}} \times 5.1 \text{ (bilirubin standard, mg/dL)}$$

$$\Delta A = \text{Test A} - \text{Blank A}$$

29.6. Lowry protein assay

The Lowry method (Lowry, Rosebrough et al. 1951) is one of the most venerable and commonly used protein assays, which is based on the reaction of protein with the

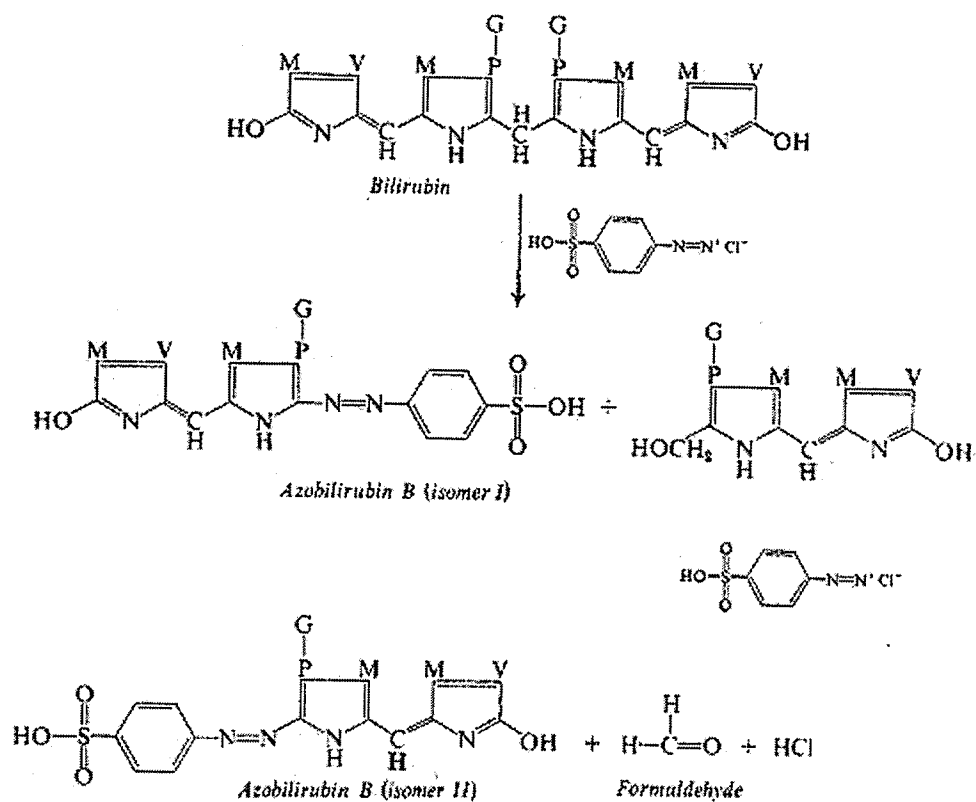


Figure 17. Formation of isomers I and II of azobilirubin B through the reaction of bilirubin glucuronide with diazotized sulfanilic acids. Unconjugated bilirubin (deglucuronided) reacts in the same way, resulting in isomers I and II of azobilirubin A. M represents methyl $-\text{CH}_3$; V vinyl $-\text{CH}=\text{CH}_2$; P propionate $-\text{CH}_2\text{CH}_2\text{COO}^-$; G glucuronate.

copper(II) ions under alkaline conditions and the subsequent reduction of folin phenol reagent (phospho-molybdic-phosphotungstic reagent) by the copper-catalyzed oxidation of aromatic acids. Color of the reaction system is changed to blue from yellow (Figure 18). The Lowry method is sensitive to low concentrations, ranging from 0.01 to - 0.3 mg of protein per ml. A wide variety of chemicals, however, interfere with this method. These include some organic buffers, detergents, salts and sulphydryl reagents. These substances should be removed or diluted before running the assay. The ideal standard should be similar to the unknown.

Stock solutions in the Lowry assay included: A (2 % Na_2CO_3 in 0.1 M NaOH), B (1 % CuSO_4), and C (2 % $\text{NaKC}_4\text{H}_4\text{O}_6 \cdot 4\text{H}_2\text{O}$). Lowry assay solution was made by mixing stock solution A, B, and C in the ratio of 100:1:1 on a daily basis. Phenol reagent was made by mixing 1 part Folin-Phenol [2 N] with 1 part water before use. Bovine serum albumin (BSA) was used as standard. Sample (100 μl) was added to each test tube that contains 1.0 ml of the Lowry assay solution. The mixture was incubated for 15 min at room temperature. Then, 100 μl of Phenol reagent was added to each tube, mixed by vortex and incubated for 30 min. Absorbance was determined in a spectrophotometer at 650 nm. Protein concentration was calculated from similarly prepared BSA standard curve. All determinations were done in duplicate.

29.7. Bradford protein assay

Bradford assay is an easy and accurate alternative, which is based on the binding of protein to Coomassie Blue G-250 dye (Bradford 1976) (Figure 19). The increase in absorbance at 595 nm is proportional to the amount of protein bound over a range of 0.1 -

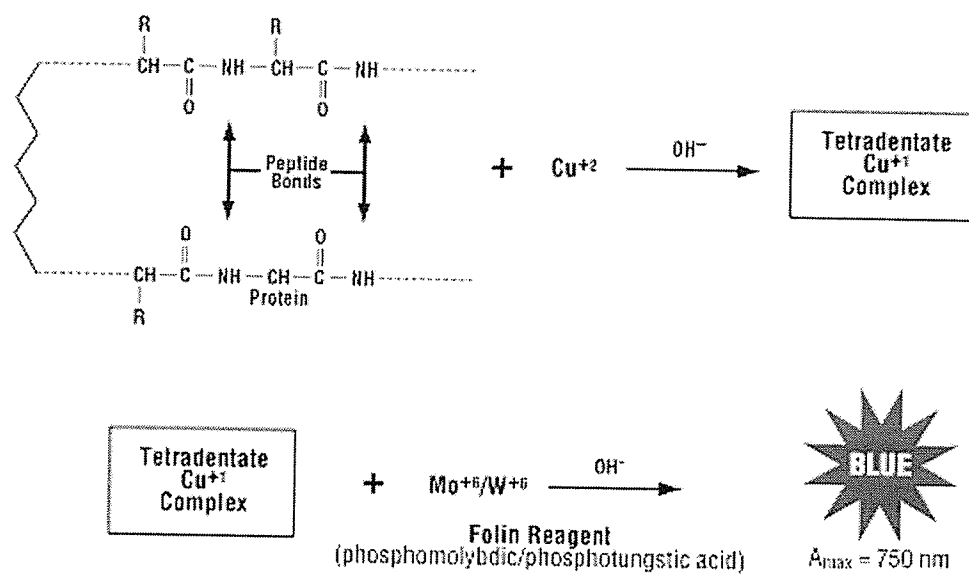


Figure 18. Reaction scheme for the Lowry Protein Assay.

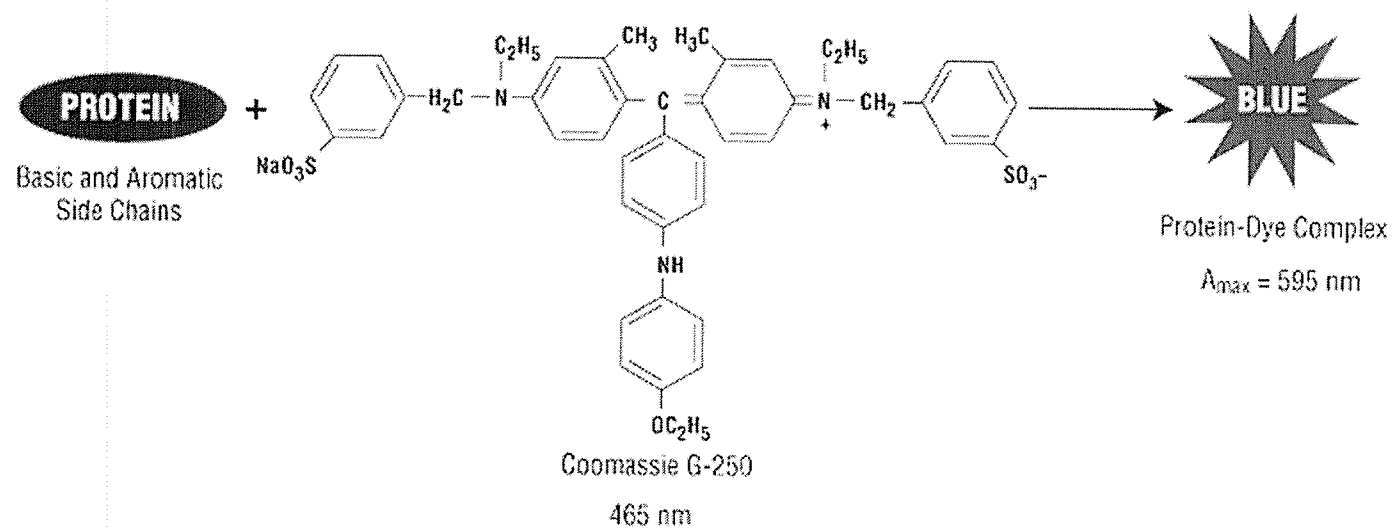


Figure 19. Reaction scheme for the Bradford protein assay (Coomassie dye based protein assays).

100 µg protein. Unlike many other assays, including the Lowry assay, the Bradford assay is not susceptible to interference by a wide variety of chemicals present in samples. Exceptionally, detergents interfere in this assay. The protein-to-protein variation in absorbance should be considered in choosing protein standard.

Bradford reagent was made by dissolving 100 mg Coomassie Blue G-250 in 50 ml 95 % ethanol, adding 100 ml 85 % (w/v) phosphoric acid to this solution and diluting the mixture to 1 liter with water. BSA (1 mg/ml) was used as standard. 100 µl of sample and 5 ml of Bradford reagent were added to a test tube. The mixture was incubated for 5 min. Absorbance at 595 nm was recorded in a spectrophotometer. Protein concentrations were obtained by comparing sample to similarly prepared BSA standard curve. All determinations were done in duplicate.

30. Statistical analysis

Results are expressed as mean \pm SEM. Appropriate statistical analysis included Students' t-test (paired and unpaired) where two groups are to be compared. Two way or one way analysis of variance (ANOVA) was used for multiple comparisons. Statistical significance differences were considered when $p < 0.05$. The n value refers to the number of animals used or number of experimental assays in each study.

IV. Results and Discussions

Section A. Identification and sequencing of rat liver FABP and other cytosolic proteins by mass spectrometry following electrophoretic separation and extraction

Introduction

In-gel proteolytic digestion is a well-established and sensitive approach for protein identification. The following procedures involve extraction of the resulting peptides from the gel, purification, mass spectrometric (MS) measurement, and search of a database for the protein capable of giving rise to the observed proteolytic fragments (peptide mass mapping) (Patterson and Aebersold 1995; Shevchenko, Wilm et al. 1996). MALDI-QqTOF (Matrix-assisted Laser Desorption/Ionization-quadrupole time-of-flight) mass spectrometer is one of the most efficient techniques recently developed, in which both MS and MS/MS measurements on a series of samples can be carried out without changing the target assembly, thus obtaining a high throughput (Shevchenko, Loboda et al. 2000). The instrument has a mass resolving power $\sim 10,000$ and mass accuracy better than 10 ppm.

The combined method of in-gel digestion with mass spectrometry has, however, some inherent problems, such as low digestion and extraction efficiency from gel, and the requirement of a large protein sample. This is especially true for smaller proteins or peptides (< 10 kDa). Thus, no enough information could be provided for analyzing amino acid sequence (mutations and post-translational modifications).

An alternative to in-gel digestion is elution of the entire protein from the gel, which normally requires at least picomoles of material, but has the advantage that the mass of proteolytic fragments and whole protein can be determined (Fridriksson, Baird et al. 1999) (Cohen and Chait 1997). The technique involves: recovering intact gel-separated proteins by direct electroelution (Fridriksson, Baird et al. 1999; Timperman and Aebersold 2000), passive solvent extraction (e.g. with a solution of formic acid/water/2-propanol (Cohen and Chait 1997), and transferring protein from gel to a nitrocellulose membrane (Anderson 1985; Aebersold, Leavitt et al. 1987; Jespersen, Talbo et al. 1993; Lui, Tempst et al. 1996) or PVDF (Wong 1992). Mass measurement of the intact protein may be followed by in-solution or on-membrane proteolytic digestion that increases the sequence coverage. In this study, we developed a new technique that uses a two-phase extraction strategy (ethyl acetate/ammonium bicarbonate) for the efficient extraction of proteins/peptides from an electrophoretic nitrocellulose membrane, and subsequent sequence analysis by MALDI-QqTOF mass spectrometry. This technique was tested using rat liver cytosolic fraction proteins.

Results

The procedures used in the proteomics of rat liver cytosolic fraction proteins are summarized in Figure 20.

Identification of Rat Liver Proteins by In-gel Digestion

Figure 21 shows proteins from the rat hepatocyte cytosolic fraction separated on a SDS-PAGE gel and visualized by staining with Coomassie blue. Peptides produced by

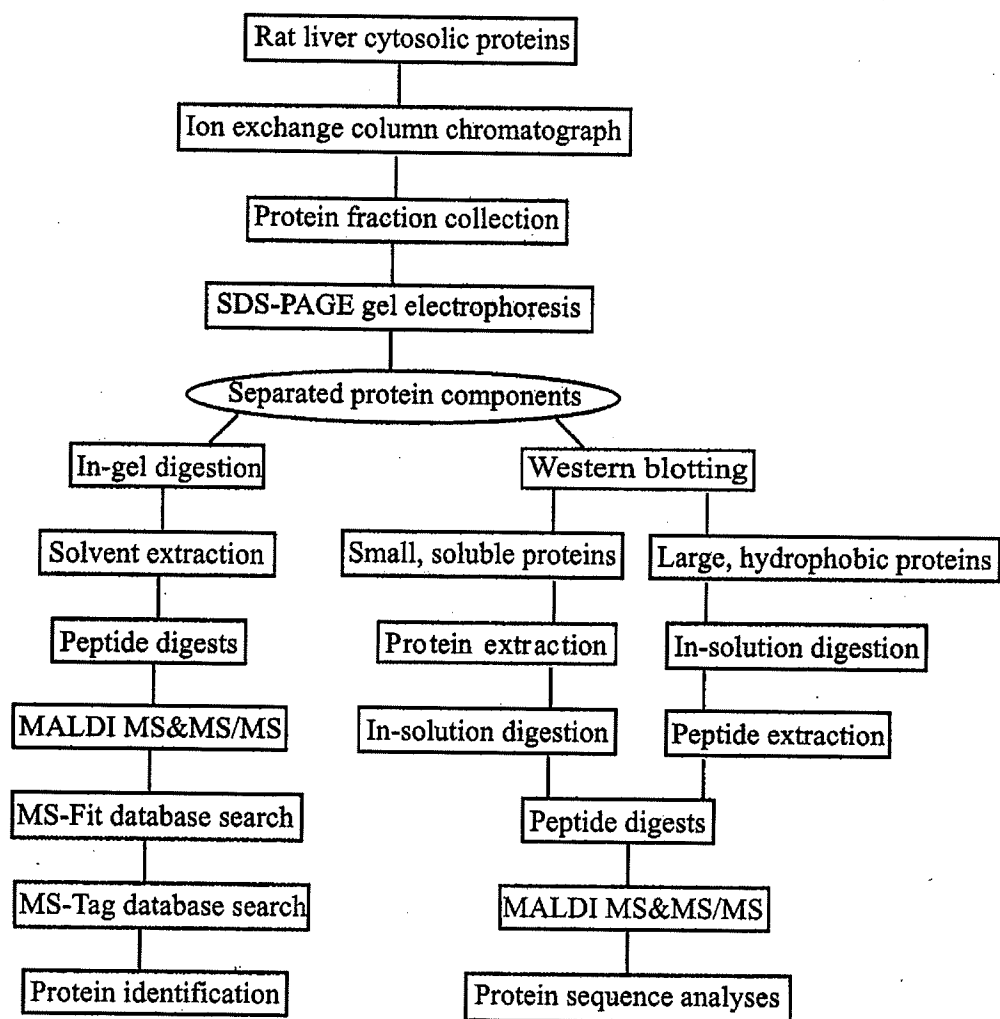


Figure 20. Summary of the identification procedure for rat liver cytosolic proteins and amino acid sequence analysis using gel electrophoresis followed by mass spectrometry.

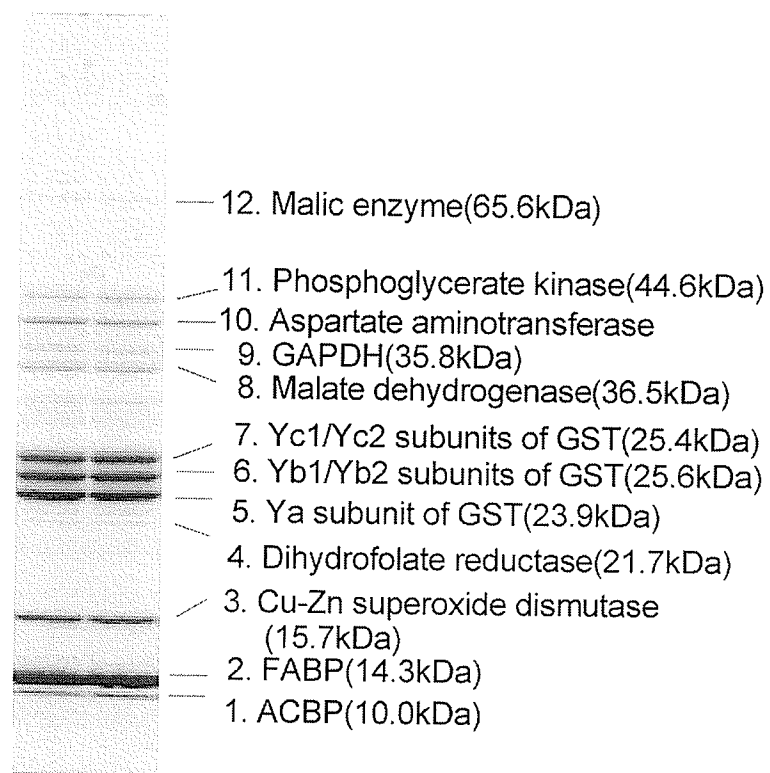


Figure 21. SDS-PAGE gel of the first fraction of rat liver cytosolic protein obtained by ion exchange chromatography using a DEAE-Sepharose column. Protein bands were visualized with Coomassie blue, then identified by in-gel digestion and MALDI QqTOF mass spectrometry. Masses are shown by calculated values of database protein sequences.

in-gel digestion of each band were analyzed by MALDI QqTOF mass spectrometry. All twelve bands represented 12 different proteins; these are Acyl-CoA-binding protein (ACBP), fatty acid binding protein (FABP), Cu-Zn superoxide dismutase, dihydrofolate reductase, Ya, Yb, and Yc subunits of glutathione S-transferase (GST), malate dehydrogenase, glyceraldehyde 3-phosphate dehydrogenase (GAPDH), aspartate aminotransferase, phosphoglycerate kinase, and malic enzyme. However, the homologous GST subunits (Yb1/Yb2, Yc1/Yc2) could not be distinguished because of protein sequence similarity and the limited number of peptides available from the in-gel digest.

One tryptic digest was not sufficient for identifying protein band #2. Two proteases sequential digestion was required. The fragments produced by *in-gel* tryptic digestion of protein band #2 after simple solvent extraction were examined by MALDI. The only prominent feature of the MALDI mass spectrum (Figure 22A) was a triplet of peaks with the side peaks separated by +16 and -48 Da from a central peak at m/z 2433.123. This typical triplet peak suggested a methionine-containing peptide ion of m/z 2433.123 with the other peaks arising from partial oxidation of methionine and the facile loss of CH_3SOH from the resulting Met sulfoxide residue (Qin and Chait 1997). A direct database search by MS-Fit using this single peptide mass was unable to identify this protein, and the MS/MS spectrum of the peptide after collision-induced dissociation (CID) was too complicated to identify its sequence. MS-Tag was also inconclusive. However, an additional digestion of the tryptic fragment with endoprotease Glu-C gave better results, which produced prominent ion peaks at m/z 1539.703 and m/z 864.421 in the MALDI mass spectrum (Figure 22B). The MS/MS spectrum of the former ion after

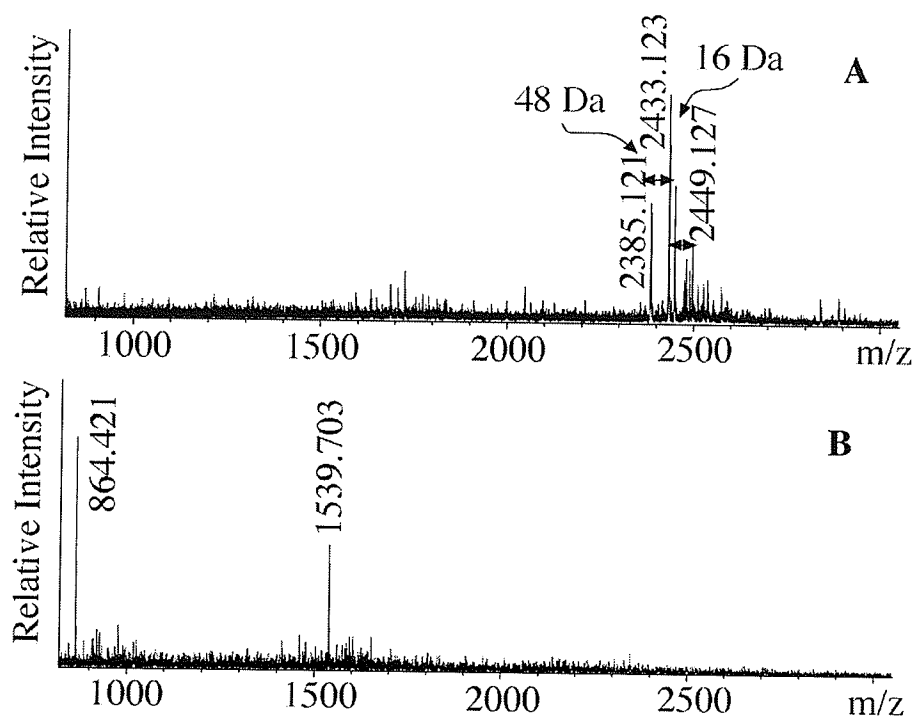


Figure 22. MALDI mass spectra of in-gel digests of FABP by (A) trypsin, (B) trypsin followed by endoprotease Glu-C.

CID revealed definitive fragmentations (Figure 23 and Table 5), which yielded the peptide sequence FSGKYQVQSQE by manual interpretation of the mass differences between adjacent pairs of peaks. Protein database searching using the deduced peptide sequence matched the residues 3-13 of FABP. MS/MS measurements on the other fragment at m/z 864.421 showed that it corresponded to residues 14-20 (NFEPFMK) with the loss of CH_3SOH from oxidized Met-19.

The ion observed earlier from the simple tryptic digest had m/z 2433.123 which was close to the value calculated from the nucleic acid sequence for the expected fragment containing residues 1-20 of the FABP (m/z 2439.111, see Table 6). The mass difference of 5.988 Da suggested the possible modifications within the two N-terminal residues (Met-1 and Asn-2) that remained to be defined by in-solution digestion.

Complete Sequence Measurements of Small Proteins by Protein Extraction Followed by In-solution Digestion.

More FABP peptide fragments were observed after protein extraction followed by in-solution digestion by either trypsin or Glu-C, as shown in Figure 24. The most abundant ion from a Glu-C digestion (at m/z 1587.710) yielded a simple MS/MS spectrum (Figure 25) corresponding to peptide residues 1-13, acetylated at the N-terminus, since it contained a complete set of acetylated b-ions as well as several y-ions of which only y-13 was acetylated. The N-terminal acetylation was further supported by the observation of a tryptic fragment at m/z 725.332 (see Figure 24A), where the measured mass was 42.013 Da higher than the calculated mass (m/z 683.319) of the N-terminal peptide for residues 1-7. This finding would explain the difference of 5.988 Da

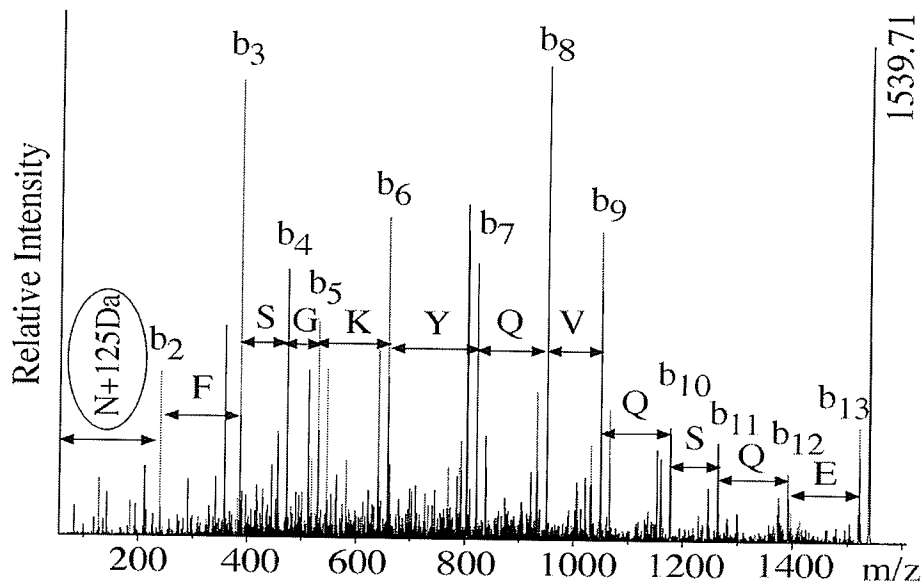


Figure 23. CID mass spectrum of the ion at m/z 1539.71. Partial amino acid residues of the peptide as shown and identified by calculating mass differences between neighboring peaks (see Table 5).

Table 5. Comparison of mass differences between adjacent b fragment ions in the MS/MS spectrum of precursor ion at m/z 1539.71 with calculated mass of the deduced amino acid residues.

b ion	m/z(Obs.)	$b_n - b_{n-1}$ (Da)	Residue	m(Calc.,Da)	error(Da)
b1	-	-	-	-	-
b2	240.087	-	-	-	-
b3	387.160	147.073	F, Phe	147.068	+0.005
b4	474.202	87.042	S, Ser	87.032	+0.010
b5	531.228	57.026	G, Gly	57.021	+0.005
b6	659.321	128.093	K, Lys	128.095	-0.002
b7	822.373	163.052	Y, Tyr	163.063	-0.011
b8	950.434	128.061	Q, Gln	128.059	+0.002
b9	1049.503	99.069	V, Val	99.068	+0.001
b10	1177.566	128.063	Q, Gln	128.059	+0.004
b11	1264.591	87.025	S, Ser	87.032	-0.007
b12	1392.643	128.052	Q, Gln	128.059	-0.007
b13	1521.694	129.051	E, Glu	129.043	+0.008

Values listed are monoisotopic masses.

Table 6. Protein extraction combined with enzymatic digestion to analyze the complete sequence of some rat liver proteins by MALDI QqTOF mass spectrometry.

(1) Acyl-CoA-binding protein (ACBP)	
001	M S Q A D F D K A A E E V K R L K T Q P T D E E M L F I Y S H F K Q A T V G D V
041	N T D R P G L L D L K G K A K W D S W N K L K G T S K E N A M K T Y V E K V E E
081	L K K K Y G I
(2) Fatty acid binding protein (FABP)	
001	M N F S G K Y Q V Q S Q E N F E P F M K A M G L P E D L I Q K G K D I K G V S E
041	I V H E G K K V K L T I T Y G S K V I H N E F T L G E E C E L E T M T G E K V K
081	A V V K M E G D N K M V T T F K G I K S V T E F N G D T I T N T M T L G D I V Y
121	K R V S K R I
(3) Cu, Zn superoxide dismutase	
001	A M K A V C V L K G D G P V Q G V I H F E Q K A S G E P V V V S G Q I T G L T E
041	G E H G F H V H Q Y G D N T Q G C T T A G P H F N P H S K K H G G P A D E E R H
081	V G D L G N V A A G K D G V A N V S I E D R V I S L S G E H S I I G R T M V V H
121	E K Q D D L G K G G N E E S T K T G N A G S R L A C G V I G I A Q

Observed peptide fragments: “——” tryptic digest; “.....” Glu-C digest; “-----” Asp-N digest.

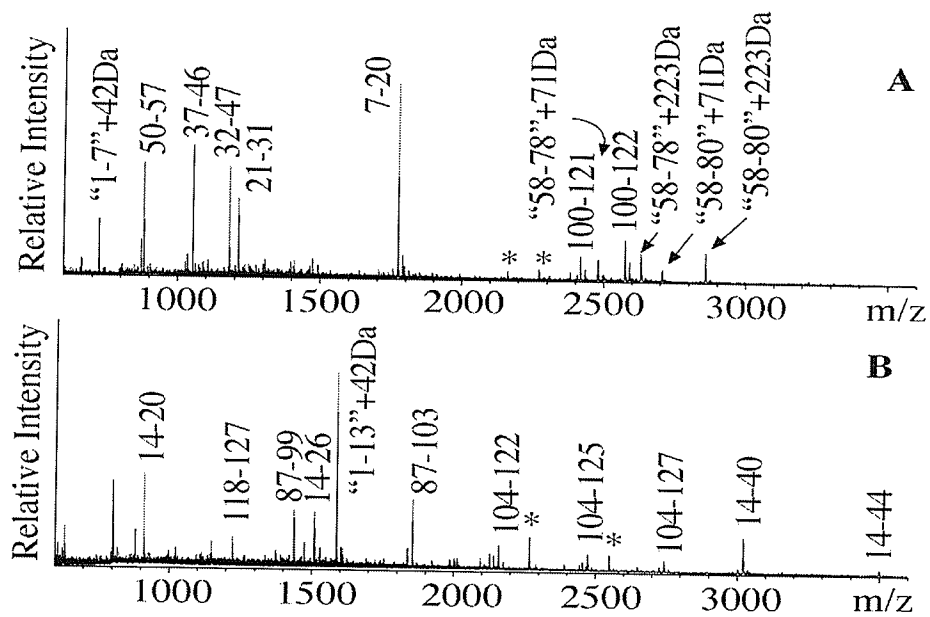


Figure 24. MALDI mass spectra of the FABP digests using protein extraction. (A) trypsin, (B) endoprotease Glu-C. The symbol * designates trypsin autolysis fragments.

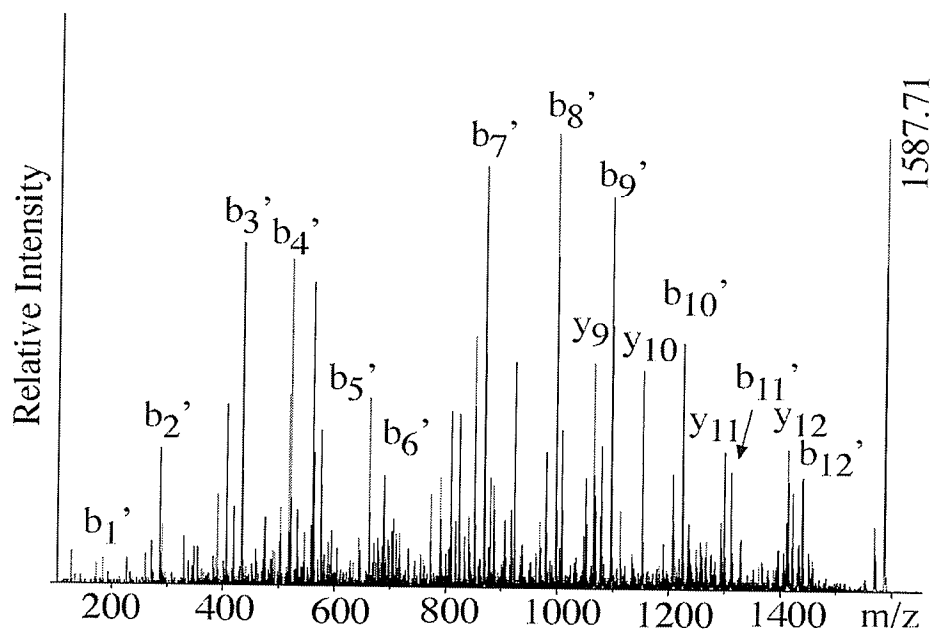


Figure 25. CID mass spectrum of the ion at m/z 1587.71. The peptide sequence was deduced as MNFSGKYQVQSQE with the N-terminus acetylated. Superscript ' indicates a 42 Da mass increment of the fragment ions.

between the measured and calculated mass of the proposed N-terminal peptide (at m/z 2433.123) generated from in-gel digests; which was caused by an N-terminal oxidized acetylmethionine with one molecule of CH₃SOH deleted from its side group (131.040Da + 15.995Da + 42.011Da – 63.998Da = 125.048Da instead of 131.040 Da, a calculated difference of 5.992 Da). Likewise, one molecule of CH₃SOH loss in the resulting peptide 1-20 (m/z 2433.123), caused by the oxidized methionine at residue 19 (as indicated above in the in-gel Glu-C digest, Figure 22B), could account for the presence of a lower mass peak at m/z 2385.121 (Figure 22A).

A similar protein extraction procedure was performed on other isolated rat liver proteins to determine their complete amino acid sequences. ACBP, FABP and Cu-Zn superoxide dismutase have been completely sequenced by various enzymatic digestions as summarized in Table 6. Similar to FABP sequence analyses, ACBP required further digestion by trypsin or Asp-N to cover its total protein sequence. The N-terminus of ACBP also was determined to be acetylated by MS/MS measurements. In contrast, full sequence coverage was obtained for Cu-Zn superoxide dismutase by a Glu-C digestion. Figure 26 showed the direct peptide mapping of a Glu-C digest of Cu-Zn superoxide dismutase, which revealed most of the peptide fragments (residues 12-21, 22-40, 41-78, 79-100, 101-109, 110-121, 122-133 and 134-153) except for the N-terminal residues 1-11 (Ho and Crapo 1987), which was also acetylated.

Observation of Chemical Modifications from Gels

In addition to the oxidation of methionine residues in liver FABP, the cysteine residues are highly susceptible to chemical modification by acrylamidation resulting from

traces of nonpolymerized acrylamide in gels (Shevchenko, Wilm et al. 1996). This results in a shift of 71 Da in the mass of any peptide containing a modified cysteine. We also observed another adduct ion $[MH + 223]$ in the MALDI mass spectra (Figures. 24A and 26), and MS/MS analyses indicated that the modification occurred at the cysteine residue (Figure 27). Presumably it was formed by N, N, N-tri-methyldiylne-acrylamide $[(CH_2=CHCONH)_3CH]$, calculated mass 223.096 Da], resulting from a radical reaction of unpolymerized acrylamide with its cross-linking agent N, N-bis-methylene-acrylamide. Similar to the typical triplet peaks (MH-48, MH and MH+16) of the methionine presence, the presence of the adduct ion triplet (MH, MH+71 and MH+223) signified the presence of cysteine in a peptide extracted from gels.

Sequence Measurements on Larger Proteins by In-solution Digestion followed by Peptide Extraction.

Partial sequence information on the GST subunits, asparate aminotransferase, and phosphoglycerate kinase was obtained using in solution tryptic digestion followed by the peptide extraction procedure. Figure 28 illustrates a typical mass spectrum of the tryptic protein band #6 (see Figure. 21), indicating a mixture of Yb1 and Yb2 subunits of GST. Mass measurements and MS/MS analyses showed that the observed peptides encompassed 65-100% of the total protein amino acid sequences as indicated in Table 7, including the presence of two proteins in individual bands.

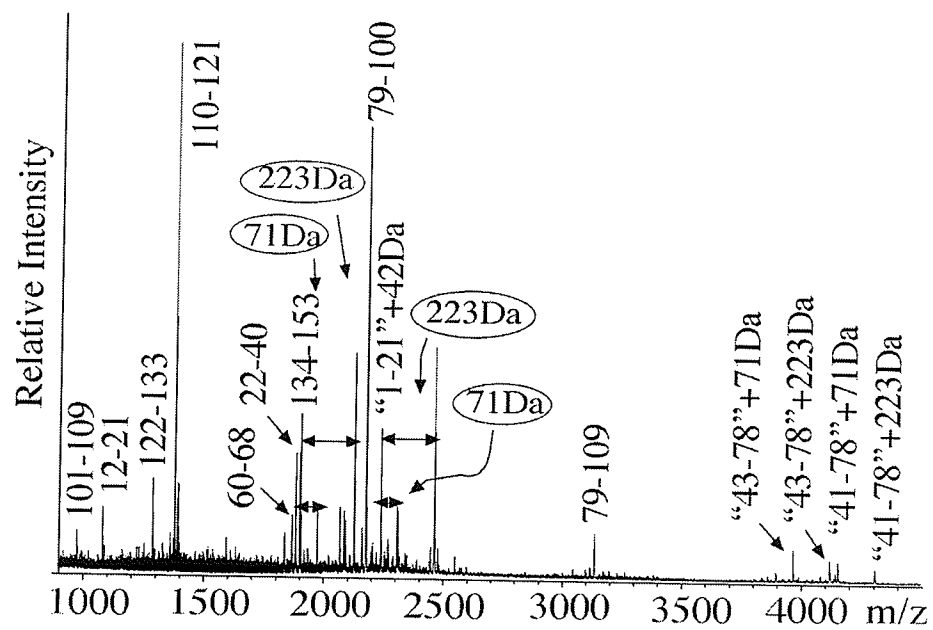


Figure 26. MALDI mass spectrum of the endoprotease Glu-C digested Cu-Zn superoxide dismutase using the protein extraction procedure.

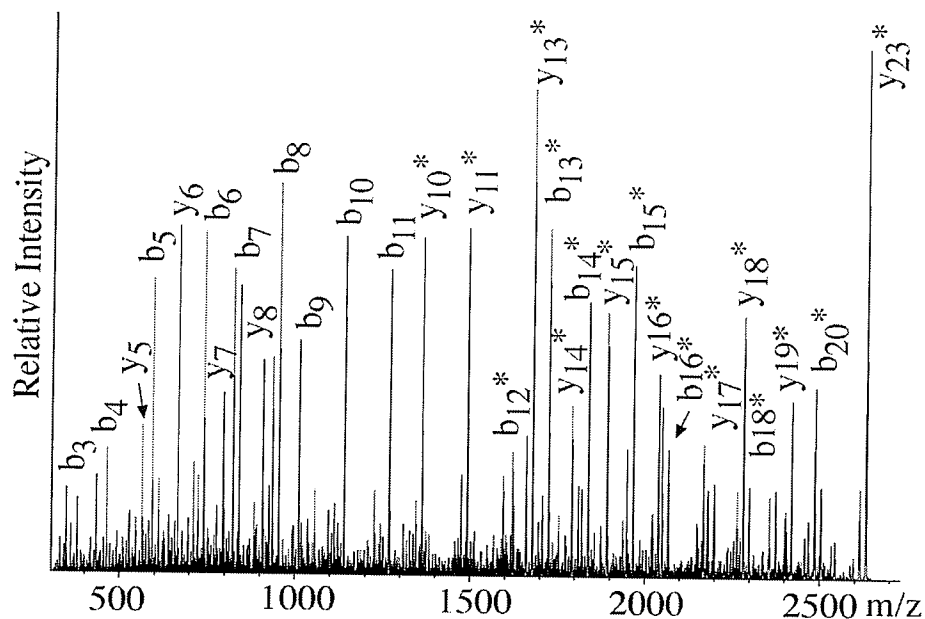


Figure 27. CID mass spectrum of the ion at m/z 2632.14 from a tryptic FABP. The symbol * represents a mass increment of 223 Da of product ions from b_{12} and y_{10} , which showed that the peptide sequence VIHNEFTLGEEC*ELETMTGEK was modified only at the cysteine residue.

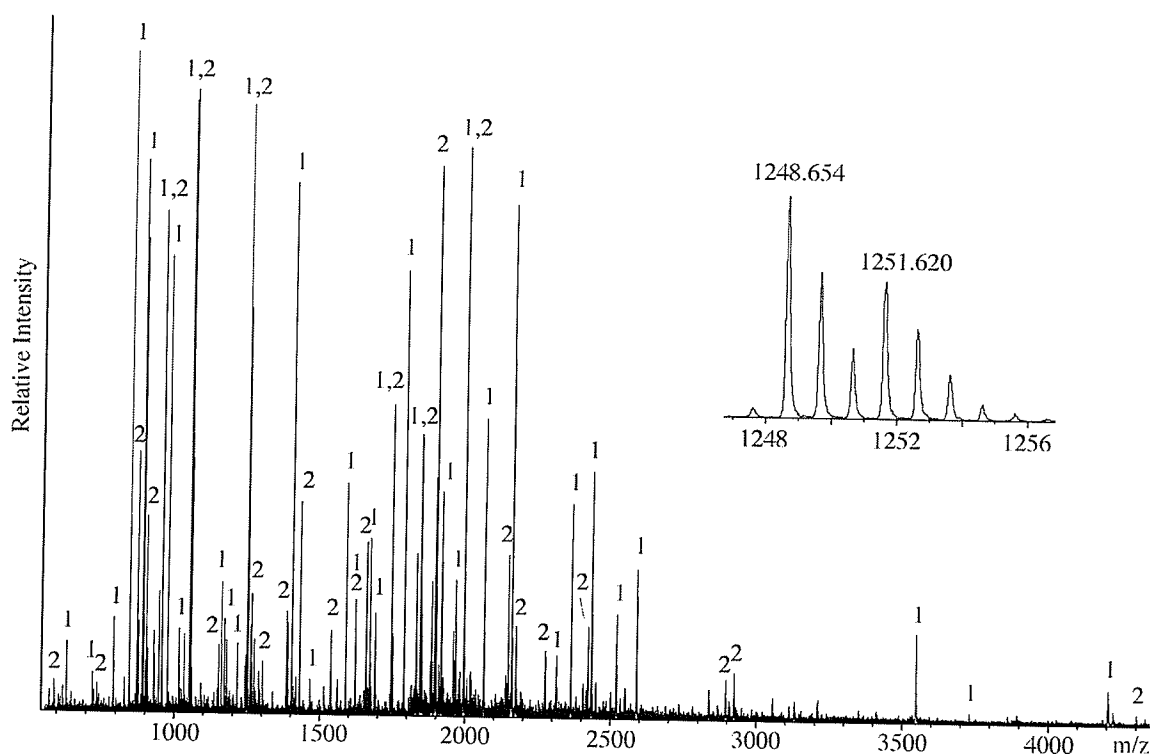


Figure 28. MALDI mass spectrum of a tryptic protein band #6. More than 82 peptide fragments revealed a protein mixture of Yb1 (1) and Yb2 (2) subunits of glutathione S-transferase (GST) with the sequence coverage of 91.3% and 75.6%. The inset shows an expanded profile of two distinguishable peaks at m/z 1248.654 (Yb1) and m/z 1251.620 (Yb2), corresponding to the N-terminal peptide (residues 1-10) of the proteins assuming the Met at the N-terminus of Yb1 subunit was deleted.

Table 7. Protein sequence analyses by MALDI QqTOF mass spectrometry following peptide extraction of the tryptic digests.

Band No.	Protein identified	Mass (kDa)	Coverage	Modifications
5	Glutathione S-transferase Ya	23.9	88.4%	N-terminal acetylation Glu ¹⁷ mutated to Asp
6	Glutathione S-transferase Yb1	25.9	91.3%	Met deleted at the N-terminus
	Glutathione S-transferase Yb2	25.6	75.6%	
7	Glutathione S-transferase Yc1	25.2	100%	Met deleted at the N-terminus
	Glutathione S-transferase Yc2	25.4	65.6%	
10	Asparatate aminotransferase	47.4	76.8%	Truncated protein
11	Phosphoglycerate kinase	44.6	90.6%	Met deleted at the N-terminus N-terminal acetylation Disulfide binding of Cys ⁹⁹ -Cys ¹⁰⁸

Molecular mass of the protein was calculated from a predicted sequence in the database (NCBIInr).

Discussion

The confidence of protein identification in proteomic research is very important. It is highly desirable to obtain more information about the complete protein amino acid sequence, including any post-translational modifications. This study developed an alternative technique that employs a two-phase extraction procedure, without the need for in-gel digestion. This technique allows the direct and complete amino acid sequence determination of cytosolic proteins from small to large, as well as the efficient identification of post-translational modifications.

Results of this study indicated that the observed post-translational modifications on the cysteine residues were introduced by SDS-PAGE gel separation and methionine residue oxidation in liver FABP. Since the cysteine was reduced prior to gel electrophoresis, the *in vivo* glutathionylation (Hitomi, Odani et al. 1990) or cysteinylation (Dormann, Borchers et al. 1993) of rat liver FABP were not found in this study. However, in the report of Murphy *et al* (Murphy, Edmondson et al. 1999), MALDI /TOF analysis showed the free thiol group in the cysteine residues of rat liver FABP isoforms. These findings suggest that cysteine and methionine residues of rat liver FABP are highly susceptible to oxidation and free radical reaction during the procedures of analysis. Therefore, these residues may contribute a putative antioxidation function to liver FABP. It is known that oxidation and modification of reducing amino residues are linked to some disease progress and drug management (Poirier, Joubert-Caron et al. 2003; Kinumi, Kimata et al. 2004; Low, Leow et al. 2004; Requena, Dimitrova et al. 2004). The technique developed in this study would provide a direct analytical approach to the

investigation of the effects of disease states on protein modification and ultimately on drug uptake and utilization.

The methodology of two-phase extraction procedures, together with amino acid sequence determination of rat liver cytosolic proteins by MALDI QqTOF MS offers several advantages. The primary advantage is its ability to obtain complete amino acid sequencing that is independent of protein size and hydrophobicity. This time-saving procedure offers the investigator a greater opportunity to determine the amino acid sequence modifications of proteins separated by gel electrophoresis. High sequence coverage of a protein made it possible to distinguish complicated homologous proteins or isomerases, such as Yb1/Yb2 and Yc1/Yc2 subunits of glutathione S-transferase (GST). Use of in-solution digestion rather than in-gel digestion overcomes many of the problems associated with the latter method including controlling the enzymatic digestion. The detection limit of the two-phase protein/peptide extraction method (at low picomole level) is suitable for the analysis of very small amounts of intracellular proteins. The two-phase extraction procedure is especially useful for the analysis of a wide range of gel-separated proteins, therefore, it promises to become a versatile analytical technique for protein sequences.

Section B. Expression and effects of L-FABP on hepatic fatty acid uptake and liver regeneration following hepatic hepatectomy

Introduction

LCFAs are essential for the synthesis of new membrane components and cellular metabolic energy. L-FABP is involved with the intracellular transportation and disposition of LCFAs and many other ligands that are deemed important in the regulation of hepatocyte growth. Thus, L-FABP has been suggested to be associated with hepatocyte mitotic activity. However, examining the effect of changes in L-FABP level in an animal model of mitosis is not known

Compared to the other hepatic mitotic models (using hepatotoxins, e.g., CCl_4), the 70% partially hepatectomized animal model is not associated with significant tissue injury and inflammation, and the initiation of regenerative stimulus is precisely defined. Whether this surgical intervention indeed stimulates L-FABP mRNA expression and increases the L-FABP level is not known. In this study, we determined the time course of L-FABP mRNA expression and L-FABP levels following 70% partial hepatectomy (PHx) using Northern and Western blot, respectively. To elucidate one of the roles for L-FABP in PHx, [^3H]-palmitic acid clearance in hepatocytes isolated from 24 hours post-PHx and control animals was assessed. L-FABP level was reduced in the PHx model by dexamethasone pre-treatment of animals. The liver regeneration activity was assessed by PCNA (proliferating cell nuclear antigen) level and [^3H]-thymidine incorporation.

Results

L-FABP mRNA levels

Rat liver tissue collected from the different time points (0, 30 min, 1, 2, 4, 8, 12, 24 and, 48 hours) following 70% PHx were quantitated for L-FABP mRNA expression using Northern blot analysis. Results (Figure 29A upper panel) indicated that L-FABP mRNA increased within 30 min of PHx, peaked at approximately 1 hour, and returned to baseline level 8 hours post PHx. Figure 29A middle panel shows the RNA loading controls using the 28S RNA probe. L-FABP mRNA expression in sham animals did not change with time following surgical manipulation of the liver as in treated animals (Figure 29A lower panel). After correction for the mRNA levels in each sample by the loading control, relative expression of L-FABP mRNA from sham and PHx rats at various time intervals were analysed for statistical significance and plotted in Figure 29B. Overall there was a significant relationship between FABP level and time interval ($p < 0.05$). Expression of L-FABP mRNA increased significantly at 30 min ($p < 0.05$) following PHx. At 1 hour the level was $163\% \pm 17\%$ (mean \pm SE, $n=5$) that of sham. L-FABP mRNA level at 2 hours following PHx was not statistically different than the 1 hour PHx level. Thus, there was an early transient increase in L-FABP mRNA in response to PHx that lasted for 4 hours. L-FABP mRNA remained statistically indifferent with time in sham animals (Figure 29A lower panel).

L-FABP protein level

The same liver tissue as used in the L-FABP northern blot analysis was used to quantitate L-FABP level by Western blot (Figure 30A upper panel). There was a steady

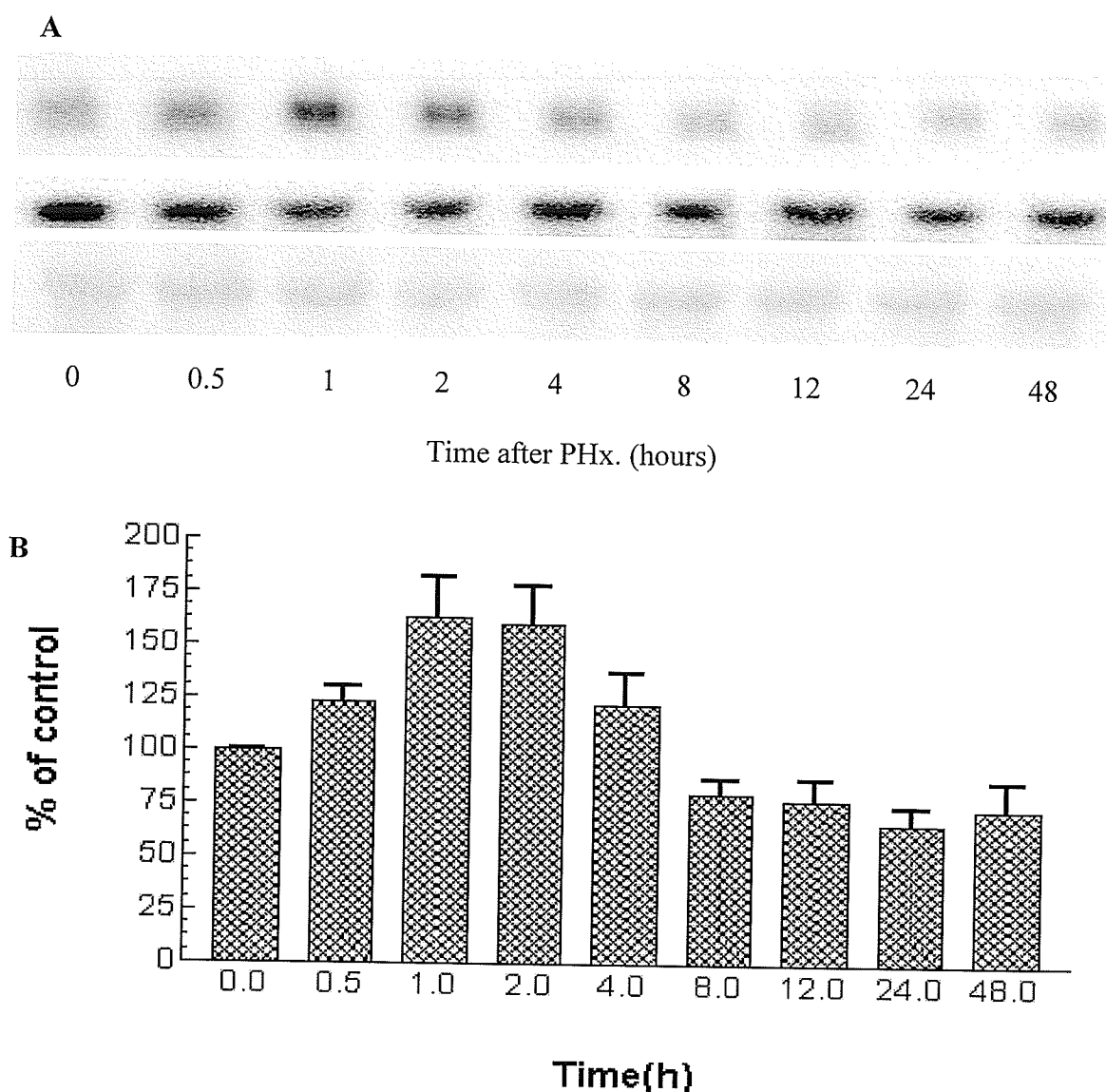
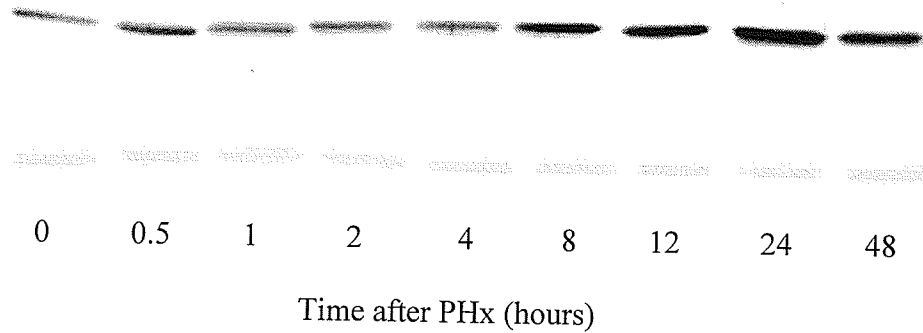


Figure 29. Northern blot analysis of L-FABP mRNA and relative expression of L-FABP mRNA at different times following PHx. A: Total RNA (20 μ g) from different time points after partial hepatectomy was separated by electrophoresis and transferred to membranes. Membranes were hybridized with 32 P labeled L-FABP cDNA (upper panel) and 28S rRNA cDNA as loading control (middle panel). Sham control (lower panel) showed no statistical change with time. B: The density of L-FABP mRNA and 28S rRNA were obtained using the NIH Image program. The relative expression of L-FABP mRNA versus 28S rRNA from 5 different samples was displayed against time following PHx. The data represent mean \pm SEM, n=5.

A



B

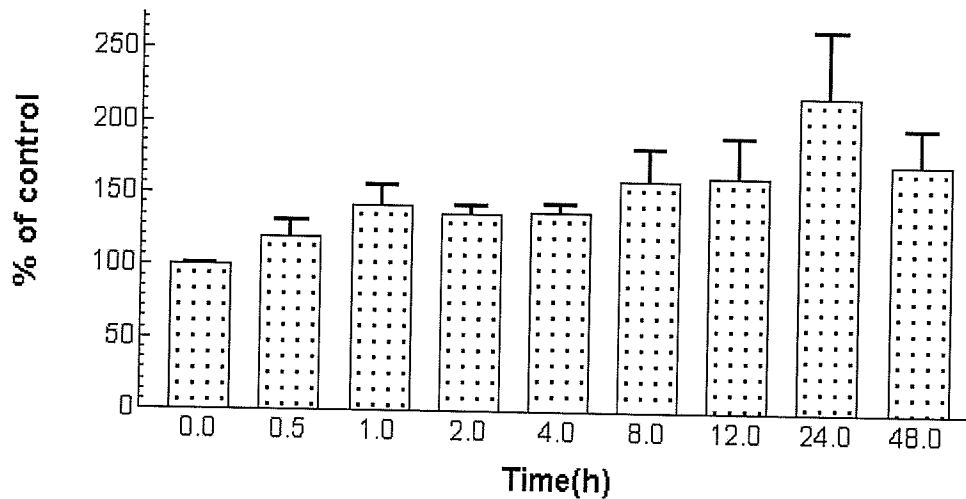


Figure 30. Western blot analysis of L-FABP levels at different time points following PHx. Cytosol protein (5 μ g) from each time point was incubated with L-FABP antisera and visualised using the ECL kit (upper panel). Sham (lower panel) showed no significant change in L-FABP with time ($p>0.05$). B. Density of L-FABP was obtained using an NIH Image program and expressed as a percentage of sham. Data represent mean \pm SEM, $n=5$.

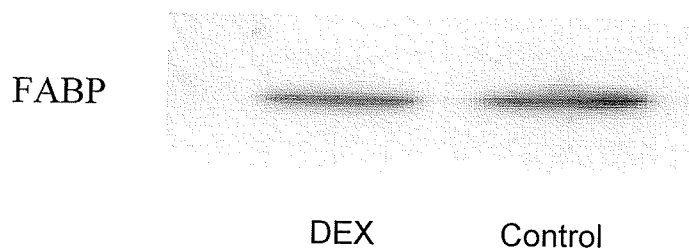
increase in FABP level in response to PHx ($p<0.05$). FABP level increased within 30 min and peaked at 24 hours PHx ($219 \pm 41\%$, $p<0.05$, Figure 30B). Sham control (Figure 30A lower panel) showed no significant change in FABP level over time.

To further elucidate the role of L-FABP in the regenerative process we administered dexamethasone to reduce the L-FABP level (Foucaud, Niot et al. 1998). At 24 hours PHx, L-FABP was reduced by 29% compared to the control group (see Figure 31, $p<0.05$). This was associated with reduced mitotic activity as determined by decreased [^3H]-thymidine incorporation into DNA (48%) and decreased PCNA levels (39%) (Figure 32 and Figure 33, respectively; $p<0.01$).

Hepatocyte [^3H]-palmitate clearance

One of the functions of L-FABP is to facilitate the intracellular transport of long-chain fatty acids. Uptake of long-chain fatty acids is known to parallel the L-FABP levels (Burczynski, Zhang et al. 1997; Burczynski, Fandrey et al. 1999). Therefore, it may be expected that during the regenerative process uptake of long-chain fatty acids also is increased. To elucidate the role of L-FABP in the uptake process during liver regeneration we investigated the [^3H]-palmitate clearance by hepatocytes isolated from the same livers in which the L-FABP levels were assessed. Figure 34 shows [^3H]-palmitate clearance (nl/sec/ 10^6 cells) in the presence 500 μM albumin. [^3H]-Palmitate clearance was 17 ± 1 and 22 ± 1 nl/sec/ 10^6 cells in sham and PHx rats, respectively (mean \pm SEM, $n=8$). This represented a 29% increase in [^3H]-palmitate clearance by hepatocytes isolated from the PHx rats as compared to those isolated from the sham group ($p<0.01$).

A



B

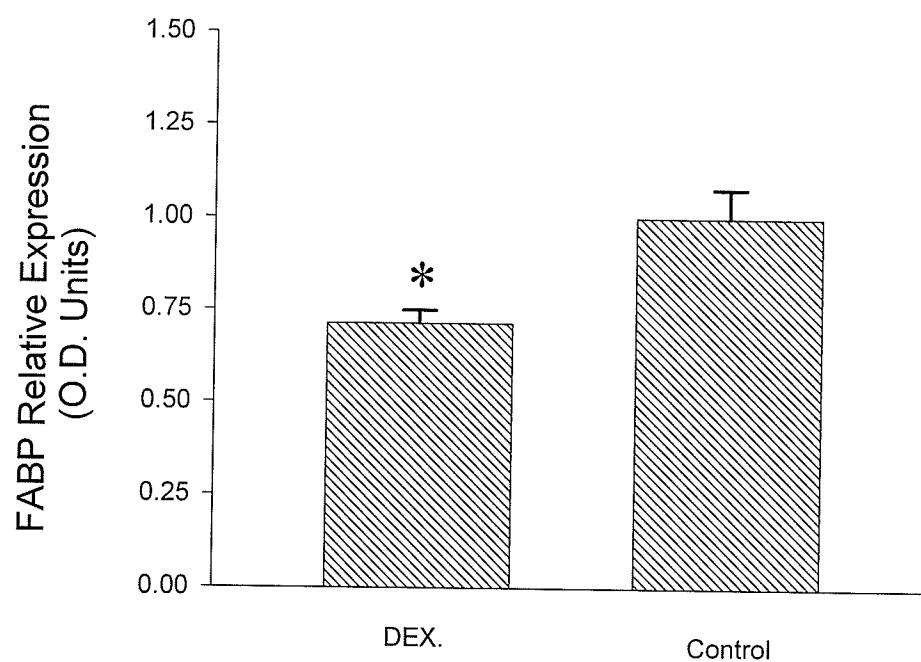


Figure 31. Western blot analysis of L-FABP levels in dexamethasone treated (DEX) and without dexamethasone treated (Control) rat livers 24 hours following 70% partial hepatectomy (30A). Figure 30B shows the L-FABP relative expression (optical density units) in DEX and control animals; mean \pm SEM ($n = 4$); * $p < 0.05$.

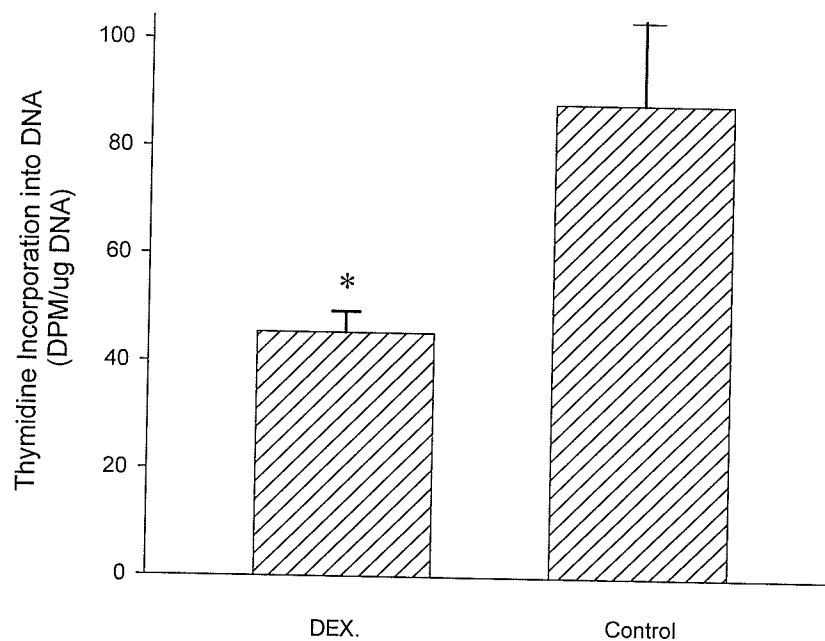


Figure 32. [^3H]-Thymidine incorporation into hepatic DNA in regenerating rat livers from Control (without dexamethasone treated) and dexamethasone treated (DEX) animals 24 hours following 70% partial hepatectomy. Data represent the mean \pm SEM ($n = 4$); $*p < 0.05$.

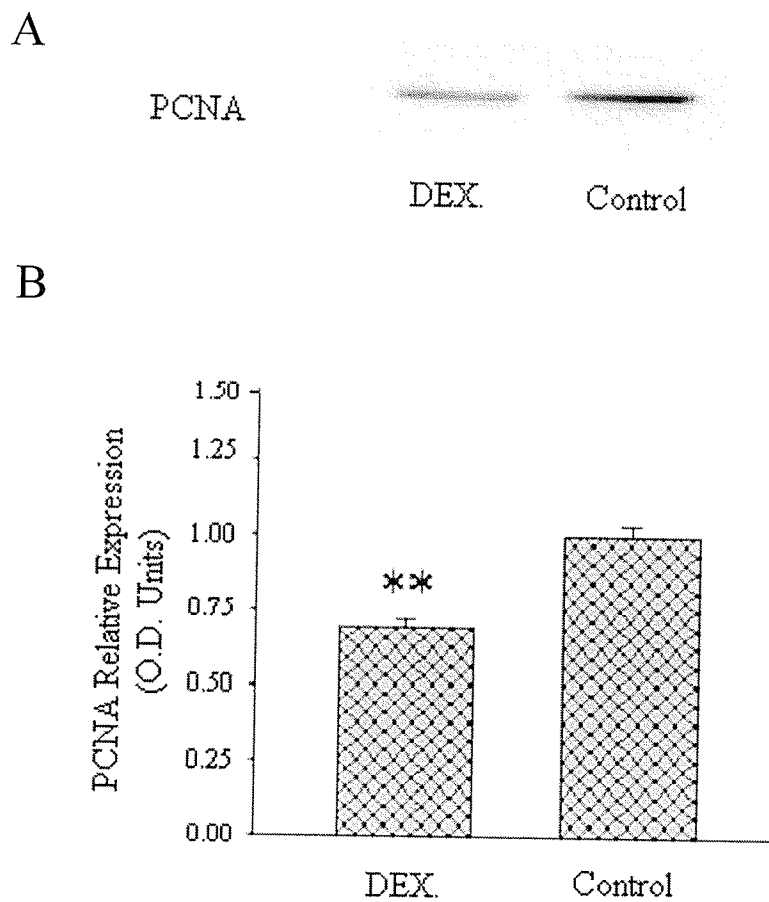


Figure 33. PCNA protein levels in regenerating rat livers from Control (without dexamethasone treated) and DEX (dexamethasone treated) animals 24 hours following 70% partial hepatectomy (Figure 33A). Figure 33B shows the PCNA relative expression (optical density units); mean \pm SEM (n = 4); **p < 0.01.

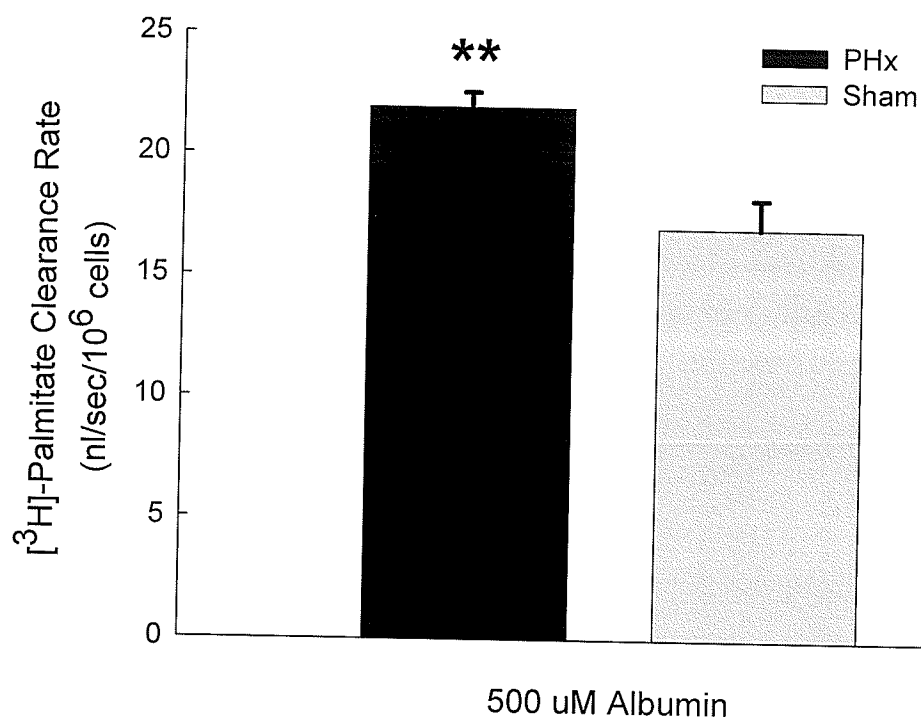


Figure 34. [³H]-Palmitate clearance by rat hepatocytes isolated from sham and 24 hour post-70% partial hepatectomized (PHx) animals. Clearance of [³H]-palmitate was expressed as nl/sec/10⁶ cells. Data represent mean \pm SEM, n=8; **p<0.01.

Discussion

The present study elucidates a role of L-FABP in a hepatic regeneration animal model. Previous work linking L-FABP to cell proliferation (mitosis) involved examining levels of this protein in isolated cell systems (cell cultures), or in carcinoma models (Sorof 1994). The latter usually arise through chemical carcinogen administration. The main difference between our current study and previous work is that we used a 70% PHx model and have investigated the L-FABP mRNA expression and protein levels from regenerating livers. This model is possibly the most popular experimental model to study hepatic regeneration (cellular proliferation) because, compared to other methods that use hepatotoxins, it is not associated with significant tissue injury and inflammation and, the initiation of the regenerative stimulus is precisely defined (removal of liver lobes). Very little information is available regarding the L-FABP levels in hepatic regeneration following PHx. Understanding the time profiles of L-FABP will help us to understand the events occurring in cellular replication following surgical intervention.

Following PHx liver regeneration occurs by proliferation of the existing mature cells in the intact organ. The entire process lasts 5 to 7 days in the rat (Michalopoulos and DeFrances 1997). The stage preceding DNA replication, called the prereplicative phase, is the phase during which time numerous metabolic changes take place. One of the initial changes that the liver undergoes in this phase is a rapid change in the rate of RNA synthesis and overall mRNA steady state levels. There are three characteristic temporal patterns of gene expression in the regulation of regenerating livers: immediate-early, delayed-early and growth related, and liver specific. One pattern of induction has two peaks coincident with the first and second G1 phases of the hepatic cell cycles, with the

initial peak representing the immediate early genes (Kren, Trembley et al. 1997). Within 30 min after PHx there is induction of immediate-early genes that encode many members of diverse transcription factor families including the Jun-Fos-LRF-1, nuclear receptor, and myc families (Taub 1996). This induction is independent of new protein synthesis. The increase in L-FABP mRNA expression observed in the present study occurred at 30 min to 4 hours, peaked between 1~2 hours following PHx, and was short lived. The time frame for the increased L-FABP mRNA expression was temporarily coincident with the induction of the immediate early-genes for liver regeneration, suggesting that the up-regulation of L-FABP production is at the transcriptional/posttranscriptional level. Also, the fact that L-FABP expression is coincident with the immediate early genes for liver regeneration, suggests that L-FABP mRNA may be one of the factors involved in the initiation of liver regeneration.

Exact timing of DNA synthesis following PHx varies with age of the animal and can be modified by hormones and dietary manipulations (Kren, Trembley et al. 1997). For younger adult rats the basal rate of DNA synthesis remains unchanged during the first 12 hours (prereplicative phase) after which there is a wave of DNA synthesis in hepatocytes that peaks at approximately 24 hours and then gradually declines. Typically, mitosis occurs 6 to 8 hours following DNA replication (Grisham 1962). This time frame is coincident with a second pattern of induction that parallels the major growth period of the liver ending 60 to 72 hours post-PHx, and includes the delayed-early and growth-regulated genes. In the current study, the increase in L-FABP level showed up-regulation at a translational level. The increased L-FABP and [^3H]-palmitate uptake also was temporally coincident with protein synthesis, suggesting that cell proliferation may be

occurring as early as 24 hours post-PHx in this model. The third pattern of induction includes liver-specific genes, which exhibit expression after the growth period.

To further elucidate the role of L-FABP in the cellular regenerative process we decreased the L-FABP level by the administration of dexamethasone to animals prior to PHx. Results showed that L-FABP level was markedly reduced (Figure 31) and that this reduction was associated with a statistically reduced mitotic activity (Figures 32 and 33). It is acknowledged that while dexamethasone treatment clearly reduced the L-FABP levels, it also may be associated with other pharmacological effects that could be related to cellular mitotic activity. However, collectively, reports from the literature using various models of mitotic activity together with the present results buttress the argument that cell proliferation following PHx occurs at 24 hours PHx (and may indeed occur earlier), and involves the intracellular disposition of long-chain fatty acids in which L-FABP is closely linked. The enhanced intracellular disposition of long-chain fatty acids in cells undergoing mitotic events in the present study is reasonable given the fact that fatty acids are critically needed for membrane synthesis as well as other intracellular events.

In summary, the present study has shown that L-FABP mRNA expression and L-FABP level increased shortly after PHx. The increased L-FABP level was associated with an increased hepatic [^3H]-palmitate clearance. Down-regulation of L-FABP by dexamethasone reduced hepatic regeneration activity. L-FABP has an important role in liver regeneration, acting as a carrier of mediators required for successful cell proliferation. We further speculate that L-FABP level may be considered as a prognostic factor for hepatic surgery (Yamazaki, Kanda et al. 1999).

Section C. Cellular Antioxidative Function of L-FABP in L-FABP Stable Transfected Chang Liver Cells

Introduction

Cellular oxidative stress is one of the factors responsible for the propagation of liver diseases, such as hepatitis, cirrhosis, and hepatoma (Yamamoto, Yamashita et al. 1998). Several primary antioxidant defence systems such as superoxide dismutase (SOD), catalase, and glutathione peroxidase (GPx) are present intracellularly. These systems scavenge reactive oxygen species (ROS) such as hydrogen peroxide, superoxide, lipid peroxides, and free radicals. Exposure to oxidative stress may, however, deplete the cellular antioxidant capacity. Therefore, other antioxidant defence systems are expected to play an important role in response to oxidative stress.

Liver fatty acid binding protein (L-FABP) is very likely to be an effective endogenous antioxidant as it has high affinity and capacity to bind long chain fatty acid oxidation products (Raza, Pongubala et al. 1989; Ek-Von Mentzer, Zhang et al. 2001). L-FABP is a 14-kDa protein abundantly found in the cytoplasm and the nucleus of hepatocytes (Bordewick, Heese et al. 1989; Fahimi, Voelkl et al. 1990). Although L-FABP consists of several forms due to post-translational modification, the amino acid sequence and fatty acid binding ability are unchanged (Murphy, Edmondson et al. 1999). Hepatocyte L-FABP concentration could be as high as 0.4 mM (Burnett, Lysenko et al. 1979) and contains a large number of reducing amino acid residues (one cysteine and seven methionine residues) in its molecular structure. With an accessible volume enclosed by the molecular surface of L-FABP of 28,600 Å³ (Thompson, Reese-Wagoner

et al. 1999), the concentration of total methionine residues in L-FABP could be as high as ~ 400 mM. It is known that methionine and cysteine amino acids are regarded as cellular scavengers of activated xenobiotics and involved in antioxidation (Bassuk, Tschlis et al. 1987). However, to date the direct role of L-FABP in oxidative stress has not been investigated. In this report, we used a L-FABP stable transfected Chang liver cell line to test the hypothesis that hepatocyte L-FABP is an important cellular antioxidant during oxidative stress induced by hydrogen peroxide and hypoxia/reoxygenation.

Results

Transfection of Chang liver cells with L-FABP cDNA

To study the role of L-FABP in cellular anti-oxidative stress, the best *in vitro* model is a hepatoma cell line which has no or low L-FABP expression. The human hepatoma cell lines of Chang liver cell, Huh7, HepG2, and PLC/PRF/5 were examined for the expression of L-FABP. As shown in Figure 35, L-FABP mRNA was detected in all cell lines with the exception of Chang liver cell. After stable transfection of Chang liver cell with pcDNA-FABP, more than 30 clones were selected for L-FABP expression identification by RT-PCR; and among them 77 % of the clones expressed the transcript mRNA of L-FABP (Figure 36). Colonies with different expression levels of L-FABP were selected for further study. L-FABP mRNA levels in the selected clones were demonstrated using regular RT-PCR and real-time RT-PCR (Figure 37). Western Blot analysis showed expression of 14 kDa L-FABP protein in pcDNA-FABP transfected Chang liver cells with different expression levels, while control cell transfected with vector (pcDNA3.1) only did not express L-FABP (Figure 38). All L-FABP expressing clones selected for subsequent study were morphologically similar to vector-transfected control cell (Figure 39).

Antioxidant effects of L-FABP

Hydrogen peroxide (H_2O_2) is a commonly used cell membrane permeable precursor of various intracellular free radicals, here it was used to generate an *in vitro* model of cellular oxidative stress. Cellular oxidative stress was monitored with the oxidation sensitive probe 2,7-dichlorofluorescein diacetate (H_2DCFDA). Various

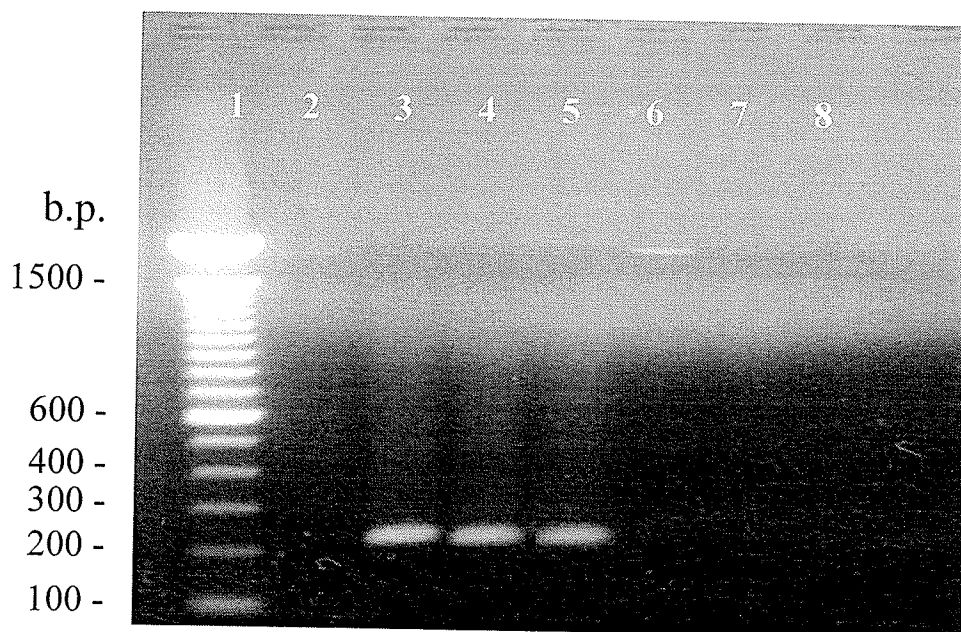


Figure 35. Expression of L-FABP cDNA in hepatoma cell lines by RT-PCR. Total RNA was isolated from different cell cultures. 1 μ g RNA was subject to RT-PCR. The expected PCR product size was 215 bp. Lane 1-Ladder; Lane 2, 6 - Chang; Lane 3- Hep G2; Lane 4-Huh 7; Lane 5-PLC; Lanes 7-Negative Controls; Lane 8 -Blank. Chang cells did not show L-FABP expression.

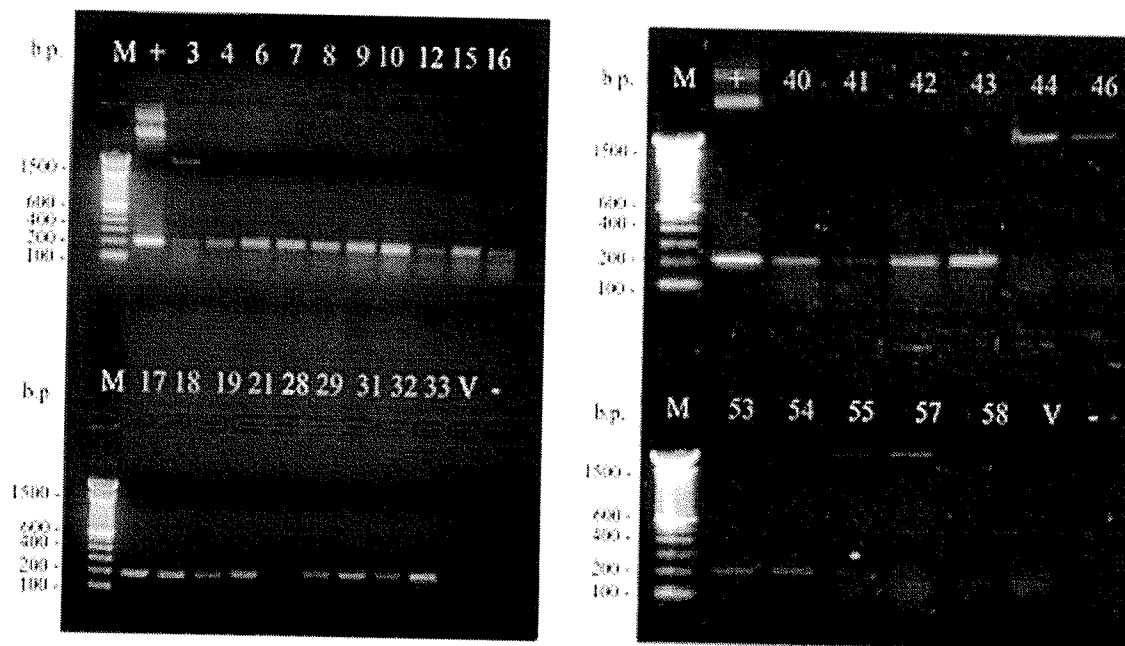


Figure 36. Selection of the pcDNA-FABP transfected Chang liver cells by RT-PCR. 23 out of 30 clones of Chang-FABP transfected cells showed L-FABP mRNA expression. M: DNA ladder; +: Human Liver Marathon-Ready cDNA as positive control; V: Vector; -: Negative control. Vector (pcDNA3.1) transfected Chang liver cell did not expressed L-FABP mRNA.

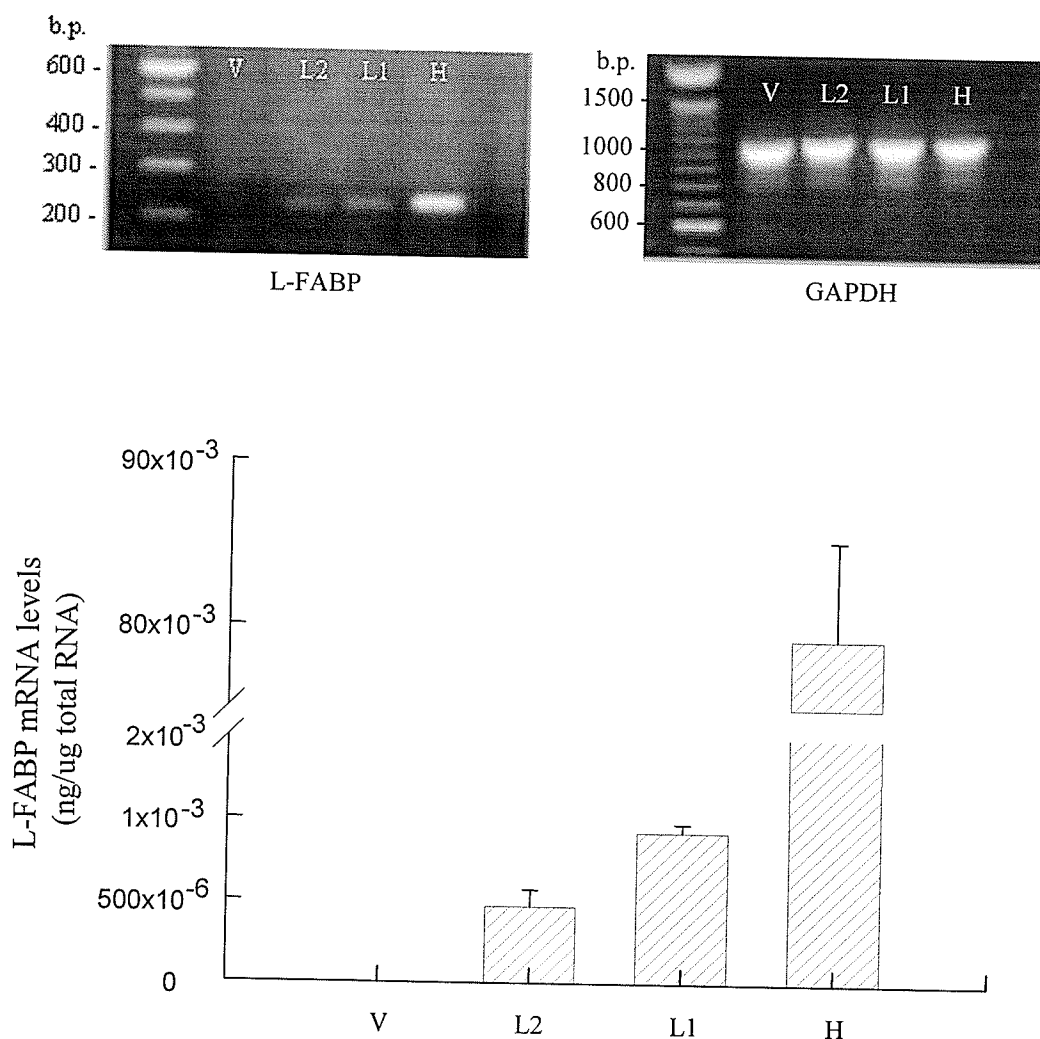


Figure 37. L- FABP mRNA expression levels in selected clones. Top images are RT-PCR images of L-FABP and loading control GAPDH in selected clones. The lower figure shows the L-FABP mRNA concentration (determined by real-time RT-PCR) in total cellular RNA in selected clones. Data represent mean \pm SEM, $n = 4$, *** $p < 0.001$. V represents vector transfected cell; H, high L-FABP expression cell; L1, low L-FABP expression cell; L2, lower L-FABP expression cell.

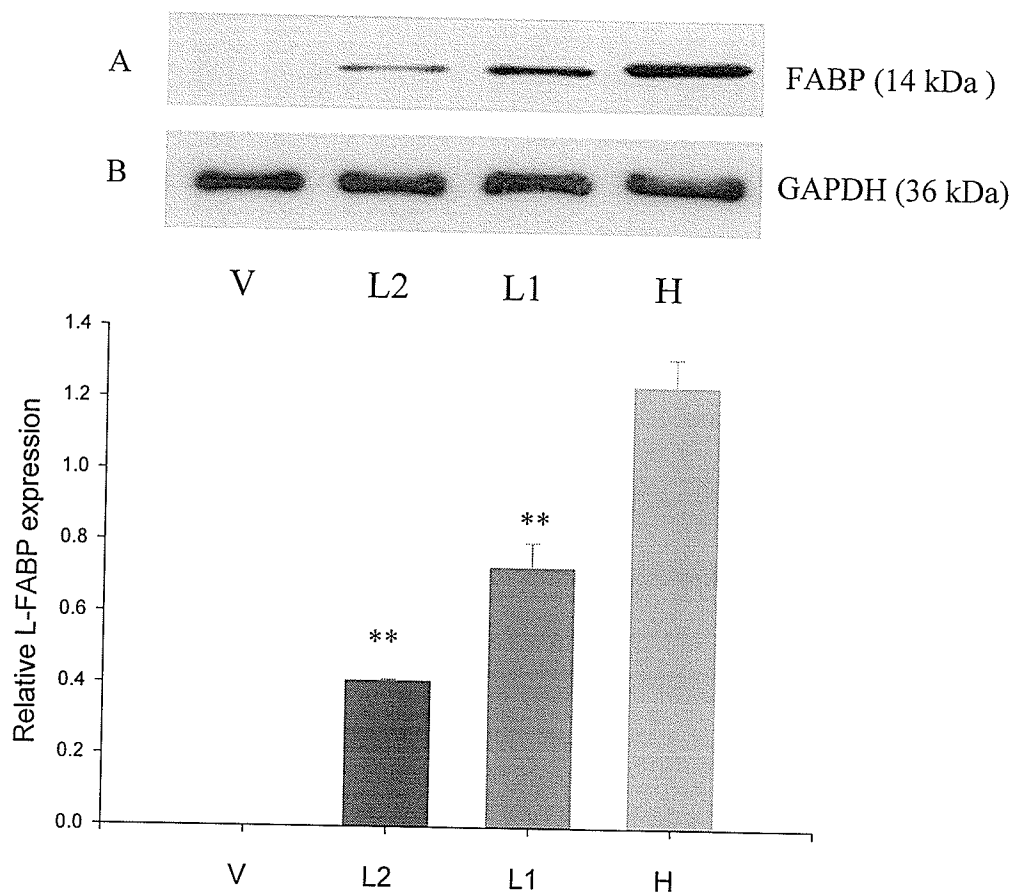


Figure 38. Western blot analysis of L-FABP expression in experimental pcDNA-FABP transfected Chang cells. Panel A shows the expression of the 14 kDa L-FABP protein. Panel B shows the expression of the 36 kDa GAPDH as loading control. V represents vector transfected cell; H, high L-FABP expression cell; L1, low L-FABP expression cell; L2, lower L-FABP expression cell. Protein densities were obtained using an NIH Image program. The relative L-FABP expression was calculated by normalizing L-FABP optical density against GAPDH. Data represent mean \pm SEM, $n = 4$. Vector (pcDNA3.1) transfected Chang cell did not show L-FABP expression. H, L1, and L2 show different expression levels, and their relative expression levels are 1.24 ± 0.08 , 0.73 ± 0.07 , and 0.41 ± 0.004 respectively. ** $p < 0.01$, one tail distribution.

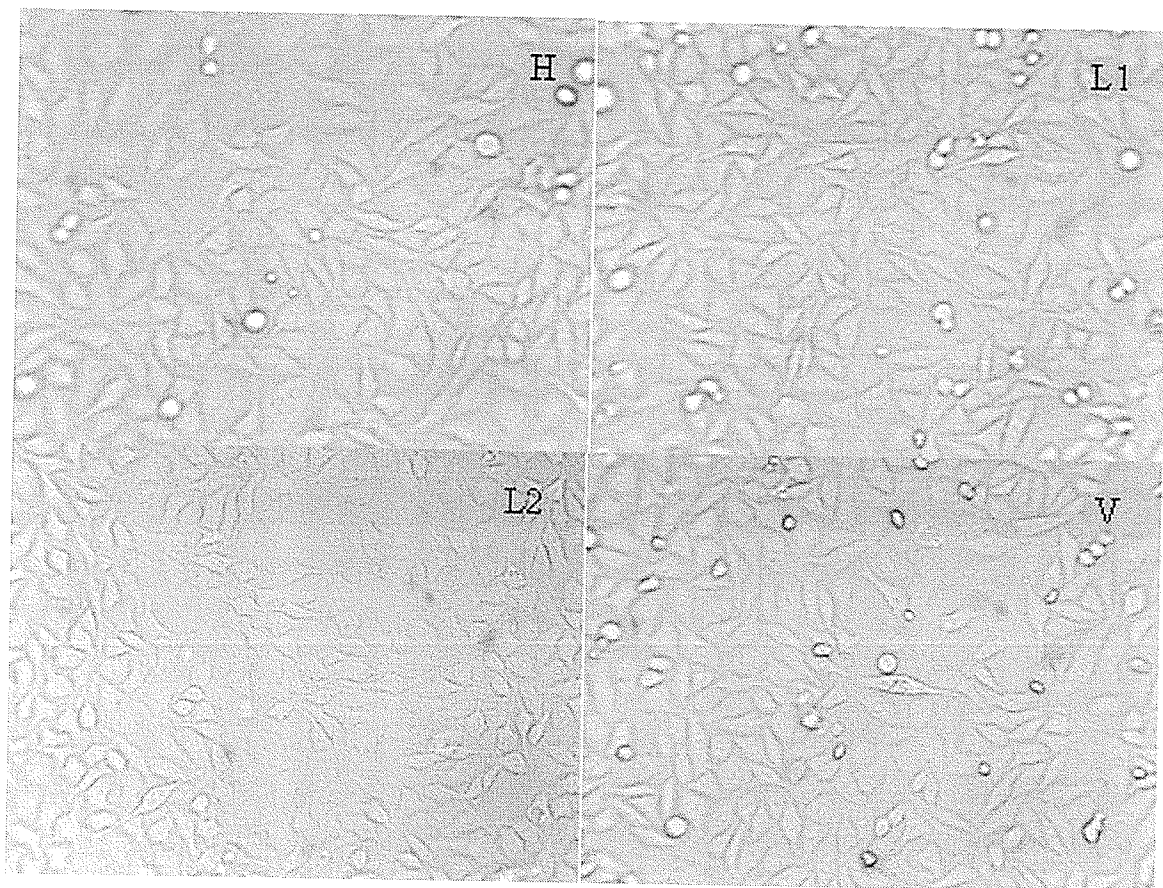


Figure 39. Images of pcDNA-FABP and pcDNA3.1 (vector) transfected Chang liver cells. Cells were cultured in 24 wells plate for 24 hours. Pictures were taken using a Cooke SensiCam CCD camera coupled to a Nikon inverted microscope with Hoffmann Modulation Contrast Optics (20 x objective). V represents vector transfected cell; H, high L-FABP expression cell; L1, low L-FABP expression cell; L2, lower L-FABP expression cell.

reactive oxygen species (ROS) and hydroperoxides oxidize H₂DCFDA, yielding the fluorescent product DCF. Native or modified albumin reportedly suppresses the fluorescence of oxidized DCF (Subramaniam, Fan et al. 2002), but this was not the case for L-FABP expressing cells in our experiments (Figure 40). DMSO, which was used to lyse cells, did not affect DCF fluorescence (Figure 41).

The pcDNA-FABP transfected Chang liver cells with different expression levels were exogenously challenged with 400 μ M H₂O₂ for 20 min at 37 °C. Total intracellular ROS in transfected cells was measured using DCF fluorescence. We observed that DCF fluorescence intensity in L-FABP transfected cells was significantly reduced ($p < 0.01$) as with L-FABP expression increased (Figure 42). The relative DCF fluorescence images were shown in Figure 43. All L-FABP expressed cells had lower DCF fluorescence intensity than the non L-FABP expressed vector-transfected control cell. This inverse relationship between L-FABP and DCF fluorescence intensity was interpreted to mean that intracellular L-FABP was able to function as an intracellular antioxidant and had the ability to play a major role in the oxidative stress induced by hydrogen peroxide.

Antioxidant effects of L-FABP on Oxidative stress induced by hypoxia/reoxygenation

Hepatic ischemia-reperfusion is related to the generation of reactive oxygen species (ROS), and results in liver injury through oxidative stress (Jaeschke 2003). The pcDNA-FABP transfected Chang cells and vector control cell were exposed to hypoxia for 3 hours then reoxygenated for another 3 hours. The DCF fluorescence intensity of each L-FABP expressed cell was lower than non L-FABP expressed vector control cell.

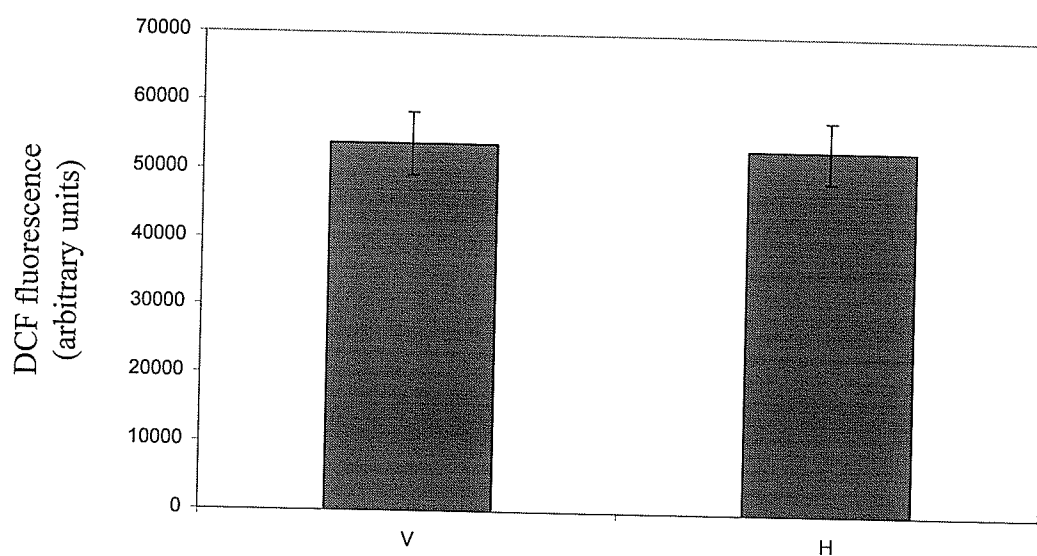


Figure 40. Testing the effect of L-FABP on the fluorescence intensity of DCF. The fluorescence intensity of 2 nM DCF was recorded in the presence of 20 μ g of cytosolic proteins from Vector (V, without L-FABP) and High L-FABP expression (H, with L-FABP) clones respectively. The results were expressed in arbitrary fluorescence units (53899 ± 4537 for V and 53277 ± 4395 for H, $p > 0.05$, $n = 6$). Fluorescence of DCF was unaffected by the presence or absence of L-FABP.

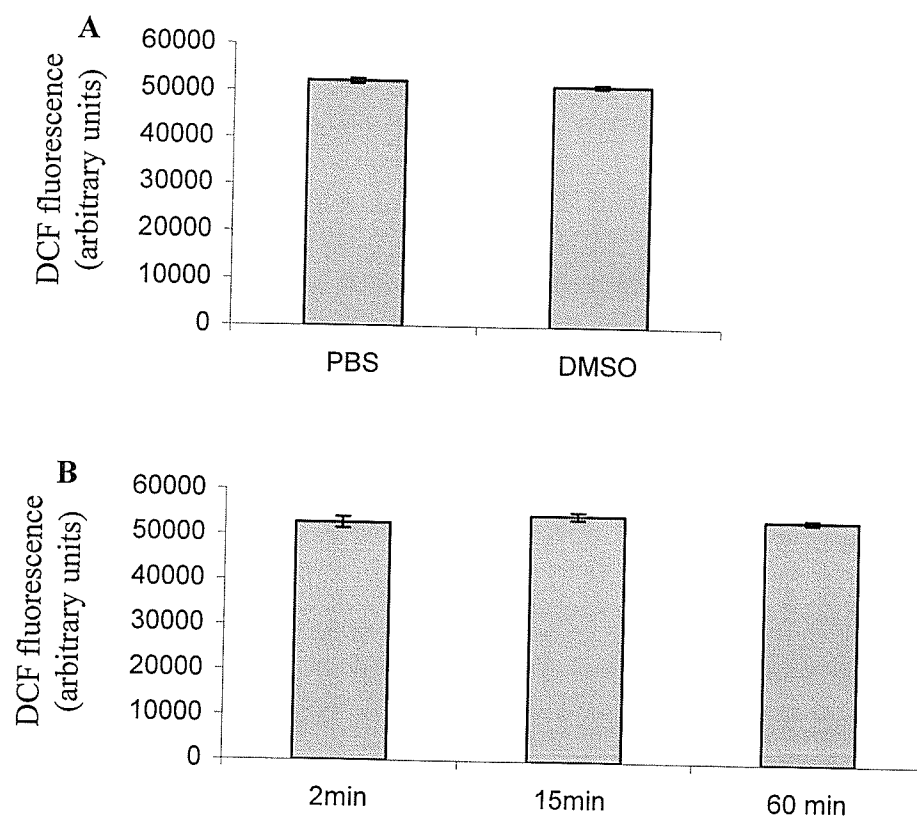


Figure 41. Testing the effect of DMSO on DCF fluorescence intensity. 2 nM DCF was made in PBS and DMSO respectively. Fluorescence intensities were measured by Fluostar Galaxy fluorescence plate reader. (A) Fluorescence of DMSO solution was measured at 2, 15, and 60 min; (B) fluorescence of DCF was unaffected by DMSO and stable over one hour ($p > 0.05$, $n = 6$).

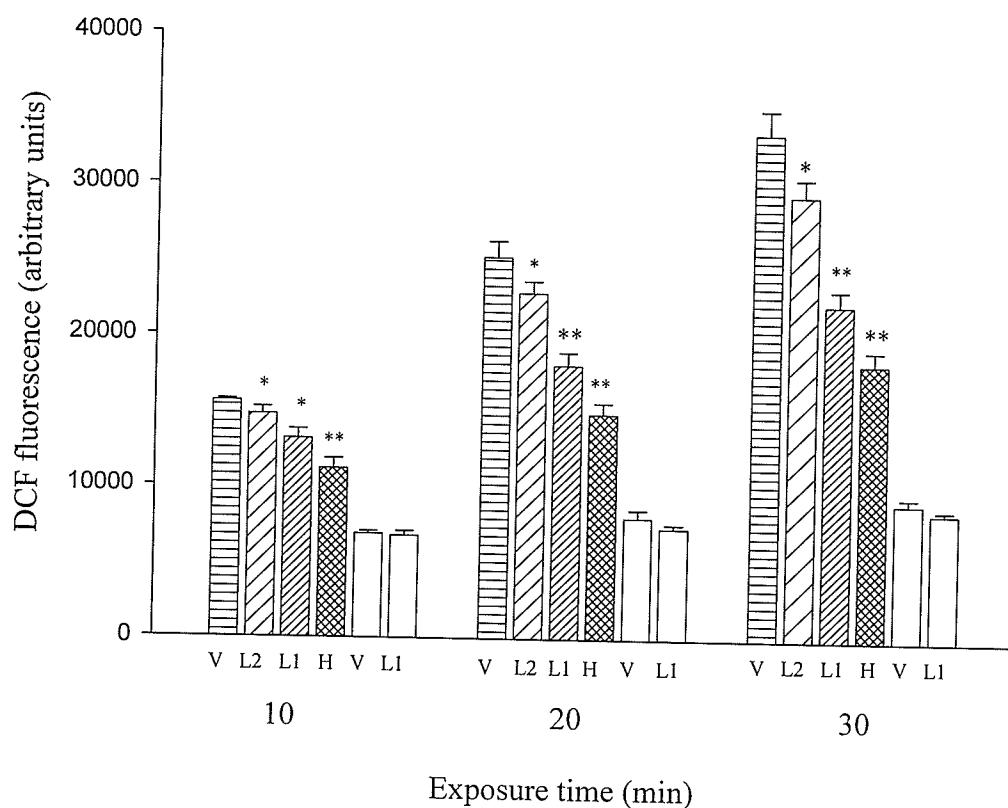


Figure 42. DCF fluorescence of pcDNA-FABP transfected Chang cells in oxidative stress induced by hydrogen peroxide. Cells were cultured in 96-well plates. 100 μ M H_2DCFDA was loaded onto cells for 30 min. Cells were subsequently exposed to 400 μ M H_2O_2 for 10, 20, and 30 min. Cellular fluorescence in each well was measured and immediately recorded. Data are represented as mean \pm SEM, $n = 8$, ** $p < 0.01$, * $p < 0.05$, one tail distribution. V represents vector transfected cell; H, high L-FABP expression cell; L1, low L-FABP expression cell; L2, lower L-FABP expression cell. Hollow bars represent negative controls of L-FABP expressed cells (L1) and no FABP expressed cells (V). No significant differences were found in negative control group. The DCF fluorescence intensity was proportional to the level of cellular reactive oxygen species (ROS). The figure shows DCF intensity reduced with increased L-FABP.

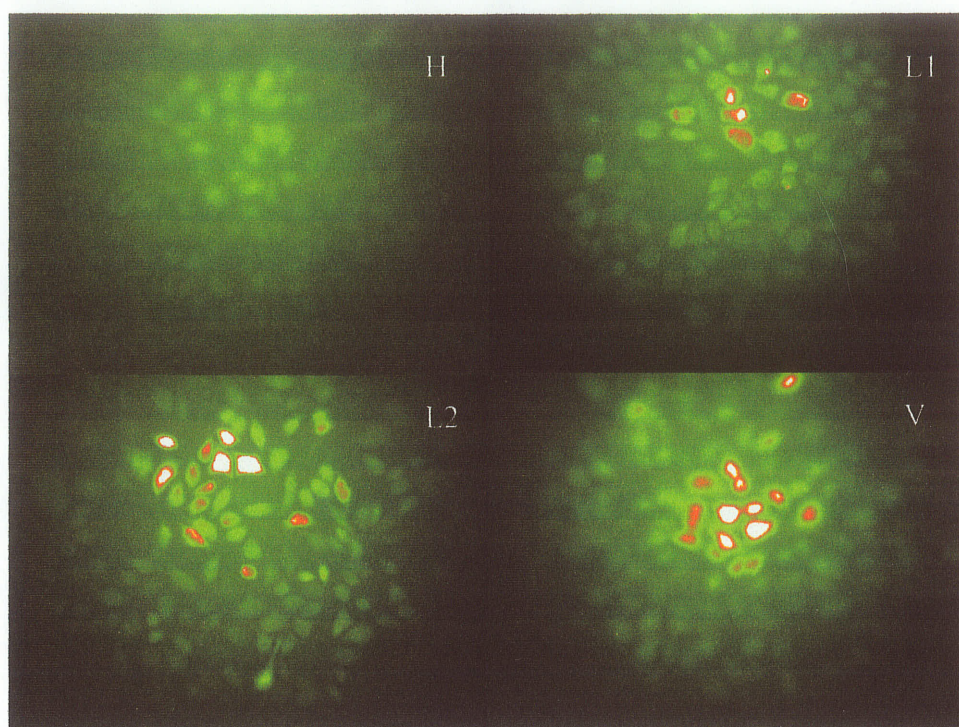


Figure 43. Representative photomicrograph depicting decreased DCF fluorescence in pcDNA-FABP transfected Chang cells in oxidative stress induced by hydrogen peroxide. Cells were cultured in 24 well plates. 100 μ M H₂DCFDA was loaded onto cells for 30 min. Cells subsequently exposed to 400 μ M H₂O₂ for 20 min. Brighter colours represent increased levels of oxidative products with “green” to “red” for elevated levels of ROS. “White” indicates saturated levels of “red”. V represents vector transfected cell; H, high L-FABP expression cell; L1, low L-FABP expression cell; L2, lower L-FABP expression cell. The DCF fluorescence intensity is reduced with increased L-FABP levels.

DCF fluorescence intensity was inversely proportional to the L-FABP expression level: the higher the L-FABP level, the lower was the DCF fluorescence intensity (Figure 44). These data show that L-FABP expression reduced the level of intracellular ROS generated during cellular oxidative stress induced by hypoxia-reoxygenation in vitro.

The protective effect of L-FABP on hepatic hypoxia/reoxygenation injury was assessed by detecting cellular lactate dehydrogenase (LDH) release. LDH is a cytosolic enzyme present within all mammalian cells. The normal plasma membrane is impermeable to LDH, but damaging cell membrane results in membrane permeability increases and subsequent leakage of LDH into the extracellular fluid. Release of LDH into culture supernatant correlates with reduced cell membrane integrity and cell viability. We used the LDH release assay to evaluate the potential damage of oxidative stress on hepatocytes with different levels of L-FABP expression. As shown in Figure 45, a significant increase in LDH release was found in all transfected Chang liver cells after hypoxia/reoxygenation ($p < 0.01$) compared to the negative control cells. As the L-FABP level decreased, more LDH was detected ($p < 0.01$) in the culture solution. These observations further reinforced the notion that L-FABP provides cytoprotection against the oxidative stress induced by hypoxia/reoxygenation. This protection is most likely due to scavenging of intracellular ROS by L-FABP.

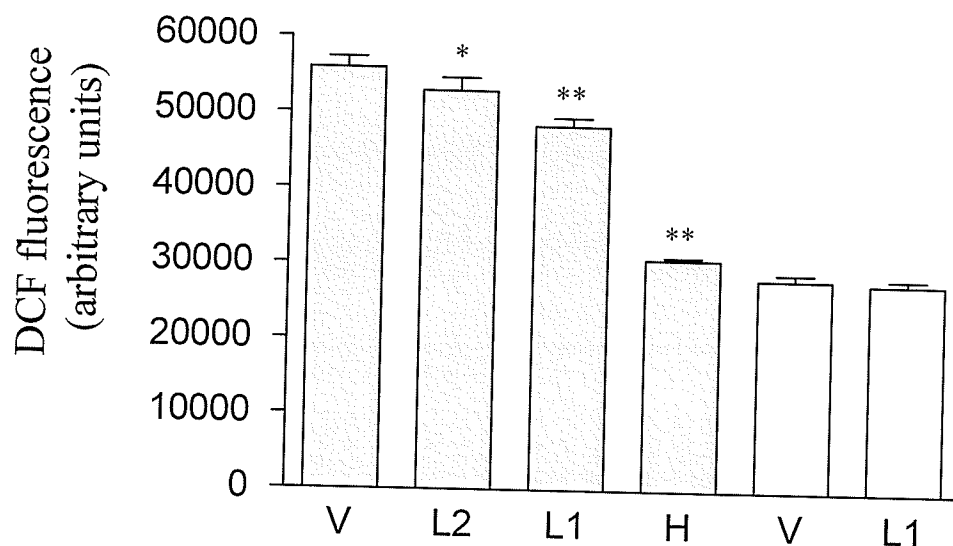


Figure 44. DCF fluorescence in pcDNA-FABP transfected Chang cells subjected to hypoxia-reoxygenation. Cells were cultured in 30-mm tissue culture dishes and exposed to hypoxia (3 hour in 95 % N₂/5 % CO₂)-reoxygenation (3 hour in 95 % O₂/5 % CO₂). After sampling 100 μ L supernatant, 100 μ M H₂DCFDA was loaded onto cells for 30 min. Cells were lysed with DMSO and harvested for DCF fluorescence measurement. Data are presented as mean \pm SEM (n = 4), ** p < 0.01, * p < 0.05, one tail distribution. Hollow bars represent negative control sample that was performed by incubating cells with 95 % O₂/5 % CO₂ for 6 hours. V represents vector transfected cell; H high L-FABP expression cell; L1, L2 low and lower L-FABP expression cells. In the negative control group, there was no significant difference in cells with different L-FABP expression levels. However, the DCF fluorescence intensity was reduced with increasing cellular L-FABP expression in the experimental group.

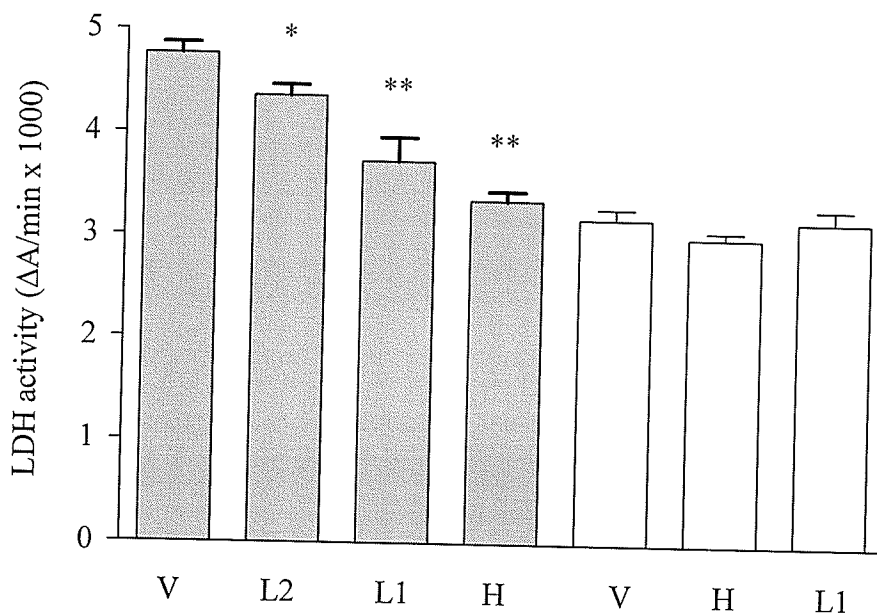


Figure 45. LDH release from L-FABP transfected Chang cells subjected to hypoxia/reoxygenation (3 hours hypoxia and 3 hours reoxygenation). Hollow bars represent negative control samples. Solid bars represent hypoxia/reoxygenation samples. Negative control experiment was performed by incubating cells with 95 % O₂/5 % CO₂ for 6 hours. LDH activity was measured as absorbance at 340 nm, expressed as the rate of absorbance change per minute. Data are presented as mean \pm SEM (n = 4), ** p < 0.01, * p < 0.05, one tail distribution. V represents vector transfected cell; H high L-FABP expression cell; L1, L2 low and lower L-FABP expression cells. In negative control samples, there were no significant differences in the cells with different L-FABP expression levels. However, LDH release was decreased with an increase in cellular L-FABP level.

Discussion

In the nearly last three decades, remarkable advances have been made in understanding the structure and biology of FABPs. Although their complete tertiary structure, gene organization, and binding properties are known, the functional aspects of these proteins are still undergoing investigation. Previous reports have suggested that FABP has protective role by: 1) controlling the availability of free fatty acids and their metabolites in the cytosol, and which prevents their cellular toxicity (Raza, Pongubala et al. 1989; Veerkamp, van Kuppevelt et al. 1993; Vork, Glatz et al. 1993; Glatz and van der Vusse 1996; Atshaves, Storey et al. 2002), 2) modulating the interaction of fatty acids with nuclear receptors (Huang, Starodub et al. 2004), 3) sequestering or removing cytotoxic drugs (Sinha, Hutter et al. 1999), and 4) trapping or scavenging reactive oxygen species (ROS) (Samanta, Das et al. 1989; Catala, Cerruti et al. 1995; Ek, Cistola et al. 1997; Ek-Von Mentzer, Zhang et al. 2001; Guajardo and Terrasa 2002). However, no significant protective effects of FABP had been observed for anti-chemical anoxia and decreased intracellular fatty acid accumulation using the FABP transfected kidney cell (MDCK) model (Zimmerman and Veerkamp 2001). Therefore, further evidence is required to elucidate the putative cytoprotective function of FABPs. Furthermore, the extent of protective function that L-FABP offers against oxidant-induced oxidative stress in cells has not been directly studied. To fill this gap, we selected Chang liver cell model, which we determined to have undetectable L-FABP mRNA, as the target for L-FABP cDNA transfection. The transfected cells with different levels of L-FABP expression were conducted to study the putative cytoprotective role of L-FABP on a simulated oxidative stress system.

Oxidative stress is involved in the pathogenesis of most chronic disease. In addition to being a cellular signal, ROS may initiate damaging biochemical reactions (Halliwell 1999). In response to high levels of ROS, cells protect themselves against oxidative stress using a variety of free radical scavengers including SOD, glutathione, and catalase. In some cases, however, (e.g., diseases or drug exposure) the titer of these enzymes may be too low to enable adequate protective function (Csonka, Pataki et al. 2000; Orellana, Rodrigo et al. 2000; Khynriam and Prasad 2002). It is likely that cells have another mechanism to deal with such high ROS levels. In this study, we investigated the effect of L-FABP cDNA transfection of Chang liver cells on oxidative stress induced by hydrogen peroxide and hypoxia/reoxygenation. DCF fluorescence intensities were higher in both experiments, suggesting elevated ROS levels in experimental cells. L-FABP expressed cells demonstrated lower DCF fluorescence intensity; this decrease of fluorescence intensity was correlated with an increased level of cellular L-FABP expression. Moreover, LDH release, a marker of cell damage, was decreased in cells that expressed L-FABP while undergoing hypoxia/reoxygenation oxidative stress. The extent of the reduction in LDH release was proportional to the cellular L-FABP expression. These results suggested a cytoprotective function of L-FABP against oxidative stress. The protective mechanism of L-FABP in oxidative stress is likely a result of the protein either inhibiting or scavenging ROS.

L-FABP is very likely to be an effective endogenous antioxidant as it has high affinity and capacity to bind long chain fatty acid oxidative products (Raza, Pongubala et al. 1989; Ek-Von Mentzer, Zhang et al. 2001). It also has a very favorable protein structure and redox conditions, such as large portion of the intracellular protein pool

(approximately 0.4 mM in hepatocyte cytosol) (Burnett, Lysenko et al. 1979), a large number of reducing amino acid residues (methionines and cysteine), and a high expression level of methionine sulfoxide reductase (Moskovitz, Jenkins et al. 1996). Oxidized methionine (methionine sulfoxide) can be reduced back to its reducing form by methionine sulfoxide reductase (Levine, Berlett et al. 1999; Moskovitz, Berlett et al. 1999). The cyclic oxidation-reduction of methionine residues of protein may contribute an important antioxidant function by the conversion of reactive oxygen species (ROS) to innocuous products (Levine, Mosoni et al. 1996; Stadtman 2004). Cysteine residue may be involved in the binding of other hydrophobic ligands or serve as an antioxidant participating in S-thiolation/dethiolation (Thomas, Poland et al. 1995; Sato, Baba et al. 1996).

We investigated the effect of L-FABP cDNA transfection of Chang liver cell on oxidative stress induced by hydrogen peroxide and hypoxia/reoxygenation. DCF fluorescence intensities were higher in both experiments, suggested elevated ROS levels in experimental cells. L-FABP expressed cells demonstrated lower DCF fluorescence intensity; this decrease of fluorescence intensity was correlated with an increased level of cellular L-FABP expression. Moreover, LDH release, a marker of cell damage, was decreased in cells that expressed L-FABP while under hypoxia/reoxygenation oxidative stress. The extent of the reduction in LDH release was proportional to the cellular L-FABP expression. These results suggested a cytoprotective function of L-FABP against oxidative stress. The protective mechanism of L-FABP in oxidative stress is likely a result of the protein either inhibiting or scavenging ROS. Collectively, our data provide evidence that support the notion that L-FABP plays a significant role as an endogenous

cellular antioxidant against the oxidative stress induced by hydrogen peroxide and hypoxia/reoxygenation.

It is known well that peroxisome proliferators up-regulate L-FABP expression through activation of peroxisome proliferator activated receptors (PPARs) (Veerkamp and Maatman 1995; Bernlohr, Simpson et al. 1997). Peroxisome proliferators increase intracellular levels of peroxisomes (Reddy and Lalwai 1983; Bentley, Calder et al. 1993) resulting in an overproduction of hydrogen peroxide (Goel, Lalwani et al. 1986; Tamura, Iida et al. 1990). Hydrogen peroxide is a precursor of ROS, and is proposed to contribute to the hepatocarcinogenic effects of peroxisome proliferators (Reddy and Rao 1989). In addition to damaging DNA, high levels of hydrogen peroxide may be expected to oxidize hepatic proteins and lipids. Interestingly, few studies have examined the effect of peroxisome proliferators on hepatic protein oxidation and lipid peroxidation, but the results were contradictory (Perera, Katyal et al. 1986; Tomaszewski, Agarwal et al. 1986; Elliott and Elcombe 1987). Moreover, recent studies indicate that hepatic levels of hydrogen peroxide and lipid products are not increased in the animals treated with peroxisome proliferators (Handler, Seed et al. 1992; Conway and Popp 1995). Contrary, nafenopin-pretreatment increased hepatic resistance to cytotoxicity induced by hydrogen peroxide in rats (Garberg, Stenius et al. 1992). Furthermore, various peroxisome proliferators have been found to be involved in cytoprotection against hepatotoxicity and oxidative stress (Tuchweber and Salas 1978; Deplanque 2004). The protection mechanism that peroxisome proliferators afford is poorly understood. The increased glutathione availability and catalase activity by clofibrate were not the primary protective pathway in the protection against acetaminophen-induced hepatotoxicity and hepatic lipid

peroxidation (Nicholls-Grzemeski, Belling et al. 2000; Nicholls-Grzemeski, Calder et al. 2000; Chen, Hennig et al. 2002), there must be some other cellular defense pathway involved in the hepatic protection by clofibrate. Is liver FABP modulation likely to be this defense pathway? It is reported that clofibrate treatment increased cytosolic concentrations of L-FABP 4.7-fold (Milliano and Luxon 2001). We also found that clofibrate treatment showed hepatic protection in bile duct ligation (BDL) rats. The hepatic lipid peroxidation product was reduced by 68 % as compared to without clofibrate treated BDL rats (data are reported in the next section). Taken together with our current data, the results suggest that L-FABP is a strong candidate player in a defense pathway against oxidative stress. Future study will delineate the antioxidation function of L-FABP by using recombinant protein and gene mutation techniques.

The role of L-FABP as a cytoprotectant will be extended to investigate its involvement in liver diseases (e.g., cirrhosis), drug-induced hepatotoxicity and liver transplant damage (ischemia/reperfusion). This would make L-FABP a very powerful endogenous antioxidant, the level of which may be a relatively easy target strategic prevention of damage increased prior to and during the course of therapeutic drug management and in organ preservation.

Section D. Expression and antioxidant function of liver fatty acid binding protein in normal and bile-duct ligated rats

Introduction

Cholestatic liver disease is caused by biliary obstruction that leads to either primary biliary cirrhosis or primary sclerosing cholangitis. Although the mechanism of cholestatic liver disease is not completely understood, oxidative stress has been recognized as an important factor in the disease process (Ljubuncic, Tanne et al. 2000; Aboutwerat, Pemberton et al. 2003). One of the experimental models used to study cholestatic liver disease is the bile duct ligation (BDL) model (Kountouras, Billing et al. 1984). BDL was reported to decrease antioxidant activities of hepatic catalase, superoxidase (SOD) and glutathione peroxidase (GTPx) (Orellana, Rodrigo et al. 2000), and liver mitochondria antioxidative capacity and glutathione (GSH) (Krahenbuhl, Talos et al. 1995). Thus, other endogenous antioxidant systems may have a critical role in protecting the liver from extensive damage.

L-FABP has been postulated to be an intracellular protective buffer of LCFAs and their CoA and carnitine esters to maintain a low concentration of the unbound form of these substances within the cell, and also may act as a trapper or scavenger to inhibit or clear cytotoxins and superoxide species thus protecting cells (Khan and Sorof 1990; Kaikaus, Sui et al. 1993; Ek-Von Mentzer, Zhang et al. 2001; Luebker, Hansen et al. 2002). Furthermore, L-FABP forms a large portion of the intracellular protein pool and contains a large number of methionines and cysteine residues which have the potential to function as antioxidants (Thomas, Poland et al. 1995; Levine, Berlett et al. 1999). In this study, I tested the hypothesis that L-FABP has an important function as a cytoprotectant

against oxidative stress. The expression and antioxidative function of L-FABP in an animal model of cholestatic liver disease induced by bile duct ligation (BDL) were documented.

Results

Liver injury following BDL

As shown in Figure 46, bile duct proliferation and mononuclear cell infiltration were detected in the portal area of the BDL rat liver sections. Macrovascular cytoplasmic alterations of hepatocytes and many apoptotic cell lysis were observed in the BDL group. BDL was also associated with a significant proliferation of bile duct epithelial cells, inflammation, and altered liver structure.

L-FABP expression in BDL rats

Rat liver tissue was obtained at different time points (0.25, 0.5, 1, 2, 3, 7, 14, 21, 28 and 35 days) following BDL. L-FABP mRNA expression and L-FABP level at each time point were measured by RT-PCR and Western Blot respectively. L-FABP mRNA expression started to decline significantly ($p < 0.05$) after 2 days of BDL. A dramatic decrease in L-FABP mRNA expression was observed after one week of BDL (Figure 47). Reduction in L-FABP mRNA abundance caused a decrease in L-FABP protein level. After two weeks of BDL, L-FABP protein level was almost undetectable by Western blot (Figure 48).

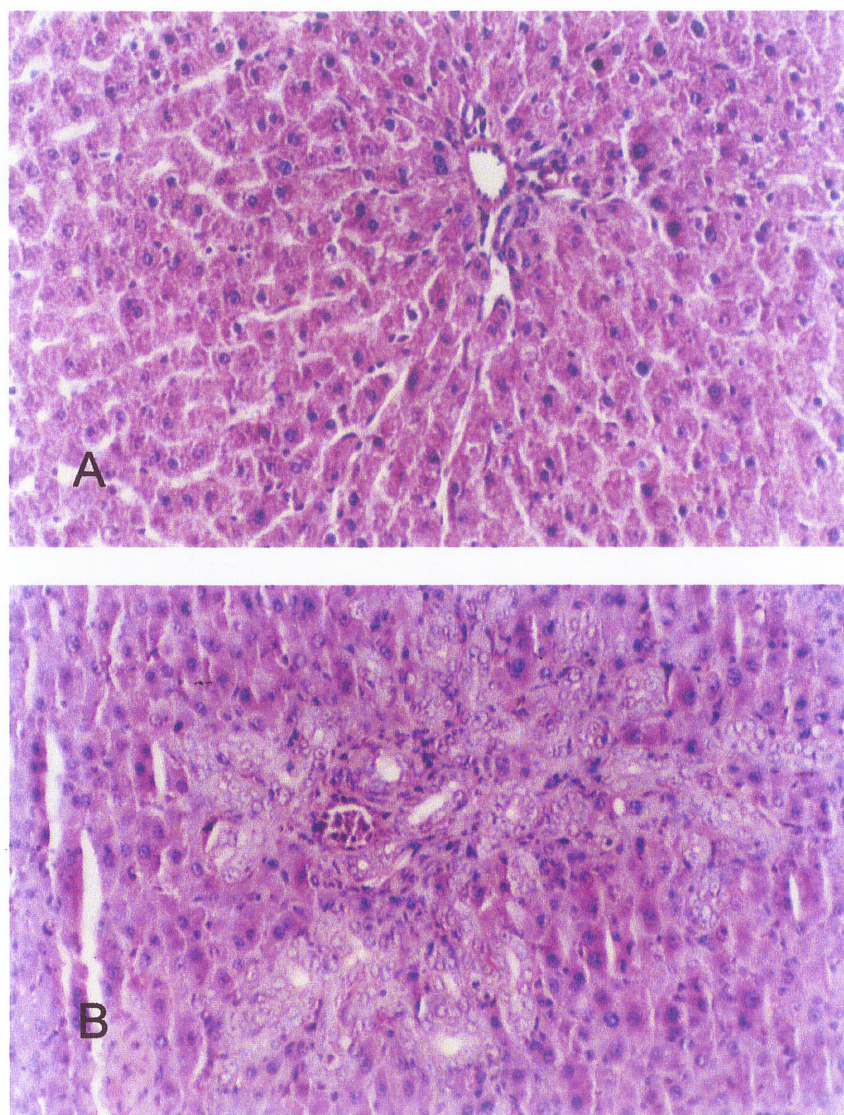


Figure 46. Liver sections from Sham and BDL rats. (A) Normal hepatocytes in portal area from the rat of Sham group. (B) Mild bile duct proliferation and mononuclear cell infiltration in portal area from the rat of two weeks post BDL group.

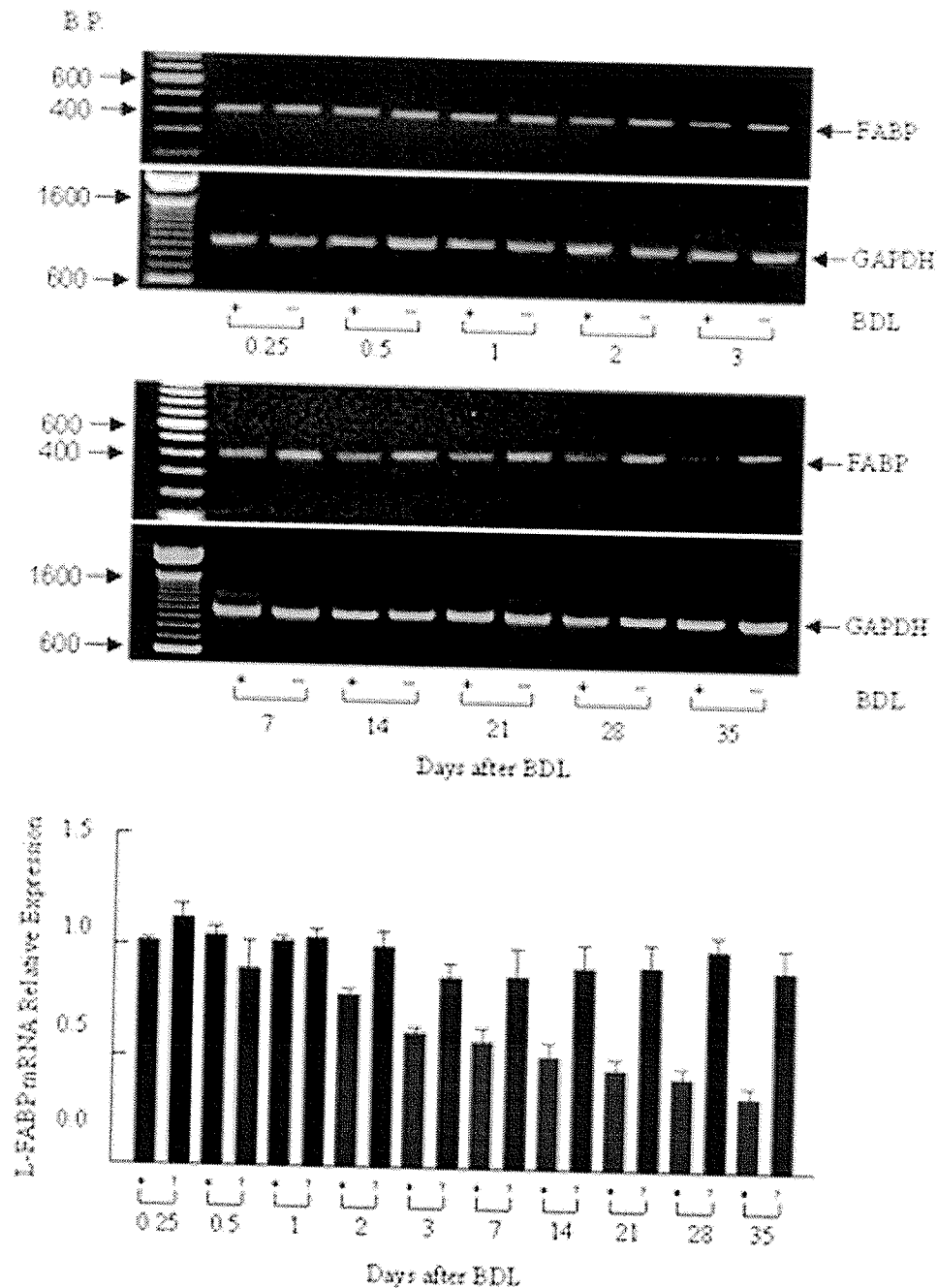


Figure 47. RT-PCR analysis of L-FABP mRNA at different times following BDL. GAPDH was used as the loading control. Optical density of each band was obtained using the NIH Image program. Relative expression of L-FABP mRNA versus GAPDH was displayed against time following BDL. Significant decrease of L-FABP mRNA level occurred after 48 hours of BDL. Data represent mean \pm SEM, $n=4$.

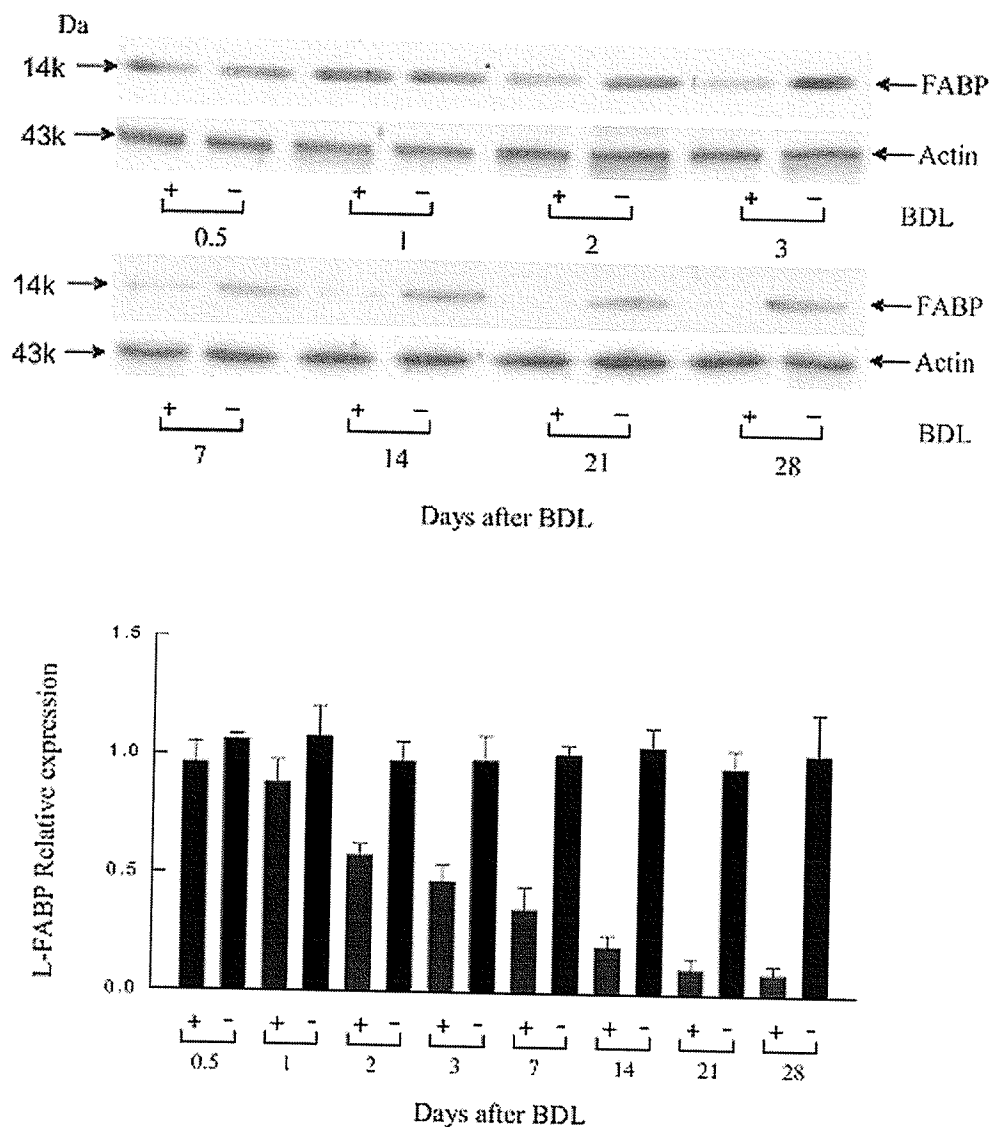


Figure 48. Western blot analysis of L-FABP levels in BDL and sham rat livers at different time points following BDL. Actin expression served as the loading control. L-FABP relative expression (optical density units) in each band was obtained using an NIH Image program and expressed as L-FABP versus Actin. Data represent mean \pm SEM, n=4. The significant change in L-FABP with time started after 48 hours of BDL, $p < 0.05$.

TBARS, Serum bilirubi, ALT and ammonia levels of the rats

Serum bilirubin, ALT and ammonia levels were examined in sham and BDL rats. Results shown in Table 8 indicate that BDL was associated with a significant increase in serum bilirubin, ALT and ammonia (increased by 3760 %, 245 %, and 266 %, respectively), reflecting liver dysfunction. It has been proposed that lipid peroxidation plays an important role in liver injury. Malonaldehyde (MDA) is one of the main end products of the lipid peroxidation process. The TBARS assay is a common method used to assess lipid peroxidation levels and thus is indicative of tissue oxidative stress. As shown in Figure 49, TBARS production was increased following BDL in a time dependent manner. A significant ($p < 0.05$) increase occurred after 7 days of BDL, indicating animals were experiencing hepatic oxidative stress and liver dysfunction. The increase in TBARS production was closely associated with the decrease in L-FABP content.

To further elucidate the association between TBARS production and L-FABP, we examined whether the reduction in L-FABP was responsible for the induction of liver lipid peroxides. To this end, rats were administered clofibrate to up-regulate L-FABP expression. L-FABP expression is known to be regulated by PPAR agonists such as clofibrate (Burczynski, Fandrey et al. 1999). As shown in Figure 50, after BDL L-FABP mRNA level was reduced to 58 % as compared to the sham group. Clofibrate restored L-FABP mRNA and protein level back to 74 % and 79 % of the sham group, respectively. The restoration of L-FABP level resulted in decreased lipid peroxidation products in both serum and liver (Table 8). Moreover, the up-regulation of L-FABP was associated with a significant decrease in serum bilirubin, ALT and ammonia levels by 193 %, 139 %, and

Table 8. Serum levels of Bilirubin, ALT, Ammonia, and TBARS and liver TBARS level in Sham, BDL, and BDL + Clofibrate treated rats. Clofibrate treatment (50 mg/100 g body weight) started at 5th day of BDL and continued for 7 days. Data are presented as mean \pm SEM, n = 4, * p < 0.05, ** p < 0.01

	Sham	BDL	BDL + Clofibrate
TBARS (nmol/mg protein)	0.176 \pm 0.041	0.394 \pm 0.029 **	0.266 \pm 0.053 *
TBARS (nmol/ml serum)	0.100 \pm 0.023	0.309 \pm 0.039 **	0.212 \pm 0.032 *
Total Bilirubin (mg/dL)	0.25 \pm 0.07	9.40 \pm 0.51 **	4.87 \pm 0.90 **
ALT (U/L)	17.43 \pm 0.99	42.67 \pm 3.35 **	30.70 \pm 3.26 *
Ammonia (umol/L)	102.6 \pm 9.4	273.1 \pm 29.6 **	205.7 \pm 16.6 *

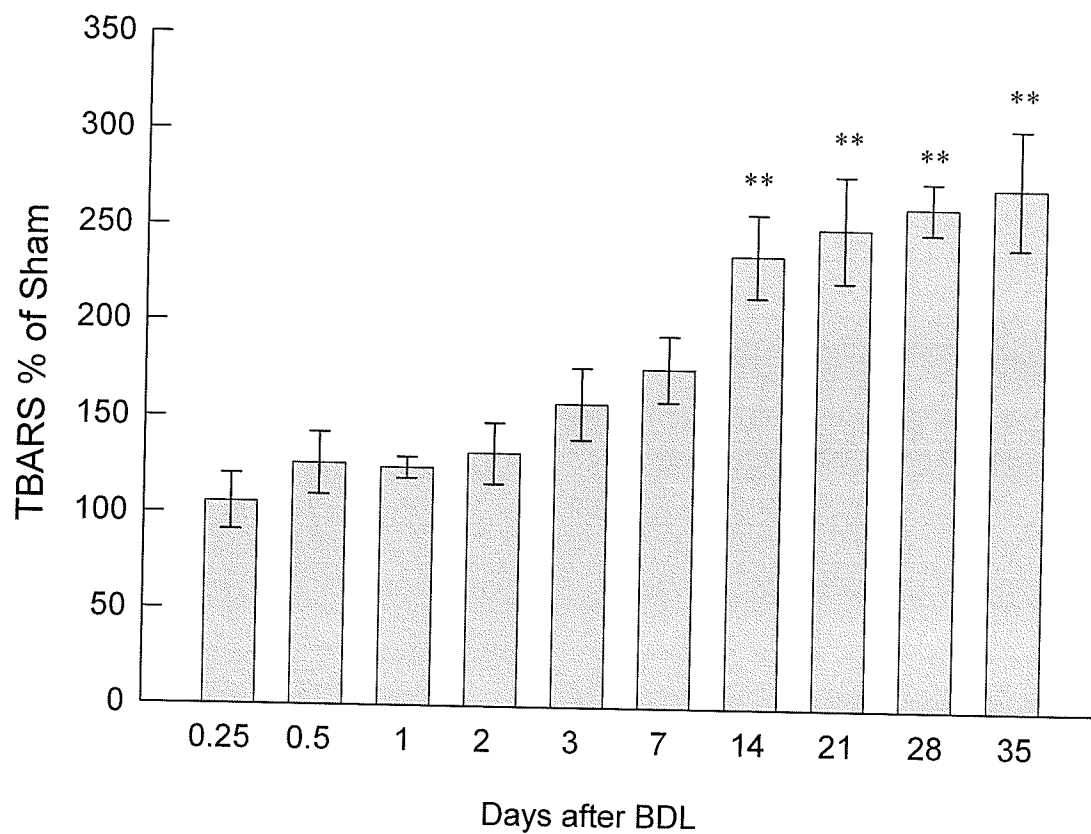


Figure 49. Increased TBARS production in liver tissue from BDL rats. Liver TBARS production was determined by measurement of absorbance at 532 nm using HPLC. The degree of lipid peroxidation was expressed as concentration of TBARS in terms of MDA equivalents per gram of liver proteins. The plot shows a significant TBARS increase in BDL rats compared to sham following 14 days of BDL (** $p < 0.01$, mean \pm SEM, $n = 4$).

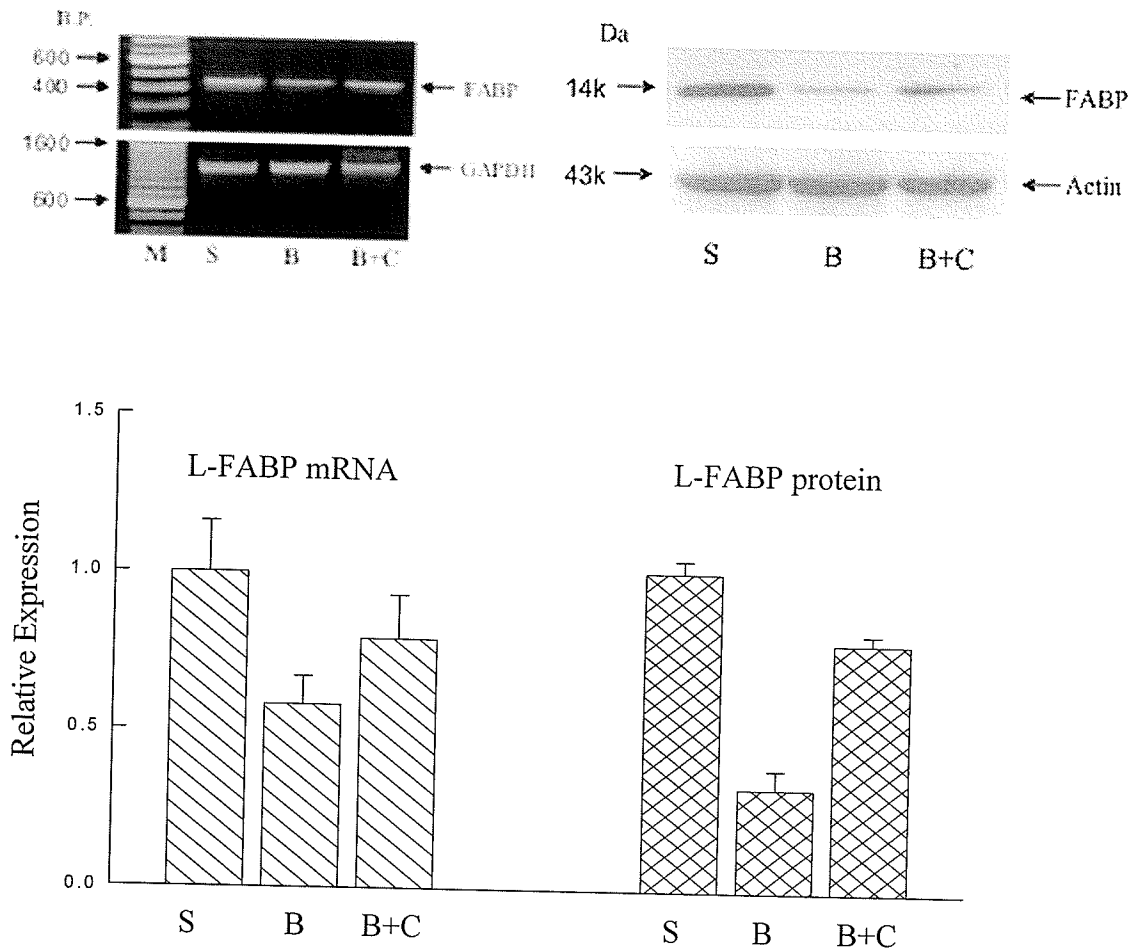


Figure 50. Clofibrate reverses reduction of L-FABP mRNA and L-FABP level in BDL rats. Clofibrate was administered to rats for 5 days (50mg/day/100 g body weight) by gavage after 7 days BDL (total time 12 days). S represents sham rats; B represents BDL rats; B+C represents BDL rats with clofibrate treatment. Lower figure represents the mean \pm SEM, $n = 4$.

133 % respectively as compared to BDL only animals (Table 8). These data indicate that L-FABP is involved in the reduction of hepatic oxidative stress and improvement of hepatic function in BDL rats.

Discussion

Bile duct ligation is a typical model of biliary disease in animals, which features proliferation of bile duct epithelial cells, hepatocellular necrosis and apoptosis, stellate cell activation, and eventually the formation of liver fibrosis and cirrhosis (Scobie and Summerskill 1965; Kountouras, Billing et al. 1984). BDL has been associated with hepatic mitochondrial dysfunction that includes oxidative damage to mitochondrial proteins and lipids, and cytotoxicity of bile components such as the lipophilic bile acids (Krähenbühl, Talos et al. 1994; Krähenbühl, Talos et al. 1994; Hino, Morita et al. 2001). The detergent action and cytotoxicity of bile salts is partly responsible for the plasma membrane damage seen in BDL models which leads to further oxidative stress (Sokol, Winklhofer-Roob et al. 1995). Extensive oxidative damage results from the release of reactive oxygen species (ROS, free radicals) that most likely result from a lack of adequate ROS scavengers. For example, hepatic glutathione in BDL animals shows a continuous decrease in reduced glutathione (GSH) and an increase in oxidized glutathione (GSSG) levels (Neuschwander-Tetri, Nicholson et al. 1996; Purucker, Winograd et al. 1998; Baron and Muriel 1999). Hepatic ubiquinones (lipophilic membrane associated antioxidants) also were reported to be decreased in BDL animals (Krahenbuhl, Talos et al. 1995), as were the enzyme activities of cytosolic water soluble antioxidants such as superoxide dismutase (SOD), catalase, and glutathione peroxidase

(GTPx) (Orellana, Rodrigo et al. 2000). Exogenous antioxidants such as vitamin E or trolox, vitamin C and silymarin do not prevent the damage induced by BDL (Baron and Muriel 1999; Muriel and Moreno 2004). BDL also is associated with decreased microsomal and peroxisomal fatty acid metabolism (Orellana, Avalos et al. 1997). Since processing of intracellular long-chain fatty acids is disrupted, it is likely that L-FABP is involved in this disease state. Our results are consistent with this notion. L-FABP levels were observed to be statistically lower by day 2 of BDL. The decline in L-FABP level progressed with time following BDL. The decrease in L-FABP level may, however, be due to the reduced number of hepatocytes rather than a decline in L-FABP level within the existing hepatocytes. It is known that liver weight increases with the proliferation of biliary epithelial cells and other cell and tissue types, but the volume proportion of hepatocytes is reduced (Gall and Bhathal 1990). The reduced L-FABP levels (65 % to 90 %) in BDL rats compared with control rats one to four weeks after surgery greatly exceeded the 10 % to 30 % loss of hepatocyte fraction in BDL rats at the same period after surgery (Yamauchi, Koyama et al. 1976; Gall and Bhathal 1990; Krahenbuhl, Talos et al. 1996). Thus, we conclude that the dramatic reduction in L-FABP level in BDL animals was related to reduced protein level within the existing hepatocytes. This reduction is due to reduced L-FABP transcription

Since L-FABP forms a large portion of the intracellular protein pool, together with its methionine and cysteine residues and great binding capacity, L-FABP is likely a potentially important intracellular antioxidant in liver cholestasis. Work in this thesis project has demonstrated that L-FABP protected hepatocytes against oxidative stress induced by H₂O₂ and hypoxia-reoxygenation in a Chang gene transfection model cell line

(section 3). An increased level of L-FABP significantly reduced the level of reactive oxygen species within hepatocytes. The current study also indicated that L-FABP acts as an antioxidant in liver injury induced by BDL. The significant decrease in L-FABP occurred at 48 hours following BDL, which preceded the decrease in GSH that is known to occur 5 days following BDL (Purucker, Winograd et al. 1998). TBARS activity increased at day 3 following BDL. It is likely that the antioxidant capacity of hepatocytes is able to deal with the increased levels of reactive oxygen species (ROS) within the first few days of BDL. However, long term the antioxidant complement is unable to maintain a low ROS level. Interestingly, restoration of L-FABP expression in the liver by clofibrate reduced the ROS levels that were accompanied with reduced serum total bilirubin, alanine aminotransferase, and ammonia. Our results show that L-FABP plays a major role in preventing liver damage against oxidative stress in BDL rats. This protective effect of L-FABP may be due to the binding of peroxidized fatty acids, bile salts, and/or scavenging of ROS.

The direct antioxidant function of L-FABP is likely due to its amino acid composition. L-FABP possesses one cysteine residue at position 69 and seven methionine residues in its 127 amino acid sequence. The accessible volume enclosed by the molecular surface of L-FABP is $28,600 \text{ \AA}^3$ (Thompson, Reese-Wagoner et al. 1999). The concentration of total methionine residues in this volume of L-FABP can be as high as $\sim 400 \text{ mM}$. Cysteine residue may be involved in the binding of other hydrophobic ligands or serve as an antioxidant participating in S-thiolation/dethiolation (Thomas, Poland et al. 1995; Sato, Baba et al. 1996). Methionine residues have nucleophilic sulfur atoms and are regarded as a cellular scavenger of activated xenobiotics such as

carcinogens (Bassuk, Tsiichlis et al. 1987). Cellular oxidative stress may also be suppressed by oxidation of methionine in liver FABP to sulfoxides, that are then reduced back by the protein methionine sulfoxide reductase (Levine, Berlett et al. 1999; Moskovitz, Berlett et al. 1999). This cyclic oxidation-reduction of methionine residues of proteins may serve an important antioxidant function (Levine, Mosoni et al. 1996). The net effect of these catalytic reactions is the conversion of reactive species (ROS) to innocuous products, and driving NADPH oxidations (Stadtman 2004). Liver also has a high expression level of methionine sulfoxide reductase (Moskovitz, Jenkins et al. 1996) providing for the catalytic methionine redox homeostasis. Moreover, L-FABP binds metabolic oxidative products such as oxidized fatty acids (Raza, Pongubala et al. 1989; Ek-Von Mentzer, Zhang et al. 2001) and inactivates these reactive molecules. For these reasons L-FABP might serve as an endogenous cellular protectant, participating as a scavenger of highly reactive products resulting from metabolic reactions and/or binding of products that induce cellular oxidative damage on the surface of membranes or in the cytosol. The higher levels of L-FABP in pregnant female livers and in females compared to males (Hung, Burczynski et al. 2003) may be related to the protective role of L-FABP. In contrast, the lower levels of L-FABP in steatosis (Hung, Siebert et al. 2005) may add to the cellular oxidative damage likely to be present in non-alcoholic fatty liver disease. Further studies are required to delineate the mechanism of L-FABP antioxidant function.

It is known that L-FABP is an important carrier for a variety of substances. It carries LCFA to mitochondrial and peroxisomes (Reubsaet, Veerkamp et al. 1990; Kaikaus, Sui et al. 1993). Increase in L-FABP abundance of about 2.5 times by clofibrate (Hung, Burczynski et al. 2003) is related to increased fatty acid uptake

(Burczynski, Fandrey et al. 1999) and fatty acid β -oxidation (Kaikaus, Chan et al. 1993). It was documented that short-term cholestasis (BDL) in rats impaired mitochondrial ketogenesis, then disturbed hepatic fatty acid metabolism (Lang, Berardi et al. 2002). L-FABP is an important determinant of hepatic lipid composition and turnover, and contributes to cytosolic fatty acid binding capacity, hepatic fatty acid oxidation and ketogenesis (Martin, Danneberg et al. 2003; Erol, Kumar et al. 2004). Therefore, L-FABP may provide protection to mitochondria against oxidative damage by lipid accumulation. Reduction in L-FABP level will likely facilitate the mitochondrial production and accumulation of free radicals. Those free radicals could add to the peroxide pool of liver tissue. With a continued increase in fatty acid intake, the liver would increase its load of free radicals (Sokol, Devereaux et al. 1991). This information was consistent to our observation that BDL rats fed a high fat diet had higher mortality rates than control animals receiving a normal diet (Figure 51). Moreover, high mortality was associated with a large reduction of L-FABP in the liver (Figure 52).

The BDL model of liver disease is probably one of the best models of biliary disease. Using this model we conclude that the decreased expression of L-FABP contributes to hepatic oxidative stress and plays an important role in the pathogenesis of biliary disease. We speculate that L-FABP could be an important factor for survival in patients with biliary obstruction and high fat diet.

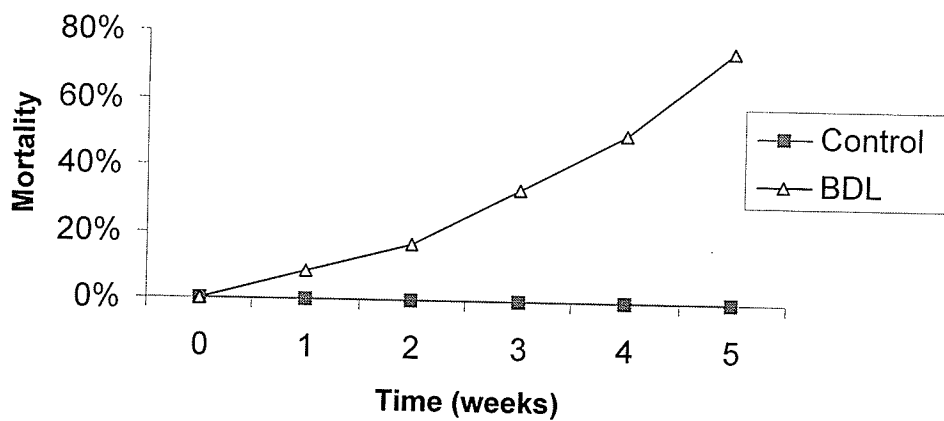


Figure 51. BDL animals fed a high fat diet (33% fat, 4,283 kcal/kg diet, 12 rats) (BDL) were associated with higher mortality rate than BDL animals fed with normal diet (Control) (n=8).

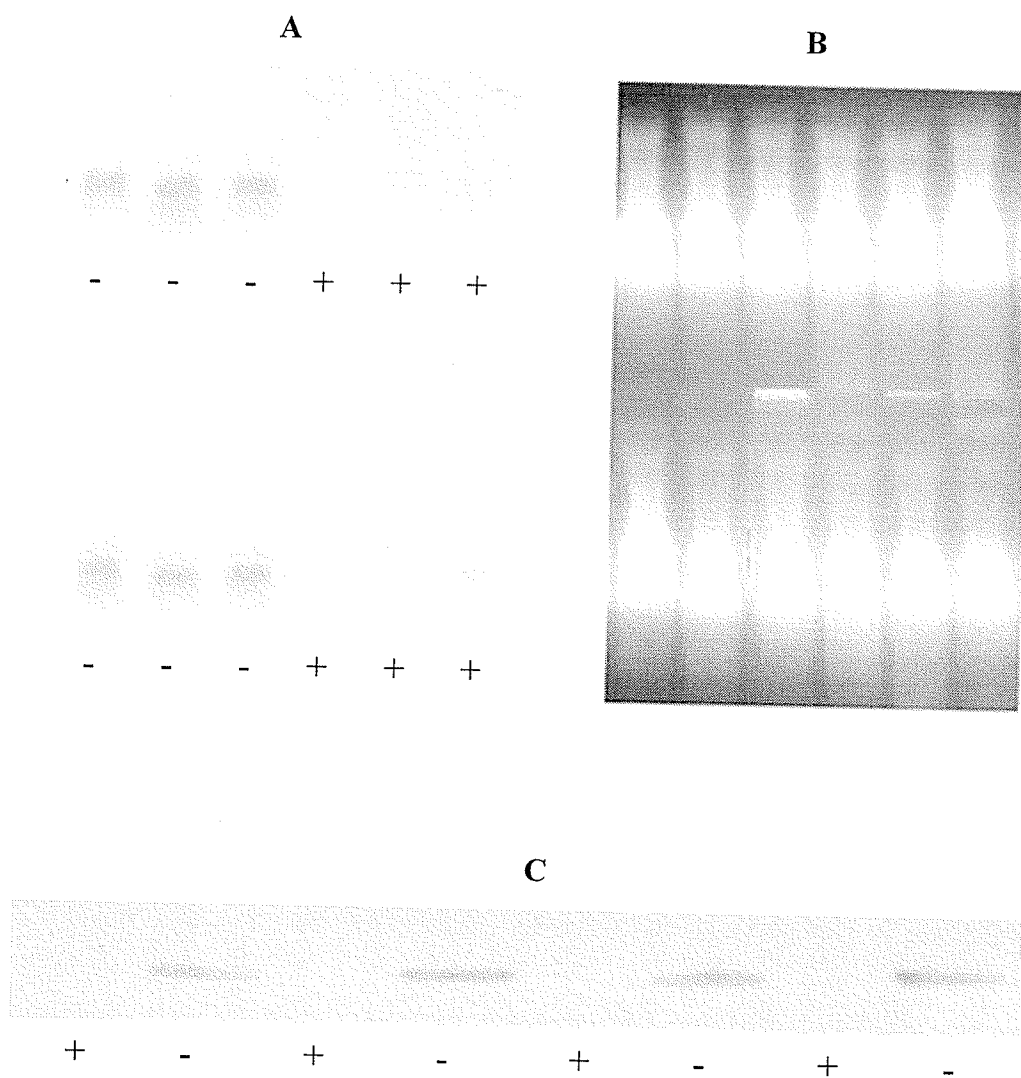


Figure 52. L-FABP mRNA and protein levels of BDL rats fed a high fat diet. 20 μ g total RNA or protein from high fat diet fed BDL or high fat diet fed sham rats was sampled for Northern or Western blot analysis. A, L-FABP mRNA levels of BDL (+) and sham (-) in Northern blot film; B, The integrity and loading of RNA in gel was visualized by UV illumination/ethidium bromide staining; C, L-FABP protein levels of BDL and sham rats in Western blot analysis.

V. Overview of FABP

Nearly three decades ago, first fatty acid binding protein – liver FABP was isolated, which initiated the discovery of a new family of intracellular fatty acid binding proteins. There are not many other protein families like FABP, for which most of the complete tertiary structures, binding properties, and tissue occurrences are well described. As a result of their interactions with LCFAs and the other ligands, FABP potentially have multiple cellular tasks. Not only in fatty acid uptake and transport but FABP also likely play a role in regulating lipid metabolism and cellular signaling pathways. The entire spectrum of putative functions of the different FABP types is still being investigated.

Recent studies demonstrate that LCFAs and their metabolites can modulate the action or localization of proteins like G-protein coupled receptors and many transcription factors including PPARs, liver X receptors, and hepatocyte nuclear factor. L-FABP has a similar binding spectrum with these proteins, and may be targeted for metabolic activation through the cross-talk of these transcription factors and the ligands that activate them. A cyclic regulation seems to exist for FABP gene expression, FABP binds a specific ligand, and the complex stimulates a transcription factor, which then activates FABP expression. Therefore, FABP may be either a positive or negative factor in FABP expression regulation. Results of my studies support the notion that FABP is an important intracellular carrier for protein and ligand cross-talk, and plays a central role in cell proliferation and metabolic response.

The modern lifestyle of humans today is often unavoidable with high caloric intake, low energy expenditure, more xenobiotics, and high stressful work or activities that lead to an unbalanced inflammatory and metabolic homeostasis, resulting in oxidative stress. Results obtained from this study raise an interesting concept that L-FABP plays a role as an endogenous cytoprotectant against oxidative stress. Deficiency or malfunctioning of FABPs has been reported in the disease process of cholestatic liver disease, cancer, diabetes, obesity, and atherosclerosis. The role of FABPs in normal and pathological processes deserves to be continually investigated.

Interestingly, FABPs were found in several parasites that are unable to synthesize fatty acids and therefore have to take fatty acids from their host for growth and survive (Esteves, Portillo et al. 2003; Ramos, Figueredo et al. 2003; Raina, Sriveny et al. 2004). Since the epitopes of these FABPs may not present in mammalian (host), therefore parasite FABPs may be good candidates for the immunotherapy or chemotherapy against these organisms infection. FABP appears to be essential for all lives. The role of FABP in energy regulation/production (substrate availability) and antioxidative stress suggests that FABP plays a pivotal role during intracellular host infections (bacterial/viral). Evolutionary selection has clearly preserved the FABP from worms to humans, implying that the conservation of FABP function may make a close link between inflammatory and metabolic responses. For most successful organism, the efficiency of FABP in these responses is likely critical to resist infection and starvation.

Finally, this thesis made novel and important findings concerning the roles of L-FABP as an intracellular mediator of cell proliferation during liver regeneration and as an important cellular antioxidant during hepatocellular oxidative stress. It provides evidence

for the clinic application and pharmaceutical specificity that L-FABP level may be considered as a prognostic factor for hepatic surgery, and regulating L-FABP may minimize hepatocyte oxidative damage and interfere with disease process during the course of therapeutic drug management and in organ preservation.

VI. References

- Aboutwerat, A., P. W. Pemberton, et al. (2003). "Oxidant stress is a significant feature of primary biliary cirrhosis." Biochim Biophys Acta **1637**(2): 142-50.
- Abumrad, N., C. Coburn, et al. (1999). "Membrane proteins implicated in long-chain fatty acid uptake by mammalian cells: CD36, FATP and FABPm." Biochim Biophys Acta **1441**(1): 4-13.
- Aebersold, R. H., J. Leavitt, et al. (1987). "Internal amino acid sequence analysis of proteins separated by one- or two-dimensional gel electrophoresis after in situ protease digestion on nitrocellulose." Proc Natl Acad Sci U S A **84**(20): 6970-4.
- Albano, E., L. Gorla-Gatti, et al. (1993). "Possible role of free radical intermediates in hepatotoxicity of hydrazine derivatives." Toxicol Ind Health **9**(3): 529-38.
- Alpers, D. H., A. W. Strauss, et al. (1984). "Cloning of a cDNA encoding rat intestinal fatty acid binding protein." Proc Natl Acad Sci U S A **81**(2): 313-7.
- Anderson, P. J. (1985). "The recovery of nitrocellulose-bound protein." Anal Biochem **148**(1): 105-10.
- Armstrong, D. and R. Browne (1994). "The analysis of free radicals, lipid peroxides, antioxidant enzymes and compounds related to oxidative stress as applied to the clinical chemistry laboratory." Adv Exp Med Biol **366**: 43-58.
- Assy, N., Y. Gong, et al. (1998). "Use of proliferating cell nuclear antigen as a marker of liver regeneration after partial hepatectomy in rats." J Lab Clin Med **131**(3): 251-6.

- Atshaves, B. P., S. M. Storey, et al. (2002). "Expression of fatty acid binding proteins inhibits lipid accumulation and alters toxicity in L cell fibroblasts." Am J Physiol Cell Physiol **283**(3): C688-703.
- Banaszak, L., N. Winter, et al. (1994). "Lipid-binding proteins: a family of fatty acid and retinoid transport proteins." Adv Protein Chem **45**: 89-151.
- Bansal, M. P., R. G. Cook, et al. (1989). "A 14-kilodalton selenium-binding protein in mouse liver is fatty acid-binding protein." J Biol Chem **264**(23): 13780-4.
- Baron, V. and P. Muriel (1999). "Role of glutathione, lipid peroxidation and antioxidants on acute bile-duct obstruction in the rat." Biochim Biophys Acta **1472**(1-2): 173-80.
- Bass, N. M. (1988). "The cellular fatty acid binding proteins: Aspects of structure, regulation, and function." International Review of Cytology **3**: 143-184.
- Bass, N. M., J. A. Manning, et al. (1985). "Turnover and short-term regulation of fatty acid binding protein in liver." J Biol Chem **260**(17): 9603-7.
- Bass, N. M., J. A. Manning, et al. (1985). "Regulation of the biosynthesis of two distinct fatty acid-binding proteins in rat liver and intestine." Journal of Biological Chemistry **260**: 1432-1436.
- Bassuk, J. A., P. N. Tschlis, et al. (1987). "Liver fatty acid binding protein is the mitosis-associated polypeptide target of a carcinogen in rat hepatocytes." Proc.Natl.Acad.Sci. USA **84**: 7547-7551.
- Bennaars-Eiden, A., L. Higgins, et al. (2002). "Covalent modification of epithelial fatty acid-binding protein by 4-hydroxynonenal in vitro and in vivo. Evidence for a role in antioxidant biology." J Biol Chem **277**(52): 50693-702.

- Bentley, P., I. Calder, et al. (1993). "Hepatic peroxisome proliferation in rodents and its significance for humans." Food Chem Toxicol **31**(11): 857-907.
- Bergmeyer, H. U. (1974). "Methods of enzymatic analysis." Academic Press, New York, NY. **2**.
- Bergmeyer, H. U. and M. Horder (1980). "International federation of clinical chemistry. Scientific committee. Expert panel on enzymes. IFCC document stage 2, draft 1; 1979-11-19 with a view to an IFCC recommendation. IFCC methods for the measurement of catalytic concentration of enzymes. Part 3. IFCC method for alanine aminotransferase." J Clin Chem Clin Biochem **18**(8): 521-34.
- Berk, P. D. (1996). "How do long-chain fatty acids cross cells membranes?" Proceedings of the Society for Experimental Biology and Medicine **212**: 1-4.
- Berk, P. D., M. Bradbury, et al. (1996). "Characterization of membrane transport processes: lessons from the study of BSP, bilirubin, and fatty acid uptake." Semin Liver Dis **16**(2): 107-20.
- Bernlohr, D. A., M. A. Simpson, et al. (1997). "Intracellular lipid-binding proteins and their genes." Annu Rev Nutr **17**: 277-303.
- Berry, S. A., J. B. Yoon, et al. (1993). "Hepatic fatty acid-binding protein mRNA is regulated by growth hormone." J Am Coll Nutr **12**(6): 638-42.
- Besnard, P., L. Foucaud, et al. (1995). "Expression of fatty acid binding protein in the liver during pregnancy and lactation in the rat." Biochimica et Biophysica Acta **1258**: 153-158.
- Billich, S., T. Wissel, et al. (1988). "Cloning of a full-length complementary DNA for fatty-acid-binding protein from bovine heart." Eur J Biochem **175**(3): 549-56.

- Bordewick, U., M. Heese, et al. (1989). "Compartmentation of hepatic fatty-acid-binding protein in liver cells and its effect on microsomal phosphatidic acid biosynthesis." Biol Chem Hoppe Seyler **370**(3): 229-38.
- Bradford, M. M. (1976). "A rapid and sensitive method for the quantitation of microgram quantities of protein utilizing the principles of protein-dye binding." Analytical Biochemistry **72**: 248-254.
- Brandes, R. and R. Arad (1983). "Liver cytosolic fatty acid-binding proteins. Effect of diabetes and starvation." Biochim Biophys Acta **750**(2): 334-9.
- Burczynski, F. J., S. Fandrey, et al. (1999). "Cytosolic fatty acid binding protein enhances rat hepatocyte [H-3]palmitate uptake." Canadian Journal of Physiology and Pharmacology **77**(11): 896-901.
- Burczynski, F. J. and B. A. Luxon (1995). "Is there facilitated uptake of fatty acids by the liver? Interpretation and analysis of experimental data." Canadian Journal of Physiology and Pharmacology **73**: 409-420.
- Burczynski, F. J., M. N. Zhang, et al. (1997). "Role of fatty acid binding protein on hepatic palmitate uptake." Canadian Journal of Physiology and Pharmacology **75**(12): 1350-1355.
- Burnett, D. A., N. Lysenko, et al. (1979). "Utilization of long chain fatty acids by rat liver: Studies of the role of fatty acid binding protein." Gastroenterology **77**: 241-249.
- Catala, A., A. Cerruti, et al. (1995). "Inhibition of microsomal chemiluminescence by cytosolic fractions containing fatty acid binding protein." Arch Physiol Biochem **103**(1): 39-43.

- Chan, L., C. F. Wei, et al. (1985). "Human liver fatty acid binding protein cDNA and amino acid sequence. Functional and evolutionary implications." J Biol Chem **260**(5): 2629-32.
- Chen, C., G. E. Hennig, et al. (2002). "Protection against acetaminophen hepatotoxicity by clofibrate pretreatment: role of catalase induction." J Biochem Mol Toxicol **16**(5): 227-34.
- Chirico, S., C. Smith, et al. (1993). "Lipid peroxidation in hyperlipidaemic patients. A study of plasma using an HPLC-based thiobarbituric acid test." Free Radic Res Commun **19**(1): 51-7.
- Coe, N. R. and D. A. Bernlohr (1998). "Physiological properties and functions of intracellular fatty acid-binding proteins." Biochim Biophys Acta **1391**(3): 287-306.
- Coe, N. R., A. J. Smith, et al. (1999). "The fatty acid transport protein (FATP1) is a very long chain acyl-CoA synthetase." J Biol Chem **274**(51): 36300-4.
- Cohen, S. L. and B. T. Chait (1997). "Mass spectrometry of whole proteins eluted from sodium dodecyl sulfate-polyacrylamide gel electrophoresis gels." Anal Biochem **247**(2): 257-67.
- Conway, J. G. and J. A. Popp (1995). "Effect of the hepatocarcinogenic peroxisome proliferator Wy-14,643 in vivo: no increase in ethane exhalation or hepatic conjugated dienes." Toxicol Appl Pharmacol **135**(2): 229-36.
- Corsico, B., D. P. Cistola, et al. (1998). "The helical domain of intestinal fatty acid binding protein is critical for collisional transfer of fatty acids to phospholipid

- membranes." PROCEEDINGS-OF-THE-NATIONAL-ACADEMY-OF-SCIENCES-OF-THE-UNITED-STATES-OF-AMERICA **95**(21): 12174-12178.
- Corsico, B., H. L. Liou, et al. (2004). "The alpha-helical domain of liver fatty acid binding protein is responsible for the diffusion-mediated transfer of fatty acids to phospholipid membranes." Biochemistry **43**(12): 3600-7.
- Csonka, C., T. Pataki, et al. (2000). "Effects of oxidative stress on the expression of antioxidative defense enzymes in spontaneously hypertensive rat hearts." Free Radic Biol Med **29**(7): 612-9.
- Custer, R. P. and S. Sorof (1985). "Mitosis in hepatocytes is generally associated with elevated levels of the target polypeptide of a liver carcinogen." Differentiation **30**(2): 176-81.
- Das, R., R. Hammamieh, et al. (2001). "Expression pattern of fatty acid-binding proteins in human normal and cancer prostate cells and tissues." Clin Cancer Res **7**(6): 1706-15.
- Davidson, N. O., C. A. Ifkovits, et al. (1993). "Tissue and cell-specific patterns of expression of rat liver and intestinal fatty acid binding protein during development and in experimental colonic and small intestinal adenocarcinomas." Lab Invest **68**(6): 663-75.
- Day, C. P. and O. F. James (1998). "Hepatic steatosis: innocent bystander or guilty party?" Hepatology **27**(6): 1463-6.
- Day, C. P. and O. F. James (1998). "Steatohepatitis: a tale of two "hits"?" Gastroenterology **114**(4): 842-5.

- de Almeida, I. T., H. Cortez-Pinto, et al. (2002). "Plasma total and free fatty acids composition in human non-alcoholic steatohepatitis." Clin Nutr **21**(3): 219-23.
- Deplanque, D. (2004). "[Cell protection through PPAR nuclear receptor activation]." Therapie **59**(1): 25-9.
- Dormann, P., T. Borchers, et al. (1993). "Amino acid exchange and covalent modification by cysteine and glutathione explain isoforms of fatty acid-binding protein occurring in bovine liver." J Biol Chem **268**(22): 16286-92.
- Dutta-Roy, A. K., N. Gopalswamy, et al. (1987). "Prostaglandin E1 binds to Z protein of rat liver." Eur.J.Biochem. **162**: 615-619.
- Dutta-Roy, A. K., M. V. Trinh, et al. (1988). "Choline-deficient diet increases Z protein concentration in rat liver." J Nutr **118**(9): 1116-9.
- Ek, B. A., D. P. Cistola, et al. (1997). "Fatty acid binding proteins reduce 15-lipoxygenase-induced oxygenation of linoleic acid and arachidonic acid." Biochim Biophys Acta **1346**(1): 75-85.
- Ek-Von Mentzer, B. A., F. Zhang, et al. (2001). "Binding of 13-hode and 15-hete to phospholipid bilayers, albumin, and intracellular fatty acid binding proteins. implications for transmembrane and intracellular transport and for protection from lipid peroxidation." J Biol Chem **276**(19): 15575-80.
- Elliott, B. M. and C. R. Elcombe (1987). "Lack of DNA damage or lipid peroxidation measured in vivo in the rat liver following treatment with peroxisomal proliferators." Carcinogenesis **8**(9): 1213-8.
- Elmadhoun, B. M., G. Q. Wang, et al. (1998). "Binding of [H-3]palmitate to BSA." American Journal of Physiology **275**(4): G638-G644.

- Erol, E., L. S. Kumar, et al. (2004). "Liver fatty acid binding protein is required for high rates of hepatic fatty acid oxidation but not for the action of PPARalpha in fasting mice." Faseb J **18**(2): 347-9.
- Esteves, A., V. Portillo, et al. (2003). "Genomic structure and expression of a gene coding for a new fatty acid binding protein from *Echinococcus granulosus*." Biochim Biophys Acta **1631**(1): 26-34.
- Fahimi, H. D., A. Voelkl, et al. (1990). "Localization of the heme-binding protein in the cytoplasm and of a heme-binding protein-like immunoreactive protein in the nucleus of rat liver parenchymal cells: immunocytochemical evidence of the subcellular distribution corroborated by radioimmunoassay and immunoblotting." Hepatology **11**(5): 859-65.
- Farrell, G. C. (1995). Drug-Induced Liver Disease. New York, Churchill Livingstone.
- Fong, D. G., V. Nehra, et al. (2000). "Metabolic and nutritional considerations in nonalcoholic fatty liver." Hepatology **32**(1): 3-10.
- Foucaud, L., I. Niot, et al. (1998). "Indirect dexamethasone down-regulation of the liver fatty acid-binding protein expression in rat liver." Biochim.Biophys.Acta **1391**: 204-12.
- Fridriksson, E. K., B. Baird, et al. (1999). "Electrospray mass spectra from protein electroeluted from sodium dodecylsulfate polyacrylamide gel electrophoresis gels." J Am Soc Mass Spectrom **10**(5): 453-5.
- Gall, J. A. M. and P. S. Bhathal (1990). "A quantitative analysis of the liver following ligation of the common bile duct." Liver **10**: 116-125.

- Garberg, P., U. Stenius, et al. (1992). "Peroxisome proliferation and resistance to hydrogen peroxide in rat hepatocytes: is development of resistance an adaptation to cytotoxicity?" Carcinogenesis **13**(10): 1751-8.
- Glatz, J. F. and J. Storch (2001). "Unravelling the significance of cellular fatty acid-binding proteins." Curr Opin Lipidol **12**(3): 267-74.
- Glatz, J. F. and G. J. van der Vusse (1996). "Cellular fatty acid-binding proteins: their function and physiological significance." Prog Lipid Res **35**(3): 243-82.
- Goel, S. K., N. D. Lalwani, et al. (1986). "Peroxisome proliferation and lipid peroxidation in rat liver." Cancer Res **46**(3): 1324-30.
- Gordon, J. I., D. H. Alpers, et al. (1983). "The nucleotide sequence of rat liver fatty acid binding protein mRNA." J-Biol-Chem **258**: 3356-3363.
- Gordon, J. I., N. Elshourbagy, et al. (1985). "Tissue specific expression and developmental regulation of two genes coding for rat fatty acid binding proteins." J Biol Chem **260**(4): 1995-8.
- Grisham, J. W. (1962). "A morphologic study of deoxyribonucleic acid synthesis and cell proliferation in regenerating rat liver; autoradiography with thymidine- H^3 ." Cancer Research **22**: 842-849.
- Guajardo, M. H. and A. M. C. Terrasa, A. (2002). "Retinal fatty acid binding protein reduce lipid peroxidation stimulated by long-chain fatty acid hydroperoxides on rod outer segments." Biochim Biophys Acta **1581**: 65-74.
- Halliwell, B. (1999). "Antioxidant defence mechanisms: from the beginning to the end (of the beginning)." Free Radic Res **31**(4): 261-72.

- Handler, J. A., C. B. Seed, et al. (1992). "Induction of peroxisomes by treatment with perfluorooctanoate does not increase rates of H₂O₂ production in intact liver." Toxicol Lett **60**(1): 61-8.
- Haq, R. U. and E. Shrago (1985). "Dietary and nutritional aspects of fatty acid binding proteins." Chem Phys Lipids **38**(1-2): 131-5.
- Hashimoto, M. and K. Sanjo (1997). "Functional capacity of the liver after two-thirds partial hepatectomy in the rat." Surgery **121**(6): 690-7.
- Hasinoff, B. B. (2002). "Dexrazoxane (ICRF-187) protects cardiac myocytes against hypoxia-reoxygenation damage." Cardiovasc Toxicol **2**(2): 111-8.
- Haunerland, N., G. Jagschies, et al. (1984). "Fatty-acid-binding proteins. Occurrence of two fatty-acid-binding proteins in bovine liver cytosol and their binding of fatty acids, cholesterol, and other lipophilic ligands." Hoppe Seylers Z Physiol Chem **365**(3): 365-76.
- Herrmann, T., F. Buchkremer, et al. (2001). "Mouse fatty acid transport protein 4 (FATP4): characterization of the gene and functional assessment as a very long chain acyl-CoA synthetase." Gene **270**(1-2): 31-40.
- Heuckeroth, R. O., E. H. Birkenmeier, et al. (1987). "Analysis of the tissue-specific expression, developmental regulation, and linkage relationships of a rodent gene encoding heart fatty acid binding protein." J Biol Chem **262**(20): 9709-17.
- Higgins, G. M. and R. M. Anderson (1931). "Experimental pathology of the liver: restoration of liver of the white rat following partial surgical removal." Arch. Pathol. **12**: 186-202.

- Hino, A., M. Morita, et al. (2001). "Effects of deoxycholic acid and its epimers on lipid peroxidation in isolated rat hepatocytes." J Biochem (Tokyo) **129**(5): 683-9.
- Hitomi, M., S. Odani, et al. (1990). "Glutathione-protein mixed disulfide decreases the affinity of rat liver fatty acid-binding protein for unsaturated fatty acid." Eur J Biochem **187**(3): 713-9.
- Ho, Y. S. and J. D. Crapo (1987). "cDNA and deduced amino acid sequence of rat copper-zinc-containing superoxide dismutase." Nucleic Acids Res **15**(16): 6746.
- Hodsdon, M. E. and D. P. Cistola (1997). "Discrete backbone disorder in the nuclear magnetic resonance structure of apo intestinal fatty acid-binding protein: implications for the mechanism of ligand entry." Biochemistry **36**(6): 1450-60.
- Hohoff, C. and F. Spener (1998). "Fatty acid binding proteins and mammary-derived growth inhibitor." FETT-LIPID **100**: 252-263.
- Huang, H., O. Starodub, et al. (2004). "Liver fatty acid-binding protein colocalizes with peroxisome proliferator activated receptor alpha and enhances ligand distribution to nuclei of living cells." Biochemistry **43**(9): 2484-500.
- Hung, D. Y., F. J. Burczynski, et al. (2003). "Fatty Acid Binding Protein Is A Major Determinant of Hepatic Pharmacokinetics of Palmitate and Its Metabolites." Am J Physiol Gastrointest Liver Physiol **284**: G423-G433.
- Hung, D. Y., G. A. Siebert, et al. (2005). "Reduced hepatic extraction of palmitate in steatosis correlated to lower level of liver fatty acid binding protein." Am J Physiol Gastrointest Liver Physiol **288**(1): G93-G100.
- Itoh, N., K. N. Nose, et al. (1979). "Purification and characterization of proinsulin mRNA from rat B-cell tumor." Eur. J. Biochem. **97**: 1-9.

- Jaeschke, H. (2003). "Molecular mechanisms of hepatic ischemia-reperfusion injury and preconditioning." Am J Physiol Gastrointest Liver Physiol **284**(1): G15-26.
- Jagschies, G., M. Reers, et al. (1985). "Bovine fatty acid binding proteins. Isolation and characterisation of two cardiac fatty acid binding proteins that are distinct from corresponding hepatic proteins." Eur J Biochem **152**(3): 537-45.
- Jespersen, S., G. Talbo, et al. (1993). "Optimization of sample recovery from the nitrocellulose support used in plasma desorption mass spectrometry and its use for multiple analyses of insulin." Biol Mass Spectrom **22**(1): 77-83.
- Jones, R. M., M. R. Prasad, et al. (1990). "Modulation of fatty acid-binding capacity of heart fatty acid-binding protein by oxygen-derived free radicals." Mol Cell Biochem **98**(1-2): 161-6.
- Kaikaus, R. M., W. K. Chan, et al. (1993). "Induction of peroxisomal fatty acid beta-oxidation and liver fatty acid-binding protein by peroxisome proliferators. Mediation via the cytochrome P-450IVA1 omega-hydroxylase pathway." J Biol Chem **268**(13): 9593-603.
- Kaikaus, R. M., Z. Sui, et al. (1993). "Regulation of pathways of extramitochondrial fatty acid oxidation and liver fatty acid-binding protein by long-chain monocarboxylic fatty acids in hepatocytes." Journal of Biological Chemistry **268**: 26866-26871.
- Kamijo, A., K. Kimura, et al. (2004). "Urinary fatty acid-binding protein as a new clinical marker of the progression of chronic renal disease." J Lab Clin Med **143**(1): 23-

- Kamisaka, H. Maezawa, et al. (1981). "A low molecular weight binding protein for organic anions (Z protein) from human hepatic cytosol: purification and quantitation." Hepatology **1**(3): 221-7.
- Kanda, T., H. Fujii, et al. (1996). "Intestinal fatty acid-binding protein is a useful diagnostic marker for mesenteric infarction in humans." Gastroenterology **110**(2): 339-43.
- Kanda, T., Y. Nakatomi, et al. (1992). "Intestinal fatty acid-binding protein as a sensitive marker of intestinal ischemia." Dig Dis Sci **37**(9): 1362-7.
- Kawashima, Y., S. Nakagawa, et al. (1983). "Effects of peroxisome proliferators on fatty acid-binding protein in rat liver." Biochim Biophys Acta **754**(1): 21-7.
- Keler, T. and S. Sorof (1993). "Growth promotion of transfected hepatoma cells by liver fatty acid binding protein." J. Cell.Physiol. **157**: 33-40.
- Ketterer, B., E. Tipping, et al. (1976). "A low-molecular-weight protein from rat liver that resembles ligandin in its binding properties." Biochem.J. **155**: 511-521.
- Khan, S. H. and S. Sorof (1990). "Preferential binding of growth inhibitory prostaglandins by the target protein of a carcinogen." Proc Natl Acad Sci U S A **87**(23): 9401-5.
- Khan, S. H. and S. Sorof (1994). "Liver fatty acid-binding protein: specific mediator of the mitogenesis induced by two classes of carcinogenic peroxisome proliferators." Proc.Natl.Acad.Sci. USA **91**: 848-852.
- Khynriam, D. and S. B. Prasad (2002). "Changes in glutathione-related enzymes in tumor-bearing mice after cisplatin treatment." Cell Biol Toxicol **18**(6): 349-58.

- Kinumi, T., J. Kimata, et al. (2004). "Cysteine-106 of DJ-1 is the most sensitive cysteine residue to hydrogen peroxide-mediated oxidation in vivo in human umbilical vein endothelial cells." Biochem Biophys Res Commun **317**(3): 722-8.
- Kountouras, J., B. H. Billing, et al. (1984). "Prolonged bile duct obstruction: a new experimental model for cirrhosis in the rat." British Journal of Experimental Pathology **65**: 305-311.
- Krahenbuhl, L., C. Talos, et al. (1996). "Progressive decrease in tissue glycogen content in rats with long-term cholestasis." Hepatology **24**(4): 902-7.
- Krähenbühl, S., C. Talos, et al. (1994). "Toxicity of bile acids on the electron transport chain of isolated rat liver mitochondria." Hepatology **19**: 471-479.
- Krahenbuhl, S., C. Talos, et al. (1995). "Reduced antioxidative capacity in liver mitochondria from bile duct ligated rats." Hepatology **22**(2): 607-12.
- Krähenbühl, S., C. Talos, et al. (1994). "Mechanisms of impaired hepatic fatty acid metabolism in rats with long-term bile duct ligation." Hepatology **19**: 1272-1281.
- Kren, B. T., J. H. Trembley, et al. (1997). "Molecular regulation of liver regeneration." Ann N Y Acad Sci **831**: 361-81.
- Landrier, J. F., C. Thomas, et al. (2004). "Statin Induction of Liver Fatty Acid-Binding Protein (L-FABP) Gene Expression Is Peroxisome Proliferator-activated Receptor- α -dependent." J Biol Chem **279**(44): 45512-45518.
- Lang, C., S. Berardi, et al. (2002). "Impaired ketogenesis is a major mechanism for disturbed hepatic fatty acid metabolism in rats with long-term cholestasis and after relief of biliary obstruction." J Hepatol **37**(5): 564-71.

- Lawrence-JW, Kroll-DJ, et al. (2000). "Ligand-dependent interaction of hepatic fatty acid-binding protein with the nucleus." Journal of Lipid Research **41**(9): 1390-1401.
- Levi, A. J., Z. Gatmaitan, et al. (1969). "Two hepatic cytoplasmic protein fractions, Y and Z, and their possible role in the hepatic uptake of bilirubin, sulfobromophthalein, and other anions." J Clin Invest **48**(11): 2156-67.
- Levine, R. L., B. S. Berlett, et al. (1999). "Methionine residues may protect proteins from critical oxidative damage." Mech Ageing Dev **107**: 323-32.
- Levine, R. L., L. Mosoni, et al. (1996). "Methionine residues as endogenous antioxidants in proteins." Proc Natl Acad Sci U S A **93**(26): 15036-40.
- Lewis, S. E., L. L. Listenberger, et al. (2001). "Membrane topology of the murine fatty acid transport protein 1." J Biol Chem **276**(40): 37042-50.
- Li, E. and A. W. Norris (1996). "Structure/function of cytoplasmic vitamin A-binding proteins." Annu Rev Nutr **16**: 205-34.
- Lieber, C. S. and C. S. Abittan (1999). "Pharmacology and metabolism of alcohol, including its metabolic effects and interactions with other drugs." Clinics in Dermatology **17**: 365-379.
- Ljubuncic, P., Z. Tanne, et al. (2000). "Evidence of a systemic phenomenon for oxidative stress in cholestatic liver disease." Gut **47**(5): 710-6.
- Loboda, A. V., A. N. Krutchinsky, et al. (2000). "A tandem quadrupole/time-of-flight mass spectrometer with a matrix-assisted laser desorption/ionization source: design and performance." Rapid Commun Mass Spectrom **14**(12): 1047-57.

- Low, T. Y., C. K. Leow, et al. (2004). "A proteomic analysis of thioacetamide-induced hepatotoxicity and cirrhosis in rat livers." Proteomics **4**(12): 3960-3974.
- Lowe, J. B., M. S. Boguski, et al. (1985). "Human liver fatty acid binding protein. Isolation of a full length cDNA and comparative sequence analyses of orthologous and paralogous proteins." J Biol Chem **260**(6): 3413-7.
- Lowry, O. H., N. J. Rosebrough, et al. (1951). "Protein measurement with folin phenol reagent." Journal of Biological Chemistry **193**: 265-271.
- Lucke, C., F. Zhang, et al. (1996). "Flexibility is a likely determinant of binding specificity in the case of ileal lipid binding protein." Structure **4**(7): 785-800.
- Luebker, D. J., K. J. Hansen, et al. (2002). "Interactions of fluorochemicals with rat liver fatty acid-binding protein." Toxicology **176**(3): 175-85.
- Lui, M., P. Tempst, et al. (1996). "Methodical analysis of protein-nitrocellulose interactions to design a refined digestion protocol." Anal Biochem **241**(2): 156-66.
- Luiken, J. J., Y. Arumugam, et al. (2001). "Increased rates of fatty acid uptake and plasmalemmal fatty acid transporters in obese Zucker rats." J Biol Chem **276**(44): 40567-73.
- Luiken, J. J., F. G. Schaap, et al. (1999). "Cellular fatty acid transport in heart and skeletal muscle as facilitated by proteins." Lipids **34**(Suppl): S169-75.
- Luxon, B. A. (1996). "Inhibition of binding to fatty acid binding protein reduces the intracellular transport of fatty acids." American Journal of Physiology **271**: G113-G120.

- Martin, G. G., H. Danneberg, et al. (2003). "Decreased liver fatty acid binding capacity and altered liver lipid distribution in mice lacking the liver fatty acid-binding protein gene." J Biol Chem **278**(24): 21429-38.
- McClarty, G. (1994). "Chlamydiae and the biochemistry of intracellular parasitism." Trends Microbiol **2**(5): 157-64.
- Memon, R. A., N. M. Bass, et al. (1999). "Down-regulation of liver and heart specific fatty acid binding proteins by endotoxin and cytokines in vivo." Biochimica et Biophysica Acta **1440**: 118-126.
- Meunier-Durmort, C., H. Poirier, et al. (1996). "Up-regulation of the expression of the gene for liver fatty acid-binding protein by long-chain fatty acids." Biochemical Journal **319**: 483-487.
- Michalopoulos, G. K. and M. C. DeFrances (1997). "Liver regeneration." Science **276**: 60-66.
- Milliano, M. T. and B. A. Luxon (2001). "The peroxisomal proliferator clofibrate enhances the hepatic cytoplasmic movement of fatty acids in rats." Hepatology **33**(2): 413-418.
- Mishkin, S., H. P. Morris, et al. (1977). "Reduced concentrations of Z protein in Morris hepatomas. Possible role in abnormal regulation of lipid metabolism." J Biol Chem **252**(11): 3626-8.
- Mishkin, S., L. Stein, et al. (1972). "The binding of fatty acids to cytoplasmic proteins: binding to Z protein in liver and other tissues of the rat." Biochem Biophys Res Commun **47**(5): 997-1003.

- Moskovitz, J., S. Bar-Noy, et al. (2001). "Methionine sulfoxide reductase (MsrA) is a regulator of antioxidant defense and lifespan in mammals." Proc Natl Acad Sci U S A **98**(23): 12920-5.
- Moskovitz, J., B. S. Berlett, et al. (1999). "Methionine sulfoxide reductase in antioxidant defense." Methods Enzymol **300**: 239-44.
- Moskovitz, J., N. A. Jenkins, et al. (1996). "Chromosomal localization of the mammalian peptide-methionine sulfoxide reductase gene and its differential expression in various tissues." Proc Natl Acad Sci U S A **93**(8): 3205-8.
- Muriel, P. and M. G. Moreno (2004). "Effects of silymarin and vitamins E and C on liver damage induced by prolonged biliary obstruction in the rat." Basic Clin Pharmacol Toxicol **94**(2): 99-104.
- Murphy, E. J., R. D. Edmondson, et al. (1999). "Isolation and characterization of two distinct forms of liver fatty acid binding protein from the rat." Biochimica et Biophysica Acta **1436**: 413-425.
- Murphy, E. J., D. R. Prows, et al. (1996). "Liver fatty acid-binding protein expression in transfected fibroblasts stimulates fatty acid uptake and metabolism." BIOCHIMICA-ET-BIOPHYSICA-ACTA **1301**: 191-198.
- Nakagawa, S., Y. Kawashima, et al. (1994). "Regulation of hepatic level of fatty-acid-binding protein by hormones and clofibric acid in the rat." Biochem J **297 (Pt 3)**: 581-4.
- Neuschwander-Tetri, B. A., C. Nicholson, et al. (1996). "Cholestatic liver injury down-regulates hepatic glutathione synthesis." J Surg Res **63**(2): 447-51.

- Newberry, E. P., Y. Xie, et al. (2003). "Decreased hepatic triglyceride accumulation and altered fatty acid uptake in mice with deletion of the liver fatty acid-binding protein gene." J Biol Chem **278**(51): 51664-72.
- Nicholls-Grzemeski, F. A., G. B. Belling, et al. (2000). "Clofibrate pretreatment in mice confers resistance against hepatic lipid peroxidation." J Biochem Mol Toxicol **14**(6): 335-45.
- Nicholls-Grzemeski, F. A., I. C. Calder, et al. (2000). "Clofibrate-induced in vitro hepatoprotection against acetaminophen is not due to altered glutathione homeostasis." Toxicol Sci **56**(1): 220-8.
- Ockner, R. K., N. Lysenko, et al. (1980). "Sex steroid modulation of fatty acid utilization and fatty acid binding protein concentration in rat liver." Journal of Clinical Investigations **65**: 1013-1023.
- Ockner, R. K., J. A. Manning, et al. (1972). "A binding protein for fatty acids in cytosol of intestinal mucosa, liver, myocardium, and other tissues." Science **177**(43): 56-8.
- Odani, S., Y. Namba, et al. (2000). "Disulfide bonds in rat cutaneous fatty acid-binding protein." J Biochem **128**(3): 355-61.
- Offner, G. D., P. Brecher, et al. (1988). "Characterization and amino acid sequence of a fatty acid-binding protein from human heart." Biochem J **252**(1): 191-8.
- Offner, G. D., R. F. Troxler, et al. (1986). "Characterization of a fatty acid-binding protein from rat heart." J Biol Chem **261**(12): 5584-9.

- Orellana, M., N. Avalos, et al. (1997). "Microsomal and peroxisomal fatty acid oxidation in bile duct ligated rats: a comparative study between liver and kidney." Gen Pharmacol **28**(4): 525-9.
- Orellana, M., R. Rodrigo, et al. (2000). "Bile duct ligation and oxidative stress in the rat: effects in liver and kidney." Comp Biochem Physiol C Toxicol Pharmacol **126**(2): 105-11.
- Palacios, A., V. A. Piergiacomi, et al. (1999). "Inhibition of lipid peroxidation of microsomes and mitochondria by cytosolic proteins from rat liver: effect of vitamin A." Int J Vitam Nutr Res **69**(1): 61-3.
- Patterson, S. D. and R. Aebersold (1995). "Mass spectrometric approaches for the identification of gel-separated proteins." Electrophoresis **16**(10): 1791-814.
- Paulussen, R. J. A., G. P. M. Jansen, et al. (1986). "Fatty acid-binding capacity of cytosolic proteins of various rat tissues: effect of postnatal development, starvation, sex, clofibrate feeding and light cycle." Biochimica et Biophysica Acta **877**: 342-349.
- Peeters, R. A., M. A. P. M. in't Groen, et al. (1989). "The binding affinity of fatty acid-binding proteins from human, pig, and rat liver for different fluorescent fatty acids and other ligands." International Journal of Biochemistry **21**: 407-418.
- Pelsers, M. M., A. Morovat, et al. (2002). "Liver fatty acid-binding protein as a sensitive serum marker of acute hepatocellular damage in liver transplant recipients." Clin Chem **48**(11): 2055-7.
- Perera, M. I., S. L. Katyal, et al. (1986). "Suppression of choline-deficient diet-induced hepatocyte membrane lipid peroxidation in rats by the peroxisome proliferators 4-

- chloro-6-(2,3-xylidino)-2-pyrimidinylthio(N-beta-hydroxyethyl)- acetamide and di(2-ethylhexyl)phthalate." Cancer Res **46**(7): 3304-8.
- Pignon, J. P., N. C. Bailey, et al. (1987). "Fatty acid-binding protein: a major contributor to the ethanol-induced increase in liver cytosolic proteins in the rat." Hepatology **7**(5): 865-71.
- Poirier, F., R. Joubert-Caron, et al. (2003). "Proteomic analysis of a lymphoma-derived cell line (DG75) following treatment with a demethylating drug: modification of membrane-associated proteins." Proteomics **3**(6): 1028-36.
- Prows, D. R., E. J. Murphy, et al. (1995). "Intestinal and liver fatty acid binding proteins differentially affect fatty acid uptake and esterification in L-cells." Lipids **30**: 907-10.
- Purucker, E., R. Winograd, et al. (1998). "Glutathione status in liver and plasma during development of biliary cirrhosis after bile duct ligation." Res Exp Med (Berl) **198**(4): 167-74.
- Qin, J. and B. T. Chait (1997). "Identification and characterization of posttranslational modifications of proteins by MALDI ion trap mass spectrometry." Anal Chem **69**(19): 4002-9.
- Raina, O. K., D. Sriveny, et al. (2004). "Humoral immune response against *Fasciola gigantica* fatty acid binding protein." Vet Parasitol **124**(1-2): 65-72.
- Ramos, C. R., R. C. Figueredo, et al. (2003). "Gene structure and M20T polymorphism of the *Schistosoma mansoni* Sm14 fatty acid-binding protein. Molecular, function, and immunoprotection analysis." J Biol Chem **278**(15): 12745-51.

- Rasmussen, H. H., T. F. Orntoft, et al. (1996). "Towards a comprehensive database of proteins from the urine of patients with bladder cancer." J Urol **155**(6): 2113-9.
- Ratcliff, C. R., and Hall, F.F. (1982). "Selected Methods of Clinical Chemistry." Edited by Willard R. Faulkner and Samuel Meites, American Association for Clinical Chemistry, Washington D.C.: 9:85.
- Raza, H., J. R. Pongubala, et al. (1989). "Specific high affinity binding of lipoxygenase metabolites of arachidonic acid by liver fatty acid binding protein." Biochem Biophys Res Commun **161**(2): 448-55.
- Reddy, J. K. and N. D. Lalwai (1983). "Carcinogenesis by hepatic peroxisome proliferators: evaluation of the risk of hypolipidemic drugs and industrial plasticizers to humans." Crit Rev Toxicol **12**(1): 1-58.
- Reddy, J. K. and M. S. Rao (1989). "Oxidative DNA damage caused by persistent peroxisome proliferation: its role in hepatocarcinogenesis." Mutat Res **214**(1): 63-8.
- Requena, J. R., M. N. Dimitrova, et al. (2004). "Oxidation of methionine residues in the prion protein by hydrogen peroxide." Arch Biochem Biophys **432**(2): 188-95.
- Reubsaet, F. A., J. H. Veerkamp, et al. (1990). "The involvement of fatty acid binding protein in peroxisomal fatty acid oxidation." FEBS Lett **267**(2): 229-30.
- Roomi, M. W., S. H. Vincent, et al. (1988). "Decreased cytosolic levels of the heme binding Z protein in rat hepatocyte nodules and hepatocellular carcinomas." Cancer Lett **43**(1-2): 55-8.

- Sacchettini, J. C., T. A. Meininger, et al. (1987). "Crystallization of rat intestinal fatty acid binding protein. Preliminary X-ray data obtained from protein expressed in *Escherichia coli*." J Biol Chem **262**(11): 5428-30.
- Sacchettini, J. C., B. Said, et al. (1986). "Rat heart fatty acid-binding protein is highly homologous to the murine adipocyte 422 protein and the P2 protein of peripheral nerve myelin." J Biol Chem **261**(18): 8218-23.
- Samanta, A., D. K. Das, et al. (1989). "Free radical scavenging by myocardial fatty acid binding protein." Free Radic Res Commun **7**(2): 73-82.
- Sato, T., K. Baba, et al. (1996). "Rat liver fatty acid-binding protein: identification of a molecular species having a mixed disulfide with cysteine at cysteine-69 and enhanced protease susceptibility." J Biochem **120**(5): 908-14.
- Schoonjans, K., B. Staels, et al. (1996). "The peroxisome proliferator activated receptors (PPARS) and their effects on lipid metabolism and adipocyte differentiation." Biochim Biophys Acta **1302**(2): 93-109.
- Schroeder, F., B. P. Atshaves, et al. (2001). "Expression of liver fatty acid binding protein alters growth and differentiation of embryonic stem cells." Mol Cell Biochem **219**(1-2): 127-38.
- Scobie, B. A. and W. H. Summerskill (1965). "Hepatic Cirrhosis Secondary to Obstruction of the Biliary System." Am J Dig Dis **10**: 135-46.
- Shevchenko, A., A. Loboda, et al. (2000). "MALDI quadrupole time-of-flight mass spectrometry: a powerful tool for proteomic research." Anal Chem **72**(9): 2132-41.

- Shevchenko, A., M. Wilm, et al. (1996). "Mass spectrometric sequencing of proteins silver-stained polyacrylamide gels." Anal Chem **68**(5): 850-8.
- Shevchuk, O., E. Baraona, et al. (1991). "Gender differences in the response of hepatic fatty acids and cytosolic fatty acid-binding capacity to alcohol consumption in rats." Proceedings of the Society for Experimental Biology and Medicine **198**: 584-590.
- Simon, T. C., K. A. Roth, et al. (1993). "Use of transgenic mice to map cis-acting elements in the liver fatty acid-binding protein gene (Fabpl) that regulate its cell lineage-specific, differentiation-dependent, and spatial patterns of expression in the gut epithelium and in the liver acinus." J Biol Chem **268**(24): 18345-58.
- Sinha, P., G. Hutter, et al. (1999). "Increased expression of epidermal fatty acid binding protein, cofilin, and 14-3-3-sigma (stratifin) detected by two-dimensional gel electrophoresis, mass spectrometry and microsequencing of drug-resistant human adenocarcinoma of the pancreas." ELECTROPHORESIS **20**(14): 2952-2960.
- Sokol, R. J., M. Devereaux, et al. (1991). "Effect of dietary lipid and vitamin E on mitochondrial lipid peroxidation and hepatic injury in the bile duct-ligated rat." J Lipid Res **32**(8): 1349-57.
- Sokol, R. J., B. M. Winklhofer-Roob, et al. (1995). "Generation of hydroperoxides in isolated rat hepatocytes and hepatic mitochondria exposed to hydrophobic bile acids." Gastroenterology **109**(4): 1249-56.
- Sorof, S. (1994). "Modulation of mitogenesis by liver fatty acid binding protein." Cancer and Metastasis Reviews **13**: 317-336.

- Sorof, S. and R. P. Custer (1987). "Elevated expression and cell cycle deregulation of a mitosis-associated target polypeptide of a carcinogen in hyperplastic and malignant rat hepatocytes." Cancer Res **47**(1): 210-20.
- Spitsberg, V. L., E. Matitashvili, et al. (1995). "Association and coexpression of fatty-acid-binding protein and glycoprotein CD36 in the bovine mammary gland." Eur-J-Biochem **230**: 872-8.
- Stadtman, E. R. (2004). "Cyclic oxidation and reduction of methionine residues of proteins in antioxidant defense and cellular regulation." Arch Biochem Biophys **423**(1): 2-5.
- Stadtman, E. R., J. Moskovitz, et al. (2002). "Cyclic oxidation and reduction of protein methionine residues is an important antioxidant mechanism." Mol Cell Biochem **234-235**(1-2): 3-9.
- Stein, L. B., S. Mishkin, et al. (1976). "Effect of fasting on hepatic ligandin, Z protein, and organic anion transfer from plasma in rats." Am J Physiol **231**(5 Pt. 1): 1371-6.
- Stump, D. D., S. L. Zhou, et al. (1993). "Comparison of plasma membrane FABP and mitochondrial isoform of aspartate aminotransferase from rat liver." Am J Physiol **265**(5 Pt 1): G894-902.
- Subramaniam, R., X. J. Fan, et al. (2002). "Cellular oxidant stress and advanced glycation endproducts of albumin: caveats of the dichlorofluorescein assay." Arch Biochem Biophys **400**(1): 15-25.

- Suzuki, T., K. Watanabe, et al. (1990). "Immunohistochemical demonstration of liver fatty acid-binding protein in human hepatocellular malignancies." J Pathol **161**(1): 79-83.
- Sweetser, D. A., J. B. Lowe, et al. (1986). "The nucleotide sequence of the rat liver fatty acid-binding protein gene. Evidence that exon 1 encodes an oligopeptide domain shared by a family of proteins which bind hydrophobic ligands." J Biol Chem **261**(12): 5553-61.
- Takahashi, K., S. Odani, et al. (1982). "Primary structure of rat liver Z-protein. A low-Mr cytosol protein that binds sterols, fatty acids and other small molecules." FEBS Lett **140**(1): 63-6.
- Tamura, H., T. Iida, et al. (1990). "Long-term effects of hypolipidemic peroxisome proliferator administration on hepatic hydrogen peroxide metabolism in rats." Carcinogenesis **11**(3): 445-50.
- Taub, R. (1996). "Liver regeneration 4: transcriptional control of liver regeneration." Faseb J **10**(4): 413-27.
- Thomas, J. A., B. Poland, et al. (1995). "Protein sulfhydryls and their role in the antioxidant function of protein S-thiolation." Arch Biochem Biophys **319**(1): 1-9.
- Thompson, J., A. Reese-Wagoner, et al. (1999). "Liver fatty acid binding protein: species variation and the accommodation of different ligands." Biochim Biophys Acta **1441**(2-3): 117-30.
- Timperman, A. T. and R. Aebersold (2000). "Peptide electroextraction for direct coupling of in-gel digests with capillary LC-MS/MS for protein identification and sequencing." Anal Chem **72**(17): 4115-21.

- Tomaszewski, K. E., D. K. Agarwal, et al. (1986). "In vitro steady-state levels of hydrogen peroxide after exposure of male F344 rats and female B6C3F1 mice to hepatic peroxisome proliferators." Carcinogenesis **7**(11): 1871-6.
- Tsuji, R., T. Tanaka, et al. (1993). "Human heart-type cytoplasmic fatty acid-binding protein in serum and urine during hyperacute myocardial infarction." Int J Cardiol **41**(3): 209-17.
- Tuchweber, B. and M. Salas (1978). "Prevention of CeCl₃-induced hepatotoxicity by hypolipidemic compounds." Arch Toxicol **41**(3): 223-32.
- Van Nieuwenhoven, F. A., A. H. Kleine, et al. (1995). "Discrimination between myocardial and skeletal muscle injury by assessment of the plasma ratio of myoglobin over fatty acid-binding protein." Circulation **92**(10): 2848-54.
- Van Nieuwenhoven, F. A., G. J. Van der Vusse, et al. (1996). "Membrane-associated and cytoplasmic fatty acid-binding proteins." Lipids **31 Suppl**: S223-7.
- Van Nieuwenhoven, F. A., P. H. Willemsen, et al. (1999). "Co-expression in rat heart and skeletal muscle of four genes coding for proteins implicated in long-chain fatty acid uptake." Int J Biochem Cell Biol **31**(3-4): 489-98.
- Vancura, A. and D. Haldar (1992). "Regulation of mitochondrial and microsomal phospholipid synthesis by liver fatty acid-binding protein." J Biol Chem **267**(20): 14353-9.
- Veerkamp, J. H. and R. G. H. J. Maatman (1995). "Cytoplasmic fatty acid-binding proteins: their structure and genes." Progress in Lipid Research **34**: 17-52.

- Veerkamp, J. H., R. A. Peeters, et al. (1991). "Structural and functional features of different types of cytoplasmic fatty acid-binding proteins." Biochim Biophys Acta **1081**(1): 1-24.
- Veerkamp, J. H., T. H. van Kuppevelt, et al. (1993). "Structural and functional aspects of cytosolic fatty acid-binding proteins." Prostaglandins Leukot Essent Fatty Acids **49**(6): 887-906.
- Vergani, L., M. Fanin, et al. (1990). "Liver fatty acid-binding protein in two cases of human lipid storage." Mol-Cell-Biochem **98**: 225-30.
- Vinores, S. A., J. J. Churey, et al. (1984). "Normal liver chromatin contains a firmly bound and larger protein related to the principal cytosolic target polypeptide of a hepatic carcinogen." Proc Natl Acad Sci U S A **81**(7): 2092-6.
- Vork, M. M., J. F. Glatz, et al. (1993). "Release of fatty acid-binding protein and long chain fatty acids from isolated rat heart after ischemia and subsequent calcium paradox." Mol Cell Biochem **123**(1-2): 175-84.
- Wang, G., F. Burczynski, et al. (2002). "Infection of myocytes with chlamydiae." Microbiology **148**(Pt 12): 3955-9.
- Wang, G., Q. M. Chen, et al. (2004). "Enhanced expression of cytosolic fatty acid binding protein and fatty acid uptake during liver regeneration in rats." Mol Cell Biochem **262**(1-2): 41-9.
- Wang, H. and J. A. Joseph (1999). "Quantifying cellular oxidative stress by dichlorofluorescein assay using microplate reader." Free Radic Biol Med **27**(5-6): 612-6.

- Wolfrum, C., T. Borchers, et al. (2000). "Binding of fatty acids and peroxisome proliferators to orthologous fatty acid binding proteins from human, murine, and bovine liver." Biochemistry **39**: 1469-1474.
- Wolfrum, C., C. M. Borrmann, et al. (2001). "Fatty acids and hypolipidemic drugs regulate peroxisome proliferator-activated receptors alpha - and gamma-mediated gene expression via liver fatty acid binding protein: a signaling path to the nucleus." Proc Natl Acad Sci U S A **98**(5): 2323-8.
- Wolfrum, C., C. Buhlmann, et al. (1999). "Variation of liver-type fatty acid binding protein content in the human hepatoma cell line HepG2 by peroxisome proliferators and antisense RNA affects the rate of fatty acid uptake." Biochim Biophys Acta **1437**(2): 194-201.
- Wong, S., Padua, A., and Henzel, W. J. (1992). "Protein and peptide recovery from PVDF membranes." Techniques in Protein Chemistry: 3-9.
- Woodford, J. K., J. R. Jefferson, et al. (1993). "Expression of liver fatty acid binding protein alters plasma membrane lipid composition and structure in transfected L-cell fibroblasts." Biochim Biophys Acta **1145**(2): 257-65.
- Yamamoto, Y., S. Yamashita, et al. (1998). "Oxidative stress in patients with hepatitis, cirrhosis, and hepatoma evaluated by plasma antioxidants." Biochem Biophys Res Commun **247**(1): 166-70.
- Yamauchi, H., K. Koyama, et al. (1976). "Morphometric studies on the rat liver in biliary obstruction." Tohoku J Exp Med **119**(1): 9-25.

- Yamazaki, T., T. Kanda, et al. (1999). "Liver fatty acid-binding protein is a new prognostic factor for hepatic resection of colorectal cancer metastases." Journal of Surgical Oncology **72**: 83-87.
- Yoshimoto, K., T. Tanaka, et al. (1995). "Human heart-type cytoplasmic fatty acid-binding protein as an indicator of acute myocardial infarction." Heart Vessels **10**(6): 304-9.
- Zakim, D. (1996). "Fatty acids enter cells by simple diffusion." Proceedings of the Society for Experimental Biology and Medicine **212**: 5-14.
- Zimmerman, A. W. and J. H. Veerkamp (2001). "Fatty-acid-binding proteins do not protect against induced cytotoxicity in a kidney cell model." Biochem J **360**(Pt 1): 159-65.
- Zimmermann-Ivol, C. G., P. R. Burkhard, et al. (2004). "Fatty acid binding protein as a serum marker for the early diagnosis of stroke: a pilot study." Mol Cell Proteomics **3**(1): 66-72.